NBS TECHNICAL NOTE 860

U.S. DEPARTMENT OF COMMERCE / National Bureau of Standards

NBS Reactor:
Summary of Activities July 1973 to June 1974

NATIONAL BUREAU OF STANDARDS

The National Bureau of Standards[1] was established by an act of Congress March 3, 1901. The Bureau's overall goal is to strengthen and advance the Nation's science and technology and facilitate their effective application for public benefit. To this end, the Bureau conducts research and provides: (1) a basis for the Nation's physical measurement system, (2) scientific and technological services for industry and government, (3) a technical basis for equity in trade, and (4) technical services to promote public safety. The Bureau consists of the Institute for Basic Standards, the Institute for Materials Research, the Institute for Applied Technology, the Institute for Computer Sciences and Technology, and the Office for Information Programs.

THE INSTITUTE FOR BASIC STANDARDS provides the central basis within the United States of a complete and consistent system of physical measurement; coordinates that system with measurement systems of other nations; and furnishes essential services leading to accurate and uniform physical measurements throughout the Nation's scientific community, industry, and commerce. The Institute consists of a Center for Radiation Research, an Office of Measurement Services and the following divisions:

Applied Mathematics — Electricity — Mechanics — Heat — Optical Physics — Nuclear Sciences[2] — Applied Radiation[2] — Quantum Electronics[3] — Electromagnetics[3] — Time and Frequency[3] — Laboratory Astrophysics[3] — Cryogenics[3].

THE INSTITUTE FOR MATERIALS RESEARCH conducts materials research leading to improved methods of measurement, standards, and data on the properties of well-characterized materials needed by industry, commerce, educational institutions, and Government; provides advisory and research services to other Government agencies; and develops, produces, and distributes standard reference materials. The Institute consists of the Office of Standard Reference Materials and the following divisions:

Analytical Chemistry -- Polymers — Metallurgy — Inorganic Materials — Reactor Radiation — Physical Chemistry.

THE INSTITUTE FOR APPLIED TECHNOLOGY provides technical services to promote the use of available technology and to facilitate technological innovation in industry and Government; cooperates with public and private organizations leading to the development of technological standards (including mandatory safety standards), codes and methods of test; and provides technical advice and services to Government agencies upon request. The Institute consists of a Center for Building Technology and the following divisions and offices:

Engineering and Product Standards — Weights and Measures — Invention and Innovation — Product Evaluation Technology — Electronic Technology — Technical Analysis — Measurement Engineering — Structures, Materials, and Life Safety[4] — Building Environment[4] — Technical Evaluation and Application[4] — Fire Technology.

THE INSTITUTE FOR COMPUTER SCIENCES AND TECHNOLOGY conducts research and provides technical services designed to aid Government agencies in improving cost effectiveness in the conduct of their programs through the selection, acquisition, and effective utilization of automatic data processing equipment; and serves as the principal focus within the executive branch for the development of Federal standards for automatic data processing equipment, techniques, and computer languages. The Institute consists of the following divisions:

Computer Services — Systems and Software — Computer Systems Engineering — Information Technology.

THE OFFICE FOR INFORMATION PROGRAMS promotes optimum dissemination and accessibility of scientific information generated within NBS and other agencies of the Federal Government; promotes the development of the National Standard Reference Data System and a system of information analysis centers dealing with the broader aspects of the National Measurement System; provides appropriate services to ensure that the NBS staff has optimum accessibility to the scientific information of the world. The Office consists of the following organizational units:

Office of Standard Reference Data — Office of Information Activities — Office of Technical Publications — Library — Office of International Relations.

---

[1] Headquarters and Laboratories at Gaithersburg, Maryland, unless otherwise noted; mailing address Washington, D.C. 20234.

[2] Part of the Center for Radiation Research.

[3] Located at Boulder, Colorado 80302.

[4] Part of the Center for Building Technology.

NBS Reactor: Summary of Activities July 1973 to June 1974

Robert S. Carter

Reactor Radiation Division
Institute for Materials Research
U.S. National Bureau of Standards
Washington, D.C. 20234

t. Technical note no. 860

U.S. DEPARTMENT OF COMMERCE, Frederick B. Dent, *Secretary*
NATIONAL BUREAU OF STANDARDS, Richard W. Roberts, *Director*

Issued April 1975

National Bureau of Standards Technical Note 860
Nat. Bur. Stand. (U.S.), Tech. Note 860, 143 pages (Apr. 1975)
CODEN: NBTNAE

U.S. GOVERNMENT PRINTING OFFICE
WASHINGTON: 1975

For sale by the Superintendent of Documents, U.S. Government Printing Office, Washington, D.C. 20402
(Order by SD Catalog No. C13.46:860).
Price $2.05

FOREWORD

The National Bureau of Standards Reactor was built not only to serve the needs of the NBS but also those of the greater Washington Scientific Community and other government agencies. The Reactor Radiation Division was established to operate the reactor and to foster its scientific and technological use. Toward this end, the Division has a small nucleus of scientists experienced in the use of reactors for a wide range of scientific and technical problems. In addition to pursuing their own research and developing sophisticated experimental facilities, they actively seek out and encourage collaboration with other scientists, engaged in challenging programs, whose work can benefit from use of the reactor, but who as yet do not have the reactor experience necessary to take full advantage of the facilities available. The Division also provides irradiation services to a wide variety of users as well as engineering and other technical services.

The reactor operates at 10 MW and is designed to provide a broad spectrum of facilities ranging from intense neutron beams to extensive irradiation facilities, making it one of the most versatile high flux research reactors in the country. Thus it is able to serve a large number of scientists and engineers in a broad range of activities both within and outside the NBS.

This report attempts to summarize all the work done which is dependent on the reactor including a large number of programs outside the Division. The first section summarizes those programs based primarily on Reactor Radiation Division (RRD) initiatives whereas the second and third sections summarized collaborative programs between RRD scientists and other NBS or non-NBS scientists respectively. The fourth section summarizes NBS work originating entirely outside of RRD which requires no collaboration with RRD scientists. The section entitled, "Service Programs" covers those programs originating outside NBS but for which RRD provides irradiation services. The remaining sections are self-explanatory.

ABSTRACT

This report summarizes all those programs which depend on the NBS reactor. It covers the period from July 1973 through June 1974. The programs range from the use of neutron beams to study the structure and dynamics of materials through nuclear physics, and neutron standards and neutron radiography to sample irradiations for activation analysis, isotope production and radiation effects studies.

Key words: Activation analysis; crystal structure; diffraction; isotopes; molecular dynamics; neutron; nuclear reactor; radiation; radiography.

Cover photograph: Reactor Building
National Bureau of Standards
Gaithersburg, Maryland

TABLE OF CONTENTS

TABLE OF CONTENTS

TABLE OF CONTENTS

A. REACTOR RADIATION DIVISION PROGRAMS

NEUTRON SCATTERING STUDIES OF HYDROGEN IN TRANSITION METALS

New results have been obtained in our continuing studies of the binding and diffusion of hydrogen isotopes in bcc (refractory) and fcc transition metals. This work is being done in collaboration with scientists from the Argonne and Oak Ridge National Laboratories. The study of the microscopic behavior of such metal-hydrogen systems is of considerable interest for a variety of reasons including the possible use of the refractory metals and alloys in nuclear fusion reactors and hydrogen storage systems and the discovery of superconductivity in palladium alloy hydrides. During the past year we have (1) completed our first study of the details of the hydrogen diffusion process in a single crystal of a bcc metal (tantalum), (2) completed the preparation of a large single crystal of β-phase $PdD_{0.63}$ and measured the lattice dynamics of this crystal by coherent neutron scattering--the first such measurement yet accomplished and (3) we have completed the first measurements in our study of the lattice dynamics in a bcc metal-hydride (α=NbD_x). The latter two experiments are being analyzed to derive information on the effects of interestitional hydrogen on the electronic structure and intermetallic forces in fcc and bcc metals.

1. Hydrogen Diffusion in a Single Crystal of Tantalum - J. M. Rowe
J. J. Rush

Analysis has been completed of a detailed neutron quasielastic scattering study of the diffusion of a defect concentration of hydrogen in a tantalum single crystal ($TaH_{0.02}$). This work and the other hydride studies described below have been carried out in collaboration with H. E. Flotow of Argonne National Laboratory.

It was clear to us from our own and other previous neutron studies of hydrogen diffusion in the TaH_x, VH_x and other hydride systems using polycrystalline samples that extending our research to single crystal samples was highly desirable in order to obtain more detailed information on the diffusion mechanisms. Such measurements yield a much more extensive data set as a function of crystal orientation and eliminate the averaging over crystallite orientations which obscures theoretical analysis of quasielastic scattering results on polycrystals. In the present experiments neutron spectra (incident E_o=5 meV, ΔE_o=0.26 meV) were measured at 584 K at seven different orientations ψ of the single crystal with respect to the incident beam and over a range of momentum transfers (Q) from 0.5 to 2.5Å^{-1}.

Examples of the symmetrized scattering functions $\tilde{S}(\vec{Q},\omega)$ in the small energy transfer region obtained from our measured neutron spectra are shown in figure 1. In order to test the applicability of the two most probable simple jump models for hydrogen in Ta, i.e., instantaneous jumps between near-neighbor octahedral or tetrahedral interstitial sites, we chose first to fit the detailed shape of the measured quasielastic peaks directly to the predictions of these models with the residence time τ as a parameter. Both of these models predict a quasielastic scattering peak composed of a sum of lorentzians with Q-dependent widths and weighting factors depending on the type of occupied sites. It turns out that neither of these models comes close to providing a satisfactory fit over the entire set of measured quasielastic peaks. This result is in sharp contrast to our recent study of hydrogen diffusion in a single crystal of (fcc) palladium, in which all the data were fit very well by a model assuming instantaneous jumps between octahedral sites. On the other hand, we were able to fit all the observed quasielastic peaks very well to a single resolution-broadened lorentzian with the width of the lorentzian as a fitting parameter. These fits are shown by the solid lines in figure 1. Such a result is surprising, since no model involving simple jump diffusion between octahedral and tetrahedral sites, including o↔t and second neighbor jumps predicts such a lineshape dependence.

The unusual nature of our results is further illustrated in Fig. 2, where the full-widths at half maximum of the observed quasielastic peak vs. $\vec{Q}$ (for different values of ψ) are shown along with the linewidths predicted from the octahedral and tetrahedral jump models. It can be seen that both the linewidths and their variation with $\vec{Q}$ shows are quite different, on the whole, from the predictions of the two models. Most

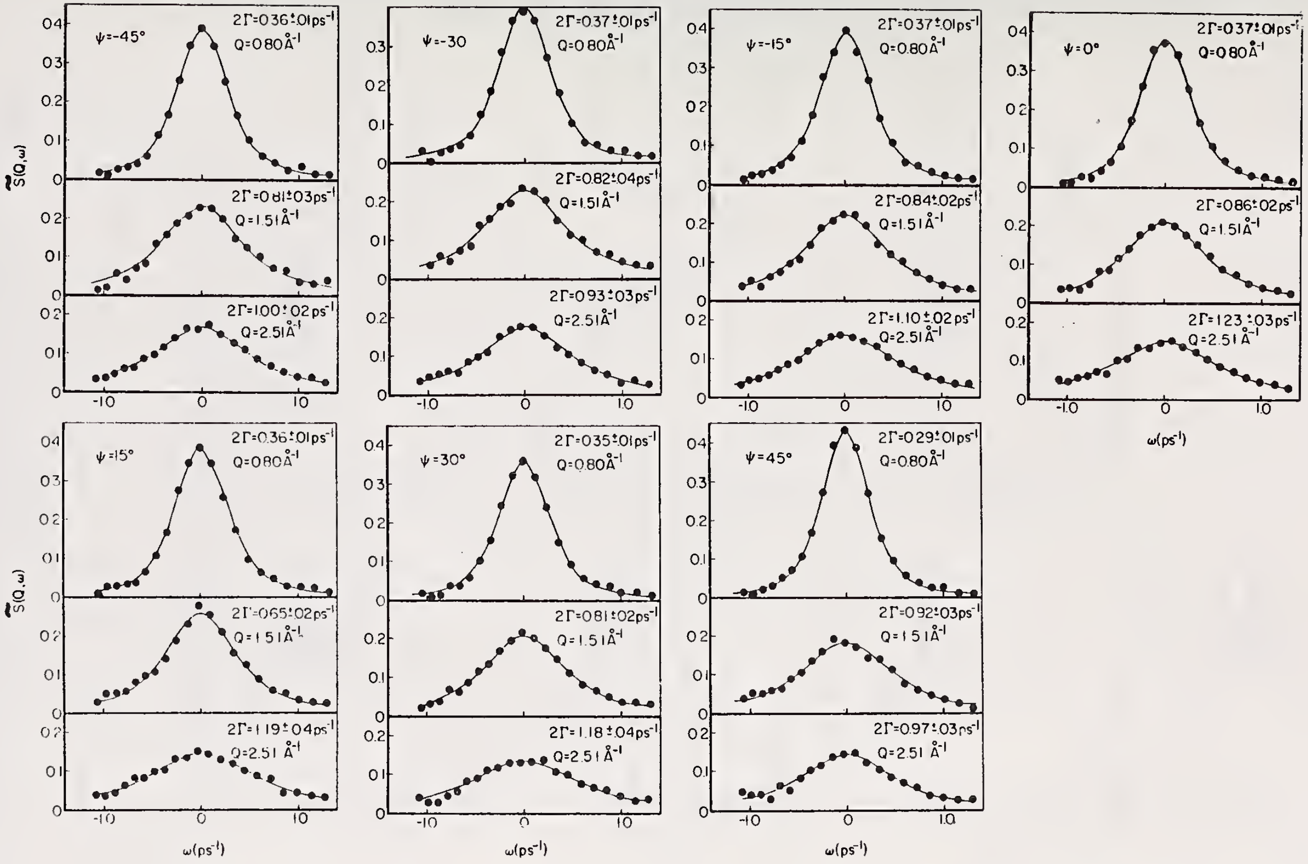

Fig. 1. Symmetrized scattering laws $\tilde{S}(\vec{Q},\omega)$ vs. ω for $TaH_{0.02}$ at 584 K for several values of momentum transfer ($|\vec{Q}|$) and crystal orientation ψ. The solid lines represent the resolution-broadened lorentzians fitted as described in the text.

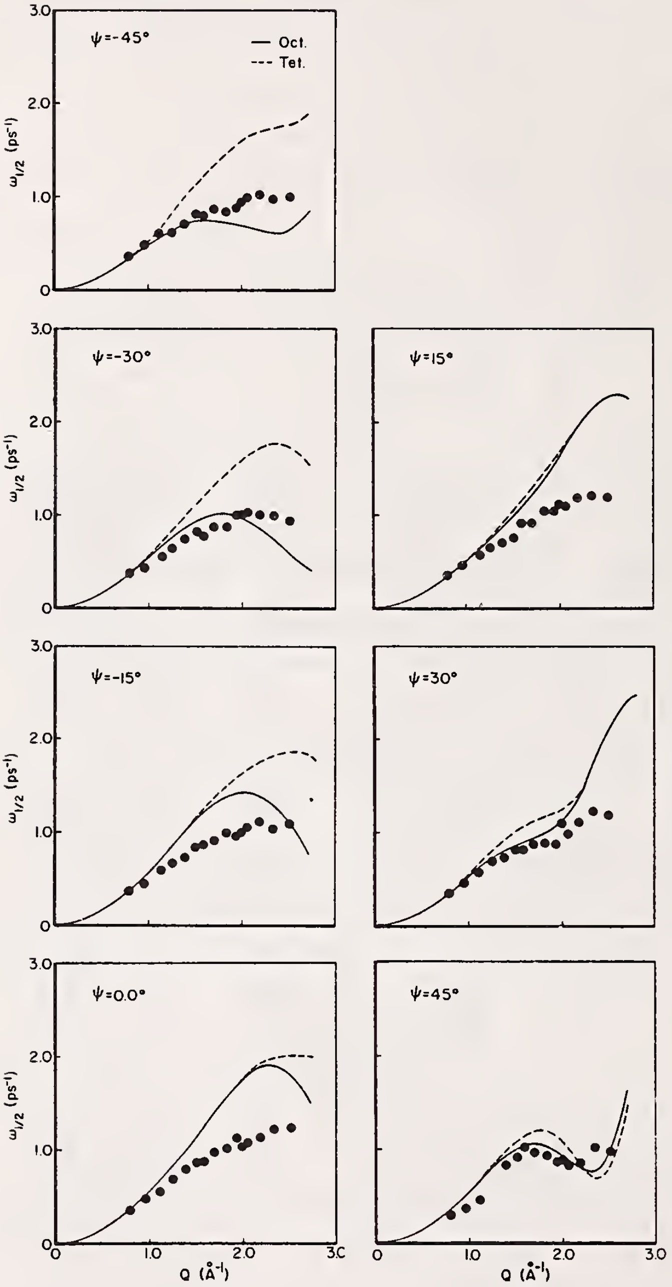

Fig. 2. Experimental full widths at half-maximum, $\omega_{1/2}$, vs. $|\vec{Q}|$ measured for various crystal orientations. Theoretical linewidths for the octahedral and tetrahedral models are also shown.

notably the experimental results are much more isotropic than those predicted by any simple jump model involving these interstitional sites. We note here that the linewidth values at small Q, which reflect diffusion behavior over large distances, predict a macroscopic diffusion constant ($2.8\text{x}10^{-5}\text{cm}^2\text{s}^{-1}$) which is in excellent agreement with macroscopic diffusion measurements using the Gorsky effect. Moreover the mean-square vibration amplitude ($\overline{u^2}$) derived from the total quasielastic scattering intensities is 0.04Å^2, in reasonable agreement with the values given previously in our report on quasielastic scattering by polycrystalline TaH_x. In addition, the τ values obtained from the "best fits" of the tetrahedral and octahedral jump models to the data were 1.2 and 1.8 ps respectively, in good agreement with our previous polycrystal results.

There is no obvious explanation for the lineshapes and isotropic character of the quasielastic width curves observed in the present experiment. The results could be explained in part by assuming that the interstitial sites occupied by the hydrogen atoms are not well localized. Clearly more work, both theoretical and experimental, will be necessary in order to attain a detailed understanding of hydrogen diffusion in Ta (and in other bcc metals). Our own measurements on $\text{TaH}_{0.02}$ are being extended to larger momentum transfers.

2. Lattice Dynamics of Palladium Deuteride - J. M. Rowe and J. J. Rush

In collaboration with H. G. Smith at ORNL, we have measured the phonon dispersion relations of β-phase $\text{PdD}_{0.63}$ by coherent inelastic neutron scattering from a single crystal sample. Apart from our earlier limited investigation of α-phase $\text{PdH}_{0.03}$, these results are the first available for any metallic (non-ionic) hydride, and provide the first detailed information on the interatomic forces in such systems. The superconducting transition temperature of this sample is almost certainly less than 1 K (in contrast to the T_c's of ∿10 K recently discovered for β-phase palladium hydride samples closer to PdH_1) but the results may be valuable in understanding the superconducting behavior at higher concentrations.

The sample was prepared by adding high purity deuterium gas to a 12 mm Dx 50 mm long single crystal of palladium. The initial loading was carried out at temperatures greater than 300 C (necessarily under high pressure, ∿0.6 kbar) to avoid the two-phase region of the phase diagram. Phonon data were collected at 78, 150, 200 and 295 K. Some typical phonon groups measured at selected temperatures are shown in figure 3. Peaks due to incoherent scattering (by deuterium) are also indicated. The most important points to be noted are that the centroids of the groups do not change appreciably as a function of T, while the groups themselves broaden considerably as T increases, thus indicating strong anharmonicity. In figure 4 are shown the dispersion relations for $PdD_{0.63}$ obtained from these measurements. Data from different temperatures have been combined in this figure. The solid lines represent the results of a 12-parameter least squares fit of a fourth-nearest-neighbor Born-von Karman model to the data, with third neighbor Pd-D force constants fixed at zero values. A fit of similar quality can be obtained with a simple screened shell model. The dotted lines are the dispersion curves measured for pure Pd at 300 K. It can be seen that the $PdD_{0.63}$ acoustic modes are 20-30% lower than for pure Pd; a result quite consistent with the observed lattice expansion (∿5%).

The frequency of the optic modes near the zone centers (figure 4) is low in comparison with most other hydrides, thus employing a weak nearest neighbor PdD force constant. This is in general agreement with the results of incoherent scattering spectra, but the detailed shape of the vibration frequency distributions derived from the present work are quite different from those obtained from the incoherent scattering studies. The dispersion of the longitudinal optic modes is large. Moreover, the fact that the frequency of the LO mode in the [100] direction reaches a maximum before the zone boundary implies strong second-like neighbor D-D interactions, comparable to the first like-neighbor Pd-Pd interaction. The existence of strong effective interactions between second-neighbor deuterium atoms is an indication that electronic screening effects are important, even though the present specimen is expected to have T_c<1 K.

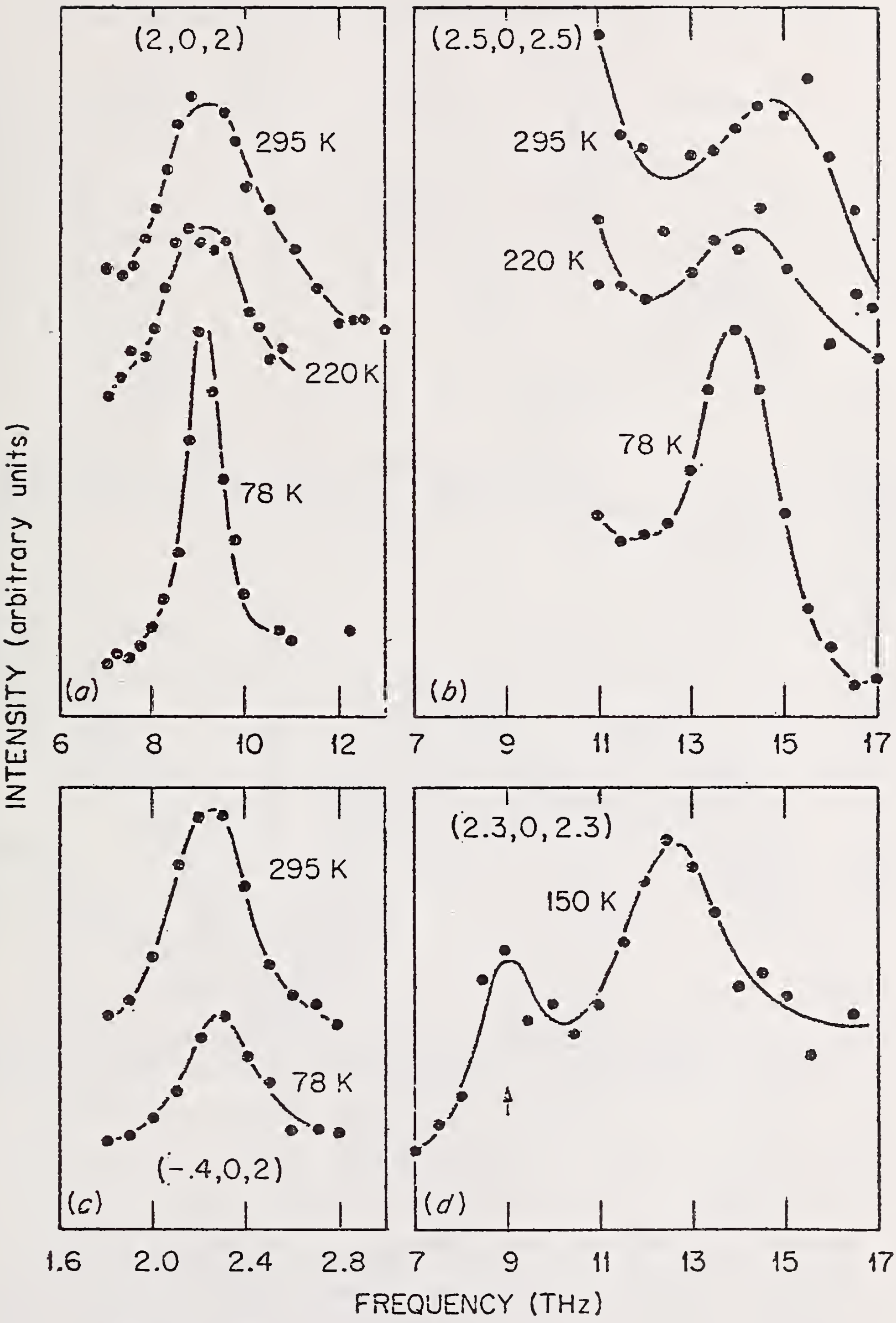

Fig. 3. Selected phonon groups at several temperatures in $PdD_{0.63}$. The arrow in part (d) indicates an incoherent peak due to the flat TO modes.

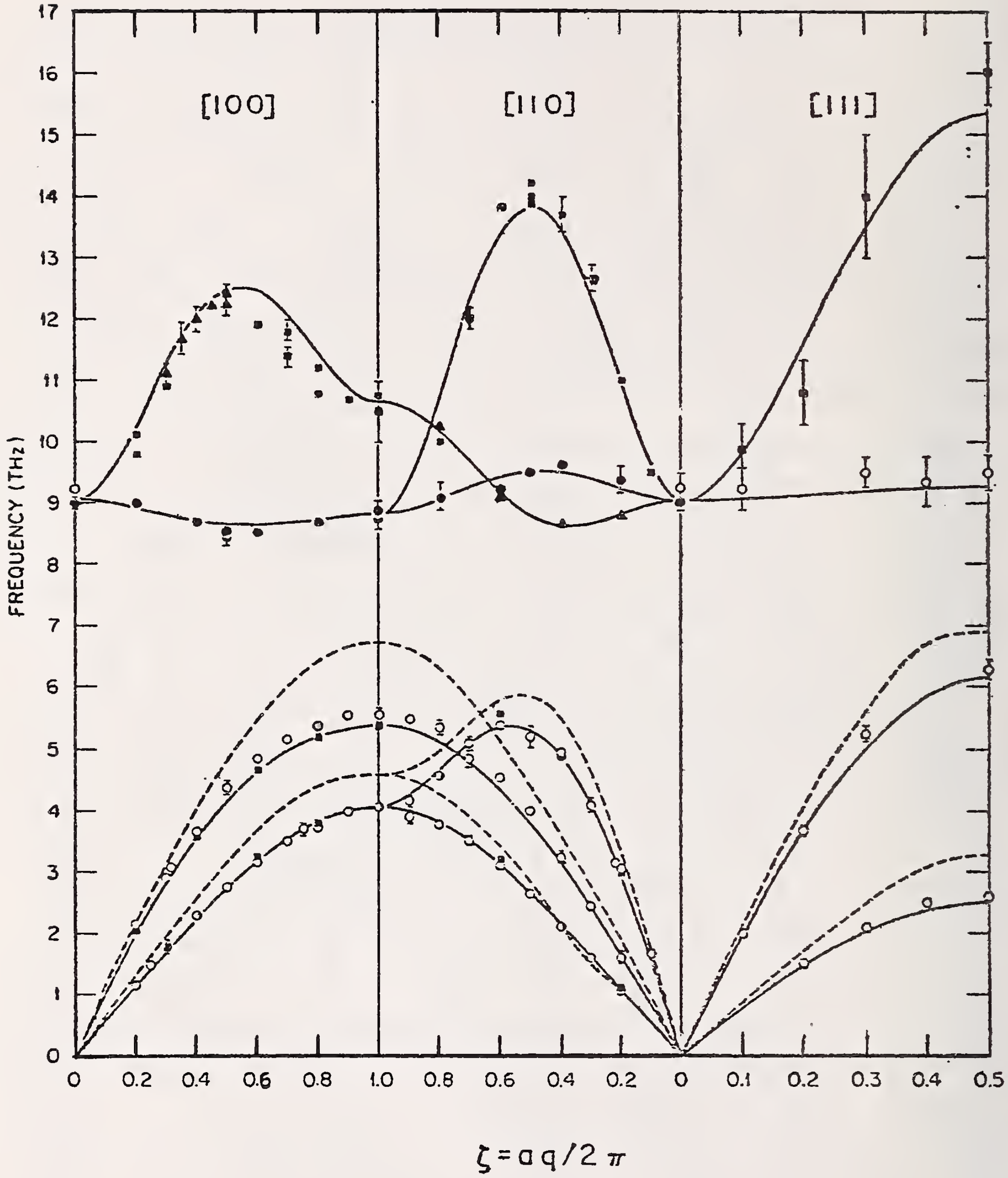

Fig. 4. Phonon dispersion curves in $PdD_{0.63}$. The solid curves are calculated based on a Born-von Kármán model with twelve parameters. The solid (open) symbols are phonon groups obtained at 150°K (295°K). The dotted curves are the dispersion curves observed for pure Pd at 300 K.

We are currently testing deuterium loading procedures to try to produce a "high" T_c ($\gtrsim$ 4 K) single crystal sample of $Pd_{\sim 0.9}$, which would allow us to study the crystal dynamics, electronic structure and anharmonic effects of the superconducting hydride closer to stiochiometry. Experiments are also in progress to remeasure the incoherent inelastic scattering spectra for the PdH and PdD at small momentum transfers, for comparison with the frequency distributions derived from our dispersion curve results.

3. Lattice Dynamics of Niobium Deuteride - J. M. Rowe, N. Vagelatos and J. J. Rush

Following up on our work on $PdD_{.63}$ discussed above, we have established a program to measure the lattice dynamics of α-phase bcc metal deuterides (we use deuterium to minimize the incoherent scattering). The first step in this program is to measure for low concentrations and we have now completed measurements of the phonon dispersion relation in $NbD_{.15}$ in the three major symmetry directions at 473 K. The sample must be maintained at temperatures above 200°C in order to avoid the two-phase (α+β) region and thus prevent destruction of the single crystal sample. For a direct comparison, we have also measured pure Nb at 473 K - our results at this temperature are in good agreement with the trends established in earlier work by the Chalk River group on the temperature dependence of phonon frequencies in pure Nb.

In an attempt to establish the effects of adding deuterium to Nb, we have fitted both the Nb and $NbD_{.15}$ to several different models including interplanar force constants, the double shell model used by Weber and Bilz to explain the lattice dynamics of transition metal carbides and Nb-Mo alloys, and to a sixth neighbor Born-von Karman model with general forces. For all of these models, we observe that the effective range of the forces decreases only slightly for the $NbD_{.15}$, suggesting that the dynamics are still dominated by long range metallic forces. These general observations are in accord with the results of Powell, Martel and Woods on Nb-Mo alloys. Therefore, we have compared our results for the difference between $NbD_{.15}$ and Nb phonon frequencies in the three symmetry directions with the same quantity for the $Nb_{.85}Mo_{.15}$ alloy measured by Powell *et al.*, as determined from the interplanar force constants given in their paper (this model fits the data very well). This comparison is shown in figure 5. The two results should agree if one could interpret the addition of D to Nb in terms of a simple filling of the electronic band states of pure Nb by the extra electrons of the deuterium, ad the rigid band model works well for the Nb-Mo alloys. From the results in the figure, this is an obvious over-simplification for the $NbD_{.15}$ alloy. There are several possible reasons for the differences shown in figure 5, including the effects of local strain, Nb-H

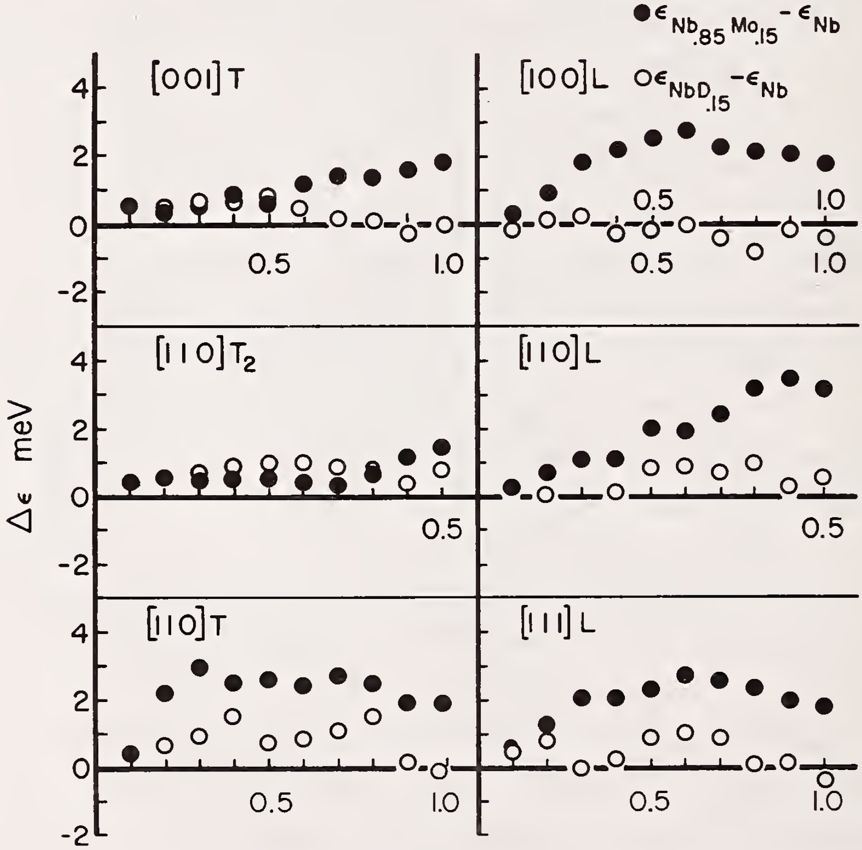

Fig. 5. Differences in phonon energies between pure Nb and $NbD_{0.15}$ and $Nb_{.85}Mo_{.15}$. ($NbD_{0.15}$-Nb) values are at 200°C at the $Nb_{0.85}$ $Mo_{.15}$-Nb) values are at 21°C.

interactions, perturbation of the Nb bands by the interstitial deuterium, lattice parameter changes, D-D interactions or temperature effects ($Nb_{.85}Mo_{.15}$ has only been measured at 293 K). Further analysis will be needed to establish which, if any, of the above factors is dominant.

We are presently preparing higher concentration alloys of NbD_x in order to explore the effects of D-D interactions.

CRYSTAL DYNAMICS, PHASE TRANSITIONS AND ORIENTATIONAL DISORDER IN IONIC AND MOLECULAR SOLIDS

Work has continued on our program to study the details of order-disorder phase transitions, interatomic forces and rotational behavior in prototype crystals by a combination of neutron scattering and optical spectroscopic techniques.

The precise nature of the orientational disorder in the high-temperature phases of broad classes of inorganic and organic materials is not generally well understood, nor is the microscopic basis of the changes in physical and thermodynamic properties associated with these order-disorder transitions. During the past year we have completed the analysis of neutron quasielastic scattering studies of orientational disorder in a single crystal of NH_4Br, and in polycrystalline RbSH in its trigonal phase. This work is also aimed at demonstrating and refining the application of the nqs method to the study of dynamical disorder in such systems. Some progress has also been made in a neutron diffraction study of the alkali hydrosulfides, which is discussed in another section of this report. In addition we have completed the first coherent neutron scattering measurements of the lattice dynamics of an ammonium halide single crystal in the high temperature (fcc) phase and have extended our optical and neutron scattering investigation of alkali cyanide crystals. Much of this work has been carried out in collaboration with Argonne National Laboratory.

1. Alkali Hydrosulfides - J. J. Rush, J. M. Rowe, R. C. Livingston

a. Quasielastic Scattering Study of Trigonal RbSH

We have completed a study of details of the dynamical disorder of the SH ions in the intermediate trigonal phase of RbSH by quasielastic neutron scattering. This is the first neutron scattering study of orientational disorder in a low-temperature phase of such a crystal.

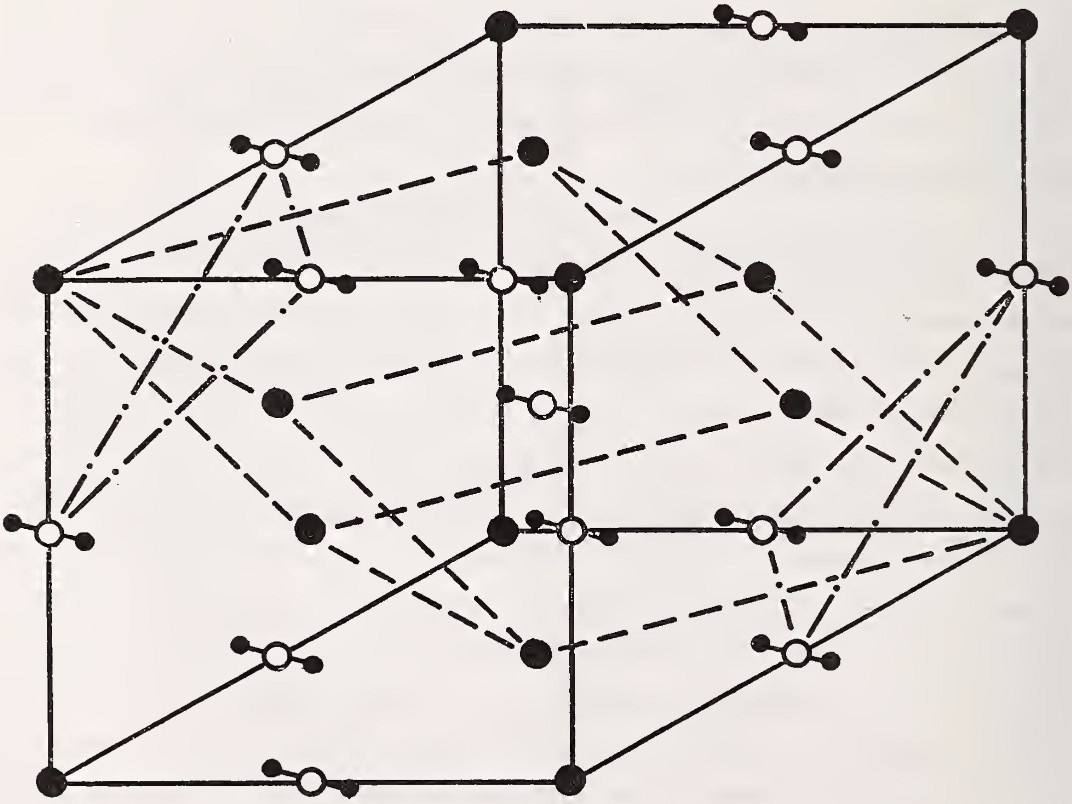

Fig. 1. Composite of the suggested crystal structures of RbSH. In the trigonal phase (dashed lines) one of the body diagonals of the original fcc cubic structure is shortened. Rb, ●; S, ○; 1/2 H, •

The experiments were carried out on a sample of RbSH whose synthesis has been described previously, using a 5 meV neutron beam with an instrumental resolution of 0.25 meV ≡ 0.40 ps^{-1} (FWHM). Time-of-flight neutron spectra were measured for the sample and a blank at 373 and 393 K (below the cubic ↔ trigonal transition at ≈403°K) over a range of scattering angles from 5 to 120°.

The structure of RbSH in both the high temperature fcc phase and the intermediate trigonal phase is shown in Fig. 1. The alignment of $(SH)^-$ ions (along the trigonal axis) shown in the figure is that deduced in our previous neutron diffraction study of isomorphous NaSH. This trigonal axis is closely related to a [111] axis in the fcc phase. For the simple case of instantaneous SH^- ion jump reorientation between only two sites (in this case 180° flips, presumably along the trigonal axis as shown in figure 1, it can be shown that the symmetrized quasielastic scattering function is given by

$$S(Q,\omega) = \ell^{-\alpha Q^2} [C_o(Q)\delta(\omega) + C_1(Q)\,L(\omega)],$$

where α is the mean-square hydrogen vibration amplitude, Q = momentum transfer/ℏ, ω = energy transfer/ℏ, $C_o = [1+ j_o(QR)]/2$ and $C_1 =]1-j_o(QR)]/2$ are the elastic and quasielastic (lorentzian) intensity factors · R = distance between H sites (twice the S-H bond distance = 2.70Å). The single lorentzian component of the predicted scattering law is given by:

$$L(\omega) = \frac{1}{\pi}\,\frac{(2/\tau)}{\omega^2+(2/\tau)^2}$$

where τ is the residence time.

In order to test this two-site jump model we have fitted our experimental results to the above scattering law experssion (broadened by the measured Gaussian resolution functions) as well as to several other models involving random orientation among the [100], [110] or [111] directions in the pseudocubic trigonal structure. Several examples of the experimental scattering laws obtained from our neutron spectra are shown in figure 2, along with the results of the fit to the two-site jump model. In figure 3 the ratio of pure elastic to total intensity in the quasielastic

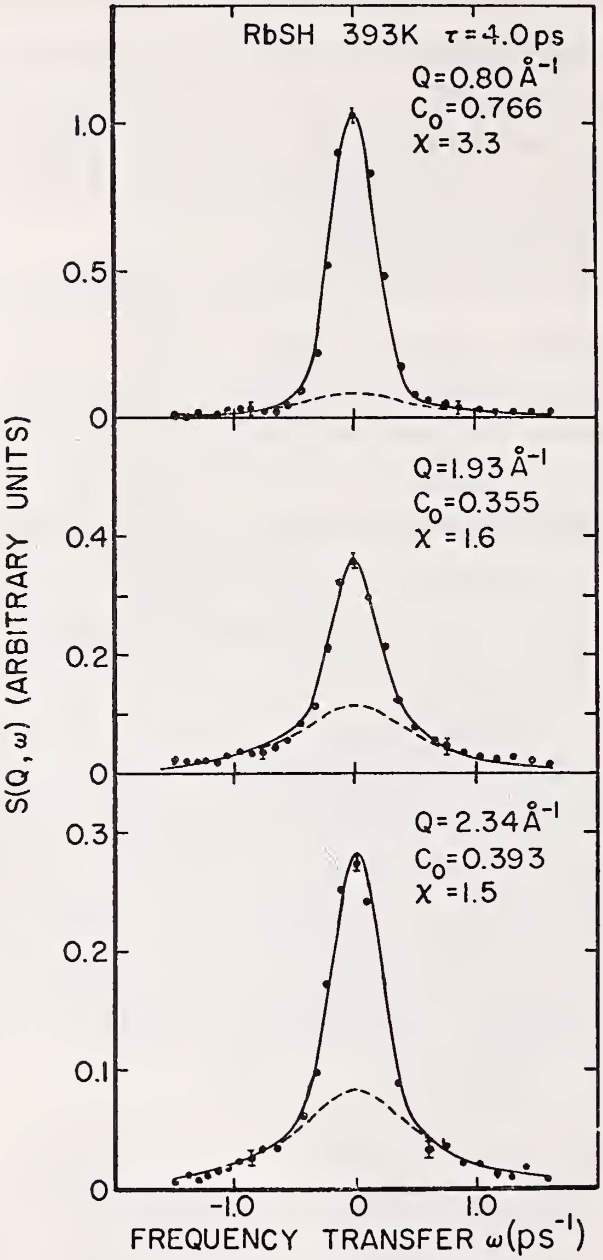

Fig. 2. Examples of the experimental quasielastic peaks for RbSH. The solid curves and elastic intensity factors C_0 represents the best fits to the observed peaks using the two-site jump model. The dashed line curves are the lorentzian components derived from the same fit.

peaks derived from the experimental results are plotted vs. Q. Also shown are the predicted intensities for the two-site model and for an eight site model involving random reorientation among all possible directions along the four body diagonal of the pseudo cubic cell (Fig. 1). From

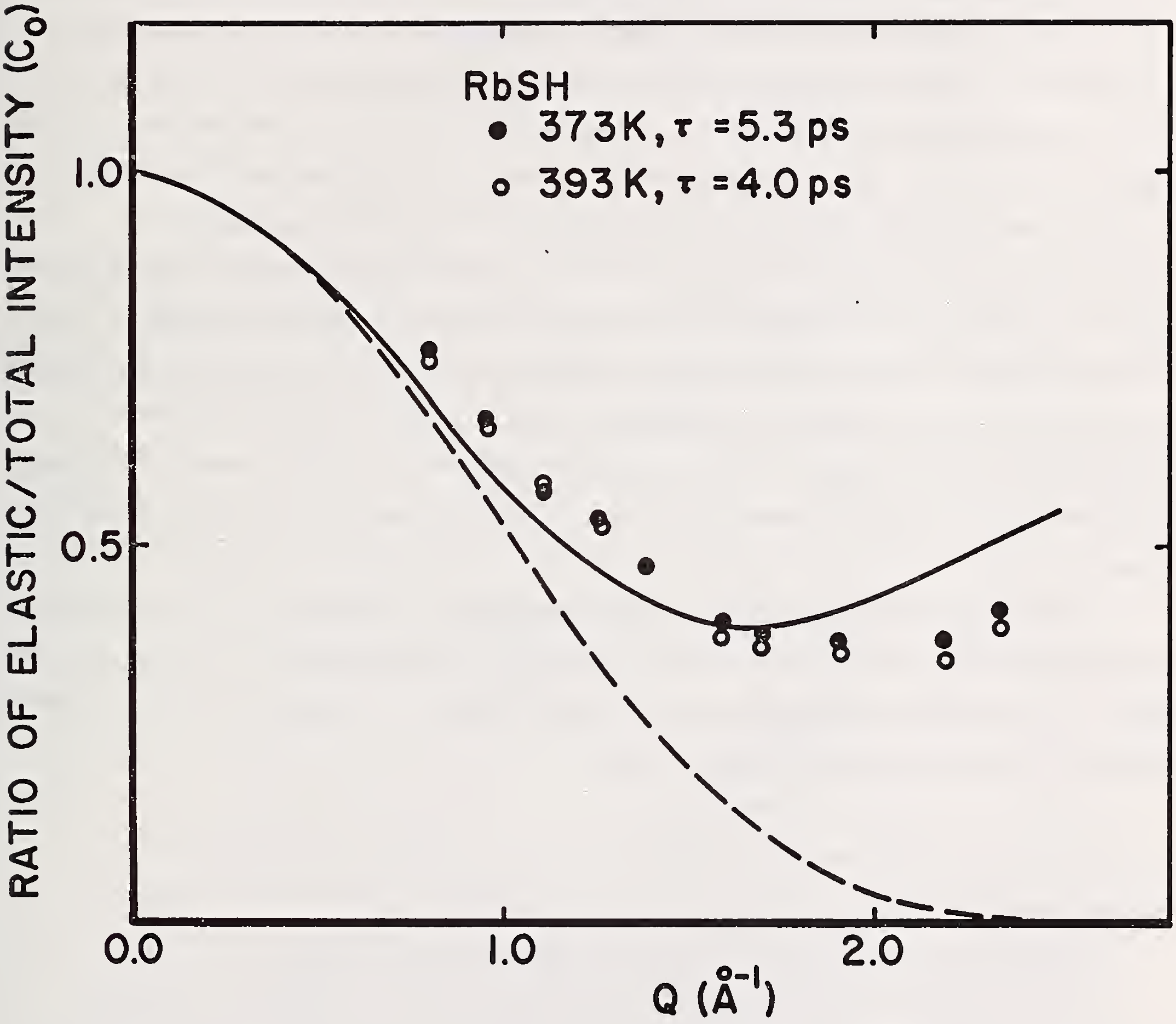

Fig. 3. Pure elastic to total intensity ratios vs. Q of the observed quasielastic peaks for RbSH. Also shown are the predicted behavior for the two-site jump reorientation model (solid line) and an eight-site model involving random reorientation among the eight possible directions along the four body diagonals of the pseudocubic cell (figure 1).

these figures it can be seen that the measured results are in reasonable agreement with the predictions of the two-site model, while the eight position model is obviously in serious disagreement. In fact on other reorientation model (free rotation, rotational diffusion, isotropic planar reorientation or jumps between more than two sites) could predict the observed behavior for the elastic component. The lack of a perfect fit could be due to several factors, including uncertainty in the S-H direction and the possibility of occasional orientation of the ions along other directions in the trigonal cell. The τ values derived from the two-site model fits at 373 and 393 K are 5.3±0.4 and 4.0±0.4 ps, respectively. These values are an order of magnitude larger than those reported previously in our neutron study of the fcc phase of RbSH. Thus a comparison of these and previous results shows that the high temperature transition in this crystal involves a change from a two fold dynamic disorder of the SH ions in the trigonal phase to a much faster ($\tau \sim 0.5$ ps) reorientation among at least six equilibrium orientations in the cubic phase.

From the present results we have also derived values for the hydrogen mean-square amplitudes (α) of 0.17 and $.19 \mathring{A}^2$ at 373 and 393 K, and (assuming a classically activated process) an activation energy for reorientation of 17±4 KJ/mol on the trigonal phase.

2. Ammonium Halides - J. M. Rowe, N. Vagelatos, J. J. Rush, R. C Livingston

a. Quasielastic Scattering in a Single Crystal of NH_4Br

The analysis of the results of a quasielastic neutron scattering study of the mechanism of ammonium ion reorientations in a single crystal of NH_4Br in the disordered CsCl phase has been completed. The aim of this investigation was both to establish the reorientation mechanism and to elucidate the advantage of single crystal measurements in detailed neutron studies of orientational disorder in solids. The potential advantages of single crystal samples in the study of molecular reorientations are similar to those mentioned previously for metal hydride studies, i.e., such measurements avoid the average over crystallite orientation which obscures polycrystalline results and provides a richer, more comprehensive data set as a function of crystal orientation.

It has been established by previous neutron diffraction and NMR studied that in the disordered CsCl phase of NH_4Br (and NH_4Cl and NH_4I) that the NH_4^+ ions in each unit cell are reorienting between two equilibrium positions so that the N-H bonds are directed at random along the [111] directions of the crystal. This dynamic disorder must involve either 90° jumps around the two-fold (C_2) axis of the $(HN_4)^+$ ions or a combination of reorientations around the two and threefold (C_3) axes.

The derivation of neutron cross-section (scattering law) expressions which describe the quasielastic spectra for reorientation around two and (or) three-fold axes of the H_4^+ ions, assuming instantaneous jumps, is straightforward, but will not be presented here. These expressions again predict a quasielastic peak (with both a purely elastic component and a broadened component comprised of a sum of lorentzians) whose shape as a function of $\vec{Q}$ is dependent on the distance between equilibrium proton sites and $\tau_2(\tau_3)$, the average time that a proton stays at a site before jumping to a new site by an NH_4^+ reorientation around a twofold (threefold) axis. Examples of the scattering laws $S_H(\vec{Q},\omega)$ obtained from experimental cross sections measured for a single crystal of NH_4Br (incident E_o = 5 meV, FWHM = 0.26 meV) as a function of momentum ($\vec{Q}$) and energy ($h\omega$) transfer and crystal orientation (ψ) are shown in figure 4. The first approach used in fitting the extensive data set provided by our single-crystal experiment was to fit the measured scattering laws to a model allowing random reorientations around both C_2 and C_3 axes, with associated residence times τ_2 and τ_3. τ_2 and τ_3 were varied using a nonlinear least squares program. The "best fit" in each fitting attempt resulted in τ values with $\tau_3 >> \tau_2$, thus providing strong evidence for a model involving only C_2(90°) reorientations. Further variations in the fitting procedures were tried, including separate fits assuming pure C_2 and C_3 reorientations. The best fit values of τ_2 obtained in this case were

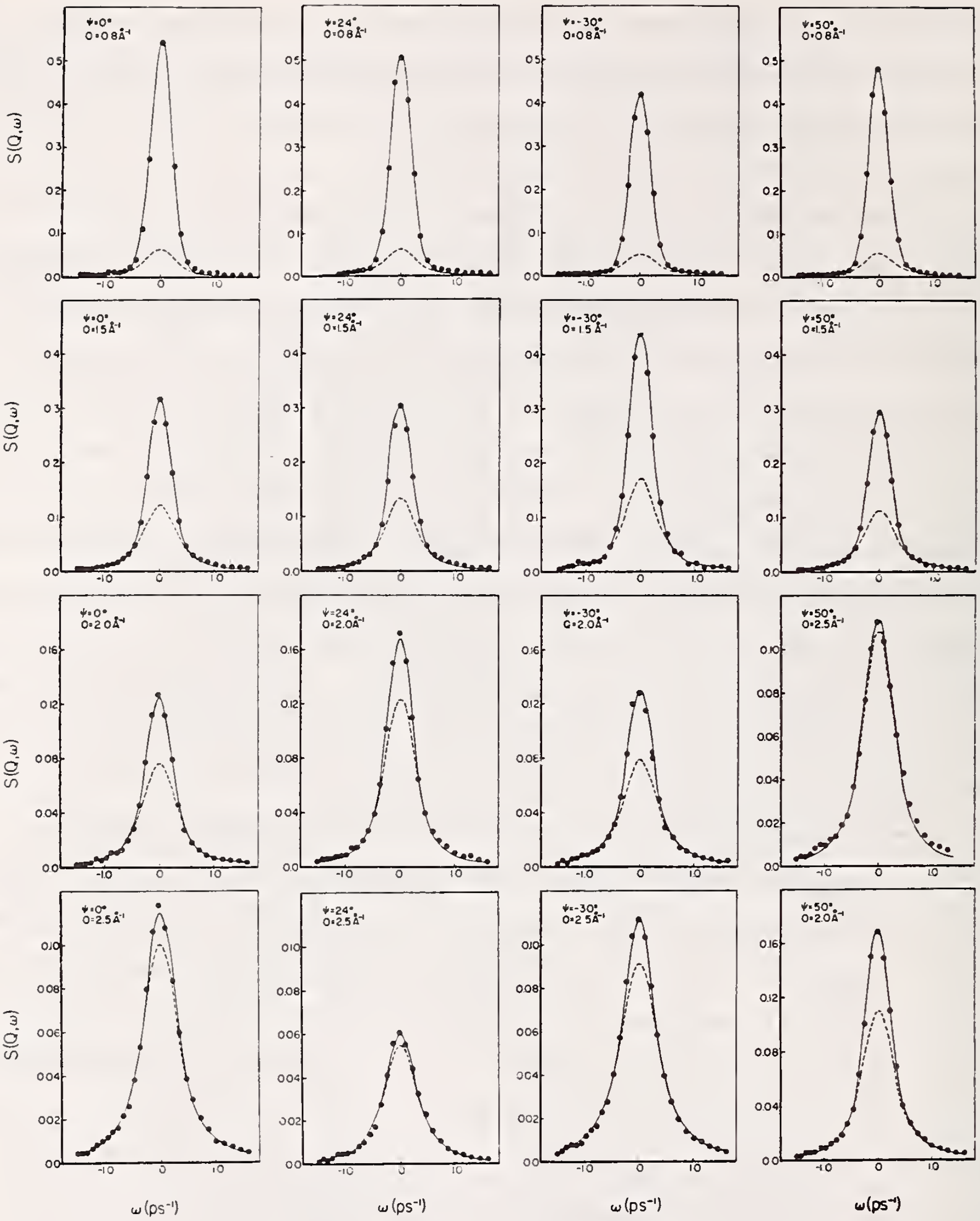

Fig. 4. Examples of the experimental scattering laws plotted vs. ω for NH_4Br at several crystal orientations (ψ) and momentum transfers. The solid lines are the "theoretical" S(Q,ω)'s (resolution-broadened) obtained by fitting to a model assuming reorientations around the C_2 axis, while the dashed lines show the lorentzian components derived from the fit.

equal for all different crystal orientations to within the fitting errors, whereas τ_3 values varied by a factor of two for various orientations--again giving strong evidence for C_2 reorientations. Finally we applied a χ^2 test for statistical significance which showed that the difference in the fits obtained for the C_2 and C_3 models was significant at the ∿0.5% level.

The extensive fitting and analysis outlined above shows conclusively that the dominent reorientation mechanism in the CsCl phase of NH_4Br is by instantaneous 90° jumps about the C_2 axes, although a small ad-mixture of C_3 jumps cannot be ruled out. The τ_2 value derived from the fitting procedure is 3.2±0.4 ps at 373 K, which is consistent with the correlation time of ∿2.5 ps predicted by extrapolation of NMR results. It should be particularly noted that the statistical reliability of this result is directly due to the large amount of data available for testing the hypotheses, and that this in turn shows that single crystal samples are essential (except for very simple cases) for the precise determination of reorientation mechanisms using neutron quasielastic scattering.

Our measurements and analyses will next be extended to a single crystal study of NH_4I in its high temperature fcc phase. Little detailed information is available on the more complex orientational disorder in the phase of the ammonium halides and in analogous phases of a wide range of molecular crystals.

b. Lattice Dynamics of Ammonium Iodide

As a result of our continuing interest in the lattice dynamics of orientationally disordered crystals and in view of the difficulties encountered in the alkali cyanide measurements, a study of the phonon dispersion relations in deuteroammonium iodide has been undertaken. Additional interest was generated by the fact that ammonium iodide has a different crystal structure at room temperature than the ammonium halides studied thus far by coherent inelastic neutron scattering[1,2,3]. At room temperature both NH_4Cl and NH_4Br (ND_4Cl and ND_4Br) crystallize with the CsCl structure, where it is relatively easy to visualize the possible orientations of the tetrahedral $NH_4^+(ND_4^+)$ ions in the CsCl lattice sites[4]. Under the same conditions NH_4I (ND_4I) has the NaCl structure where NH_4^+ (ND_4^+) ions occupy sites of octahedral symmetry and their orientations are not at all obvious[5].

Single crystals of ND_4I (up to $2x2x1cm^3$) suitable for inelastic neutron scattering measurements have been grown by slow evaporation under controlled conditions from D_2O solutions of deuterated ammonium iodide doped with urea. Deuteration of the NH_4I + urea was accomplished by several H-D exchanges consisting of dissolving the hydrogenous or partly deuterated granular mixture in D_2O, allowing the H-D exchange to reach equilibrium, and evaporating the solvent. 6-7 such exchanges resulted in approximately 99% deuteration of the ammonium iodide-urea mixture.

Dispersion curves for phonons propagating in the high symmetry directions in ND_4I at room temperature have been measured by coherent inelastic neutron scattering using the triple axis spectrometer. The results of these measurements are shown in figure 5. Acoustic phonons were well defined, the uncertainties in individual frequencies generally being 1-3%. Optic phonons were considerably more difficult to measure because of the necessarily worse resolution conditions under which these measurements were performed and the relatively low signal to background ratio due to the deuterium incoherent and multiphonon "background." This difficulty is reflected in the larger errors assigned to these phonons. Intensity and resolution limitations precluded the observation of the highest frequency LO phonons, (i.e. near the Brillouin zone center) and the entire LO[111] branch. No attempt was made to investigate the rotational or librational modes by the triple axis method. It is interesting, however, that optical translatory modes as well as acoustic modes near the zone boundary were observed for ND_4I which were difficult or impossible to observe in the equivalent phase of the alkali cyanide crystals.

At the present time, the rotational modes are being studied by the time-of-flight technique. The triple axis and time-of-flight data will be analyzed in terms of theoretical models, e.g. the shell model, which have been previously used to analyze the phonon dispersion relations of other ammonium halides. We also intend to study the phonon dispersion curves of ND$_4$I temperatures close to the NaCl→CsCl phase transition. In addition, the neutron quasielastic scattering from this crystal will be measured in order to obtain information about the orientational disorder of ND$_4^+$ ions in the fcc lattice and the rate of reorientation between energetically equivalent orientations.

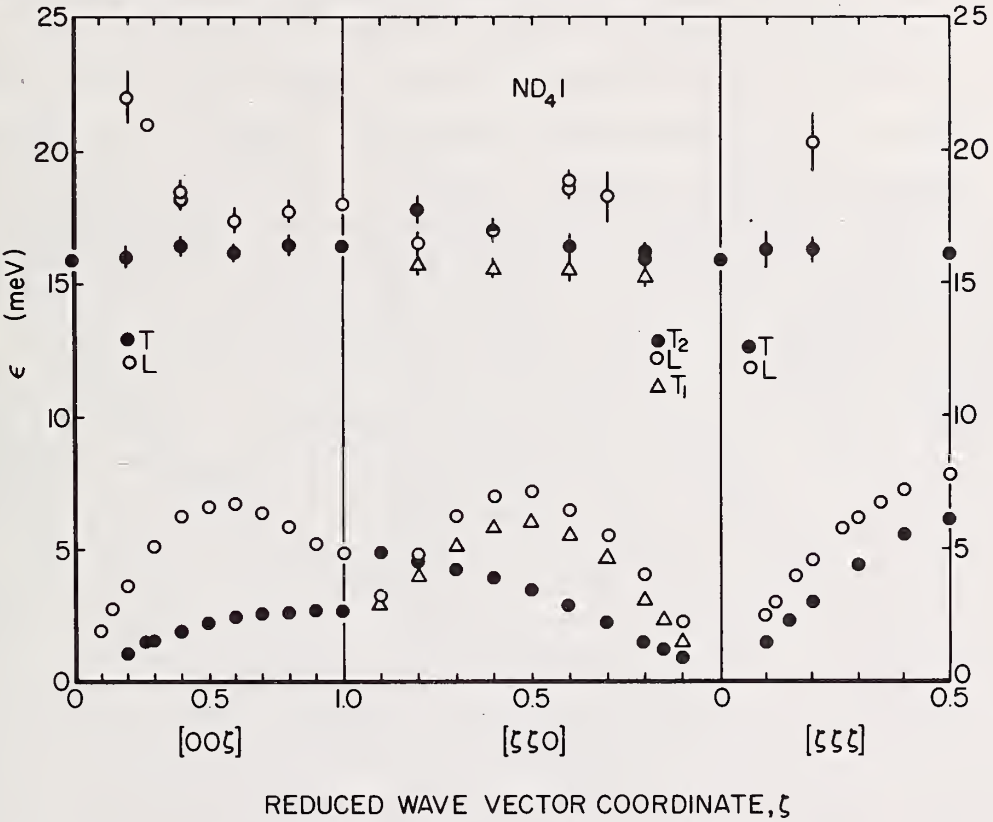

Fig. 5. Phonon dispersion curves measured for ND$_4$I at 293°K.

---

[1] Smith, H. G., J. G. Traylor, W. Reichardt, *Phys. Rev.* 181 1218 (1969).

[2] Teh, H. C., B. N. Brockhouse, *Phys. Rev.* 8B, 3928 (1973).

[3] Yamada, Y., Y. Noda, J. D. Axe, G. Shirane, *Phys. Rev.* 9B 4429 (1974).

[4] Levy, H. A., S. W. Peterson, *J. Chem. Phys.* 21, 366 (1953).

[5] Levy, H. A., S. W. Peterson, *J. Chem. Phys.* 75, 1536 (1953).

3. Lattice Dynamics of Alkali Cyanides - J. M. Rowe, J. J. Rush,
N. Vagelatos

New results have been obtained in investigation of phonons in the orientationally disordered room temperature phase (NaCl structure) of KCN and NaCN in collaboration with D. L. Price of Argonne National Laboratory. In this study use has been made of both the coherent inelastic neutron scattering and infrared reflection techniques.

The neutron measurements, mainly of phonons propagating in the [001] symmetry direction, were performed on large single crystal samples prepared at ANL. Well defined neutron groups were observed corresponding to low frequency acoustic phonons, i.e. near the center (Γ point) of the Brillouin zone. They became progressively less well defined away from the zone center and especially near the zone boundary. In general, it appears that phonons are better defined in NaCN. No optic phonons were definitively assigned in either crystal by the neutron technique.

Infrared reflection spectra for NaCN and KCN were also measured from polycrystalline pellets, using the IMR Central Raman-IR facility. As is generally the case, the observed maximum reflectance was sensitive to the pellet surface. The KCN spectrum consisted of a single well defined band which, when analyzed in terms of a single classical damped oscillator model, yielded: $TO(\Gamma)=137\pm5cm^{-1}$ and $LO(\Gamma)=225\pm20cm^{-1}$. No clear evidence of a TO mode in the above frequency region was observable by the neutron technique. The NaCN reflection spectra were not as intense or as well defined as those of KCN and similar analysis was not performed.

The apparent reasons for the difficulties encountered in the inelastic neutron scattering measurements are the very low signal to background ratio, the low Debye-Waller factor (e^{-2W}), and the coupling between the rotations and the translational modes (see also the summary of theoretical work on these systems by R. Casella in this report). The background was high because of the incoherent scattering (NaCN), multiphonon and quasielastic contributions. The Debye-Waller factor is low because of the large thermal displacements of both the metal and CN^- ions, which limits the Q-space accessible for the measurements. The rotationtranslation coupling shortens the phonon lifetimes and thus broadens the scattered neutron groups. Such effects can also be expected to influence the dynamics of a wide variety of other complex crystals exhibiting orientational disorder. Any one of the above factors could make the observation of phonons difficult. All three appear to contribute in the NaCN, KCN measurememts. Further analysis and measurements at lower temperatures KCN are planned.

4. Lattice Dynamics (Other)

a. CdTe - J. M. Rowe

In collaboration with D. L. Price, Argonne National Laboratory, Ken Zanio, Hughes Research Corporation and R. M. Nicklow, Oak Ridge National Laboratory, we have measured the lattice dynamics of a single crystal of CdTe. Because of the large neutron absorption of the naturally occurring isotopic mixture of Cd, the crystal was specially grown from a sample enriched in ^{114}Cd, a relatively non-absorbing isotope. Even after this enrichment, the absorption cross-section of the sample was more than 100 barns for thermal neutrons, so that the measurements were quite difficult and could only have been done at a very high flux reactor (the HFIR, ORNL). The results for CdTe complete the isolectronic series α-Sn, InSb and CdTe (AgI cannot be obtained in the zincblende structure), allowing a detailed study of the effects of increasing ionicity and band gap with all other parameters nearly constant. (Note that α-Sn has a zero direct band gap.) It is hoped that the availability of such complete and detailed results will stimulate renewed theoretical efforts to understand the lattice dynamics of zincblende semiconductors on a sound microscopic basis.

SYMMETRY ANALYSES OF NEUTRON SCATTERING IN CRYSTALS--APPLICATION OF TIME-REVERSAL SYMMETRY

R. C. Casella

It is well known that the number of independent parameters in the phonon dynamical matrix $C(\vec{k})$ can be reduced by accounting for crystal symmetry. Moreover, although time reversal symmetry T is known to be broken in certain weak mesonic decays[1], no evidence exists which would invalidate this principle in the electromagnetic interactions responsible for chemical binding. Hence, we may assume its validity when treating the phonon spectrum of solids as determined by neutron scattering.

Based upon the classic Wigner-Herring work in this field, I have derived an algorithm for computing the number of independent real parameters in $C(\vec{k})$ for an arbitrary space group when all space-time symmetries are taken into account.

The application of T invariance to phonons has been discussed by Maradudin and Vosko and recently by Warren[2]. My interest was motivated by discussions with M. Rowe who has indicated that programs for reducing the dynamical matrix, which have as their basis the Warren analysis, appear to contain inherent inconsistencies. I have taken an independent approach from that of Maradudin-Vosko and of Warren, opting against increasing the little group $G(\vec{k})$ to $G(\vec{k},-\vec{k})$ and then doubling $G(\vec{k},-\vec{k})$ to find the so-called co-representations for the antiunitary operators including time reversal. Instead, the method developed applies directly to the little group representations $D^{\vec{k}}(B)$ where B is a (unitary) element of the little group. Moreover, "mutiplier representations" are introduced *only* in connection with applying the Wigner-Herring test, thereby simplifying the analysis considerably.

The new algorithm can also be applied to crystals in the rigid-molecule approximation which has been treated group theoretically by myself and S. Trevino and recently applied to $NaNO_3$ by S. Trevino, H. Prask, and myself.

In collaboration with M. Rowe and S. Trevino, it is planned to apply the algorithm to specific examples.

---

[1] R. C. Casella, *Phys. Rev. Letters* 21, 1128 (1968); 22, 554 (1969).

[2] J. L. Warren, *Phys. Rev.* B9, 3603 (1974).

RIGID ROTATOR MODEL FOR KCN, NaCN

R. C. Casella

An analysis of a system of heteronuclear diatomic "free rotators" with centers of mass lying on a vibrating crystal lattice has been made. The analysis includes a fundamental field-theoretic deviation of the Debye-Waller factor within the context of the model. Expressions for the differential cross sections for elastic and inelastic neutron scattering have been obtained within the approximations of rotational transitions involving $\Delta J=\pm 1$ only and $\Delta J=\pm 1, \pm 2$ only. Line-shape factors are found which are similar to those for homonuclear diatomic liquids given by Sears.

It is planned to extend the analysis to include an additional point atom and compare the results with the neutron data of J. Rush and M. Rowe for the NaCN and KCN systems. Moreover, it may be interesting to apply our general group theoretical analysis[1] of neutron scattering from librating rigid molecules in a crystal to those systems and to examine how the structure function $F^r(\vec{k})$ varies with $\vec{k}$ along the (100) direction. This may be particularly interesting for the KCN system where neutron scattering does not pick up the optical branch (although infra red measurements of N. Vagelatos do) and the acoustics branches lose strength as $|\vec{k}|$ increases along that direction.

---

[1] R. C. Casella and S. F. Trevino, *Phys. Rev.* B6, 4533 (1972).

NEUTRON DIFFRACTION STUDY OF NaSH AND RbSH

A. Santoro and J. J. Rush

Sodium and rubidium hydrosulfides, NaSH and RbSH, exist in several crystal modifications. Below the melting point these compounds are both cubic (phase I). When the temperature is lowered, they undergo a first order transition (at ∿358 K and ∿403 K for NaSH and RbSH, respectively) into a trigonal phase (phase II) and a second transition (∿113 K and ∿123 K, respectively) into a modification (phase III) whose symmetry has not yet been determined[1].

Space group and heavy atoms positions for phases I and II have been determined by X-ray diffraction for both compounds[2]. Neutron diffraction[3] and inelastic scattering studies[4] on NaSH have shown that the SH^- ions in the cubic phase are reorienting between at least six quasi-equilibrium positions, and that in the trigonal phase they are aligned along the three-fold axis with equal probability of finding them pointing in either direction.

The x-ray results show that the heavy atoms positions in the trigonal phases of RbSH and NaSH are analogous. So far, however, the location of the hydrogen atom has not been crystallographically determined in the case of RbSH. The present neutron diffraction study was undertaken to complete the structural analysis of the trigonal modification of RbSH and to determine the structure of phase III for both compounds. In what follows we give preliminary results of our investigation.

---

[1] Rush, J. J., R. C. Livingston, G. J. Rosasco, Solid State Com., 13, 159-162 (1973).

[2] West, C. D., Zeit. Krist., 88, 97-115 (1934).

[3] Schroeder, L. W., L. A. deGraaf, and J. J. Rush, Chem. Phys. 55, 5363-5369.

[4] Rowe, J. M., R. C. Livingston and J. J. Rush., J. Chem. Phys. 59, 6652 (1973); J. J. Rush, L. A. deGraaf, and R. C. Livingston, J. Chem. Phys., 58, 1438 (1973).

1. Trigonal Phase of RbSH

The neutron diffraction powder pattern of trigonal RbSH can be readily indexed on the cell found by x-ray (a=4.525Å, α=69.3°). Of the eight lines observed in the pattern, only three are completely free from interferences if one assumes the space group $R\bar{3}m$. With such limited number of data it is only possible to test if reasonable models for the structure are consistent with the observed intensities. As refining of the thermal and positional parameters is clearly impossible, reasonable values for these parameters must be assumed. (In our case, for example, the SH^- band length was approximately the same as in NaSH, and the thermal parameters used were derived from the previous neutron scattering work.)

As for the case of NaSH, three models were considered and the comparison between observed and calculated intensities is shown in Table I for each model. In agreement with the results found for NaSH, the structure favored is the one with the SH^- ions lying along the trigonal axis and pointing with equal probability in either direction (model A).

Structures in which the hydrogen atoms are completely ordered are possible. One possibility is to orient all the SH^- ions in the same direction along the trigonal axis. This model, however, can be excluded because electrostatic interactions favor the ordering of these ions in opposite directions along the jacent trigonal axes. Other ordered structures satisfying this correlation of orientation can also be ruled out, as they would be based on unit cells larger than the one derived by x-rays and therefore, would give more diffraction lines than are actually observed.

The proposed structure of the trigonal phase of RbSH can be confirmed and better thermal and positional parameters can be obtained, by carrying out a total profile analysis of our neutron diffraction pattern*. Work in this direction is planned in the near future.

---

* This method does not make use of the individual intensities of the Bragg reflections, but used the entire shape of the powder pattern to decide between various models and to refine structural parameters. The

2. Studies on Phase III of RbSH

All the diffraction lines of phase II are present in the powder pattern of phase III, practically in the same angular positions and approximately with the same intensities. However, the pattern of phase III contains a number of extra lines. This observation strongly suggests that the structure of phase III is based on a superlattice of the trigonal lattice of phase II. This interpretation of the powder pattern is consistent with the hypothesis that the transition from phase III is associated with an ordering of the hydrogen atoms which are "disordered" between the positions uuu and $\bar{u}\bar{u}\bar{u}$ in the trigonal structure.

The smallest superlattice which indexes the powder pattern is monoclinic (a=4.52Å, b=5.14Å, c=6.85Å, β=101.2°) and it is obtained from the trigonal cell by means of the transformation $100/01\bar{1}/\bar{1}11$. There are two formula units of RbSH per unit cell.

The most reasonable model for the structure of this phase appeared to be the one with the two SH^- ions contained in the monoclinic cell still lying along the old trigonal axis, but pointing in opposite directions*. This model, however, gave results inconsistent with the experimental results. Specifically, the proposed structure predicts observable intensity for reflections which are experimentally unobserved. Attempts to orient the SH^- ions away from the trigonal axis proved equally unsuccessful. This and other inconsistencies between observed and calculated intensities may be due to shifts in the relative positions of the rubidium and sulfur atoms, or to incorrect assignment of the hydrogen positions, or to both factors.

---

*The positional parameters for this structure, referred to the monoclinic cell, are:

Rb : 1/4,1/4,1/4; 3/4,3/4,3/4
S : 1/4,1/4,3/4; 3/4,3/4,1/4
H : 1/4-2u, 1/4, 3/4-u; 3/4+2u, 3/4, 1/4+u

---

number of parameters which can be refined with this technique is comparable to that normally encountered in a single-crystal studies of moderately complex structures.

Further work planned for this structure comprise - (i) A low-temperature x-ray study which should give the positional parameters of the heavy atoms without ambiguity; (ii) The use of the total profile analysis of the neutron diffraction pattern for deciding between structures with more complex configuations of the SH^- ions. This part of our study involves the derivation of crystallographic methods for generating systematically all structural models consistent with superlattices of multiplicity higher than 2 (i.e. with unit cells containing more than 2 formula units of RbSH).

Table 1. Observed and Calculated Intensities for the Trigonal Modification (Phase II) of RbSH

HKL	I_{obs}	Model A	Model B	Model C
100	40.7	39.9	37.5	31.5
111 + 110	57.4	52.6	50.9	60.6
$1\bar{1}0$	16.1	13.9	26.2	40.2
$211 + 11\bar{1}$	41.6	42.9	30.6	21.4
210 + 200	18.7	18.4	21.2	28.4
221	unobs.	.7	1.0	4.8
$222 + 220 + 2\bar{1}0$	22.0	26.6	21.5	18.3
$21\bar{1}$	17.3	16.1	21.1	23.2
311	VW	.6	1.7	1.3
$2\bar{1}\bar{1}$	VW	4.1	8.3	7.3
321 + 310	25.2	29.2	23.6	30.1
$2\bar{2}0$	unobs.	2.8	4.9	5.5
332	VW	2.5	3.9	3.6
$3\bar{1}0$	VW	6.3	6.0	7.0
		R= 7.9%	R=16.5%	R=33.8%

For all models - S : 000 ; Rb : 1/2 1/2 1/2

Model A - 1/2H : uuu, $\bar{u}\bar{u}\bar{u}$; u=0.118

Model B - 1/6H ; $00\overset{\pm}{z}$, $0\overset{\pm}{z}0$, $\overset{\pm}{z}00$; z=0.267

Model C - 1/6H : $\overset{\pm}{x}\overset{\pm}{x}0$, $\overset{\pm}{x}0\overset{\pm}{x}$, $0\overset{\pm}{x}\overset{\pm}{x}$; z=0.235

$\langle U^2\rangle_H = 0.10\,\text{Å}^2$; $\langle U^2\rangle_S = 0.05\,\text{Å}^2$; $\langle U^2\rangle_{Rb} = 0.035\,\text{Å}^2$

DYNAMICS IN SIMPLE LIQUIDS

J. M. Rowe

As discussed in last year's report (NBS Technical Note 813), the dynamical behavior of simple liquids is at present poorly understood. Our program addresses this problem by obtaining accurate, detailed measurements of the scattering function of various simple liquids in absolute, normalized form which can then be compared to both molecular dynamics and model calculations. We are also exploring the transition from the well-understood hydrodynamic regime (very long wavelength fluctuations) to the short wavelength high-frequency regime. Some recent results for liquid rubidium, one of the simplest liquid metals are discussed below. Future work will extend the measurements to polyvalent metals and alloys.

In collaboration with J. R. D. Copley and A. Rohman, Argonne National Laboratory, the scattering function of liquid rubidium at 313K (just above the melting point) have been measured for wave-vectors between 0.3 and 5.5 $\mathring{A}^{-1}$ and compared to molecular dynamics (MD) results. The MD calculations were done for 500 atoms interacting with an effective two body potential determined from the phonon dispersion relations of the solid. As pointed out in last year's report, we were able to clearly observe evidence of propagating collective excitations for wavelengths as short as 6Å, which is a typical interatomic spacing in liquid Rb. For shorter wavelengths, no evidence of such propagating collective modes was observed. This is in complete contrast to the results for liquid argon, when no structure was observed for wavelengths as long as 10Å. The molecular dynamics calculations are in very good agreement with the details of the measurements although minor discrepancies remain. In particular, the observed propagating mode is reproduced by the MD calculation. This is shown in figure 1, where the frequency of the observed mode is plotted as points for the neutron scattering results and a line for the MD results (Note that the wave-vector transfer $\kappa=2\pi$/wavelength). The agreement at shorter wavelengths is shown in Fig. 2 by a direct

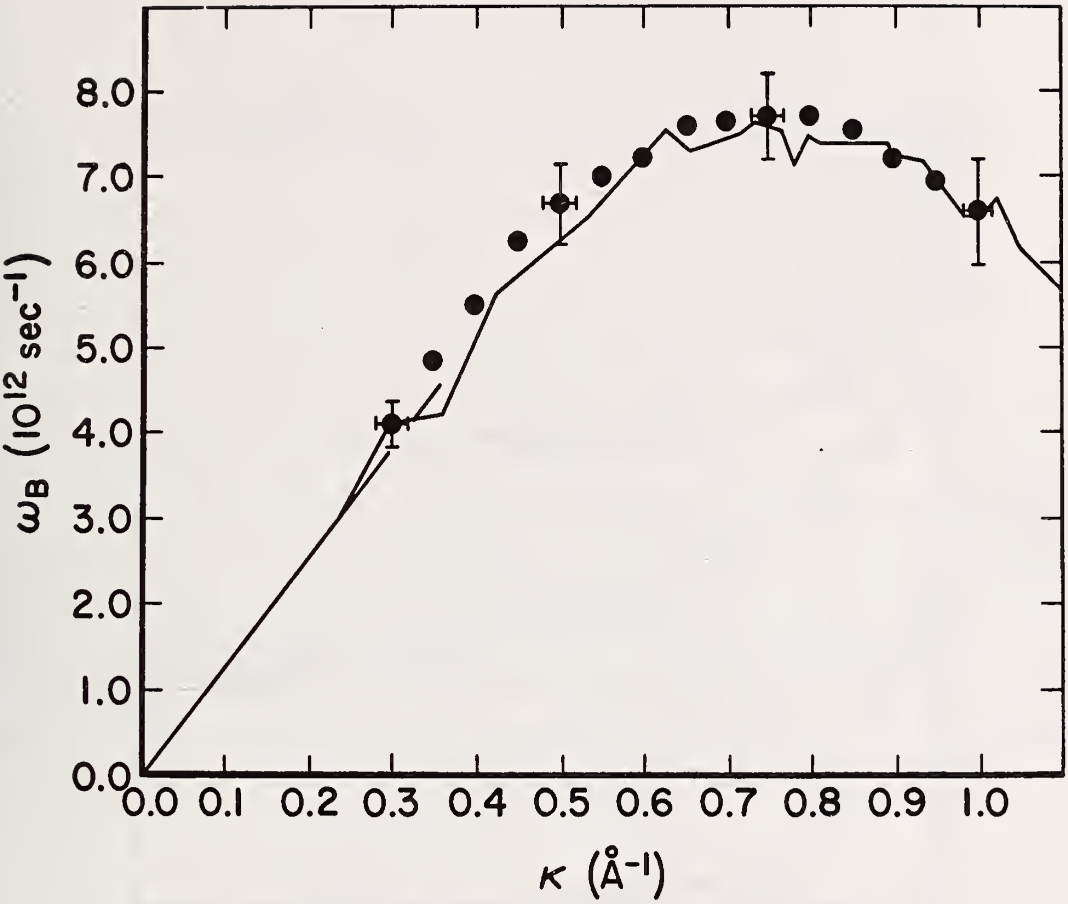

Fig. 1. A comparison of the frequency of propagating collective excitations in liquid rubidium at 313K as measured by neutron scattering (●) and as calculated by molecular dynamics (—).

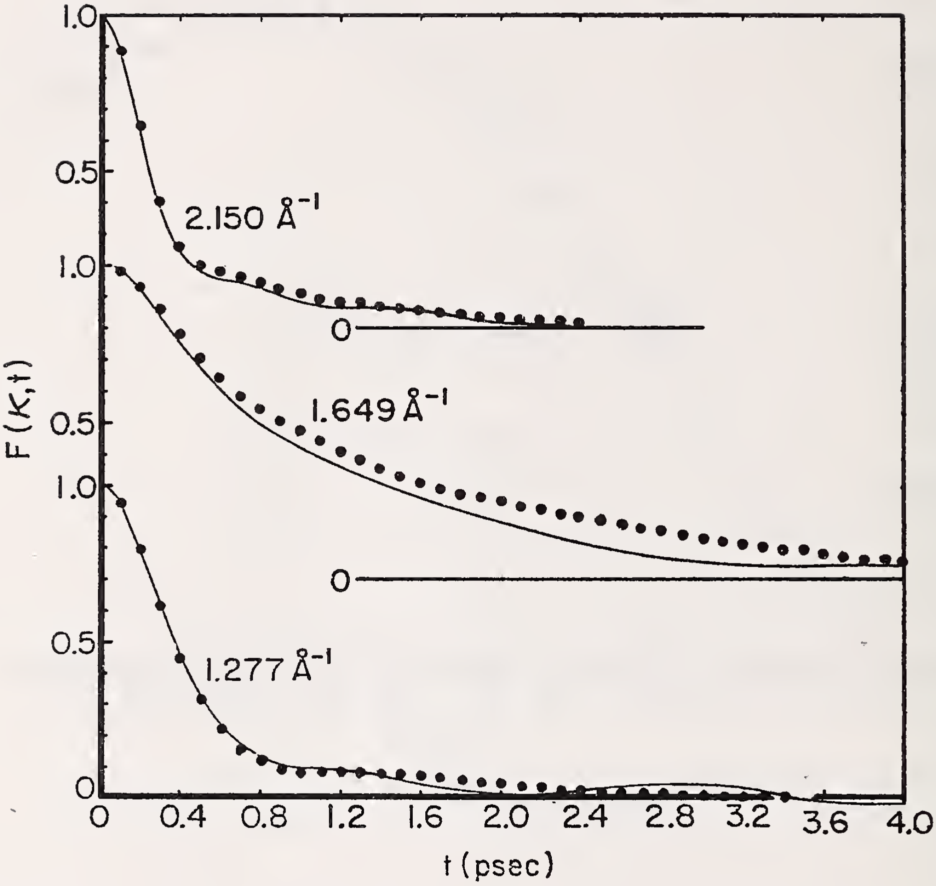

Fig. 2. A comparison of the time dependent pair correlation function of liquid rubidium at 313K as measured by neutron scattering (●) and as calculated by molecular dynamics (—).

comparison of the observed and calculated scattering function for selected values of the wave-vector transfer. The comparison is given in terms of a time-dependent correlation function simply for computational reasons.

This result, which is the most detailed comparison of experimental results to MD calculations yet attempted, has strong implications for the theory of the dynamics of simple liquids and for the reliability of MD simulations. First, it establishes clearly that one can obtain useful information about the potentials of interaction from the liquid dynamics (a point not well established earlier). Second, it shows that at least for Rb, the same potential can be used to explain both the liquid and solid dynamics to a reasonable approximation. Third, it shows that collective excitations can persist to very short wavelengths for some potentials. Fourth, it shows that the MD simulations can reproduce the dynamics of liquids even for wavelengths comparable to the size of the box for which periodic boundary conditions are applied--a point which has been the subject of much debate. Finally, more detailed investigations of other potentials will allow us to establish those features of the potential which are most sensitive to the dynamics and thus help in the testing of various proposed forms for this potential.

INTERCOMPARISON OF NEUTRON DIFFRACTOMETERS

V. W. Myers

The Neutron Diffraction Commission of the International Union of Crystallography has been involved in a program for the comparison of the available monochromatic neutron flux at various diffraction instruments around the world. NBS has collaborated in this program since its inception in 1970. During the past year, gold foils were activated in the diffracted beam of the NBSR BT-1 diffractometer and then counted. H. Alperin and L. Rauber measured the scattering from an Al_2O_3 powder specimen on this instrument also. The results for the gold foils' activities and the powder pattern where then communicated to A. F. Anderson (Institutt for Atomenergi, Kjeller, Norway). Anderson and

Sabine (Australian AEC) have issued a report describing the results of this study. They show, for example, the flux at sample position versus core flux and the flux ratio versus resolution. The NBSR BT-1 diffractometer results compare favorably with those of spectrometers at other high flux research reactors. This intercomparison study is essentially completed.

THERMAL NEUTRON FLUX MEASUREMENTS

V. W. Myers and M. Ganoczy

The data are being analyzed for the manganese sulfate bath which was used for measuring the absolute thermal neutron intensity of a beam. Boron loaded cobalt glass beads were activated in the known thermal flux and then for calibrating a NaI well detector and its associated counting system. This technique provides for the measurement of an unknown thermal flux by activating a bead in the flux and then counting it in the calibrated system.

REACTOR RADIATION DIVISION PROGRAMS

NEUTRON RADIOGRAPHY

Harold Berger, Vernon W. Myers and Martin Ganozy

A program in neutron radiography[1,2] was initiated in FY 1974. The program is expected to provide leadership in the development of standards for this expanding method of nondestructive evaluation (NDE). In addition, the neutron radiographic facilities will be used to perform application studies for NBS and other agencies and to develop techniques to make neutron radiography more useful to industry.

A neutron beam facility has been set up at the NBS Reactor thermal column. Beam characteristics can be changed in terms of beam intensity and divergence. A maximum thermal neutron intensity of $1.5x10^{7} n/cm^{2}\cdot sec$ is available at a beam divergence ratio of 30 for L/D (L is the distance from the aperture to the radiographic location, D is the aperture diameter from which the neutron beam diverges). The intensity can be decreased and the beam divergence improved from those values. Typical beam characteristics are as follows:

Thermal Neutron intensity	$2x10^{6} n/cm^{2}\cdot s$
Coverage	17.5 cm diam
Divergence	L/D = 90
Cadmium ration (gold)	600
Gamma intensity	1 R/hr.
Neutron to Gamma ratio	$6x10^{6} n/cm^{2}$ per mR

A diagram of the beam facility is shown in figure 1. Exposures may be controlled by raising and lowering either the Boral Curtain or the external shutter.

The beam facility has been used to investigate several image detection systems. Two of these are particularly useful for initial alignment radiographs and have been used to aid diffraction experiments by showing crystal placement inside furnaces and cryostats. One method utilizes Polaroid TLX film(a). An exposure of 7 seconds provides a result showing high contrast resolution better than 125 μm. The Polaroid film can be ready for viewing after 45 seconds development time. A radiographic paper, Kodak(a) type 600, has also been used with even better results (resolution of 25 μm). An exposure time of 50 seconds provides a good result and can be viewed after only 10 seconds development time. Both detectors, used with scintillator converter screens, provide a result that can be viewed within about a minute. An example of a radiograph taken on paper is shown in figure 2.

A real-time detection system, providing images at the normal television frame rate of 30 frames/s has also been investigated(a,b). The image intensifier system, normally used for x-ray detection[3], also responds to thermal neutrons because of the use of a new x-ray fluorescent screen containing the high neutron cross section material gadolinium[4]. The gadolinium oxysulfide screen used for these tests was about 0.5 mm thick and attenuated the thermal neutron beam 75 percent. Tests of spatial resolution, contrast, and speed were conducted over a thermal neutron intensity from $2.5\mathrm{x}10^3$ to $6\mathrm{x}10^6 \mathrm{n/cm}^2 \cdot \mathrm{s}$.

Motion response varied over the range of intensities. High contrast objects such as cadmium could be followed without image blur at linear velocities of 2m/min at the high intensity. At an intensity of $6\mathrm{x}10^4 \mathrm{n/cm}^2 \cdot \mathrm{s}$ any motion blurred the image.

High contrast resolution varied from 0.5 mm at the high intensity to bare discernment of gross objects (5 cm diam or larger) at the lower intensity. In terms of contrast, a 0.4 mm thick plastic step could be observed through 1.27 cm of steel at the high intensity. The plastic thickness required for observation increased as intensity was lowered. For example, at $2.6\mathrm{x}10^5 \mathrm{n/cm}^2 \cdot \mathrm{s}$ a plastic thickness of 0.5 mm was

---

(a) The use of proprietary names is for identification purposes only and does not constitute an endorsement of any particular product or apparatus.

(b) Tests performed in collaboration with the Old Delft Corporation of America, Fairfax, VA, using their image intensifier Decalix SI-12 1/2.

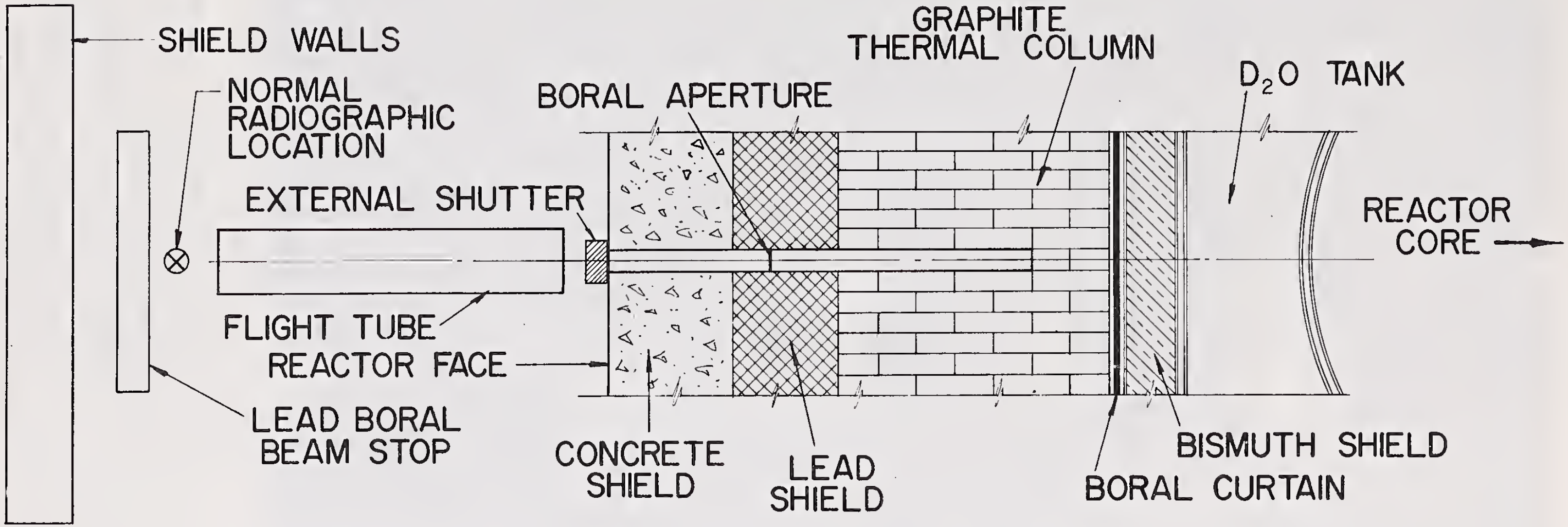

Fig. 1 A diagram of the neutron radiography facility at the NBSR thermal column.

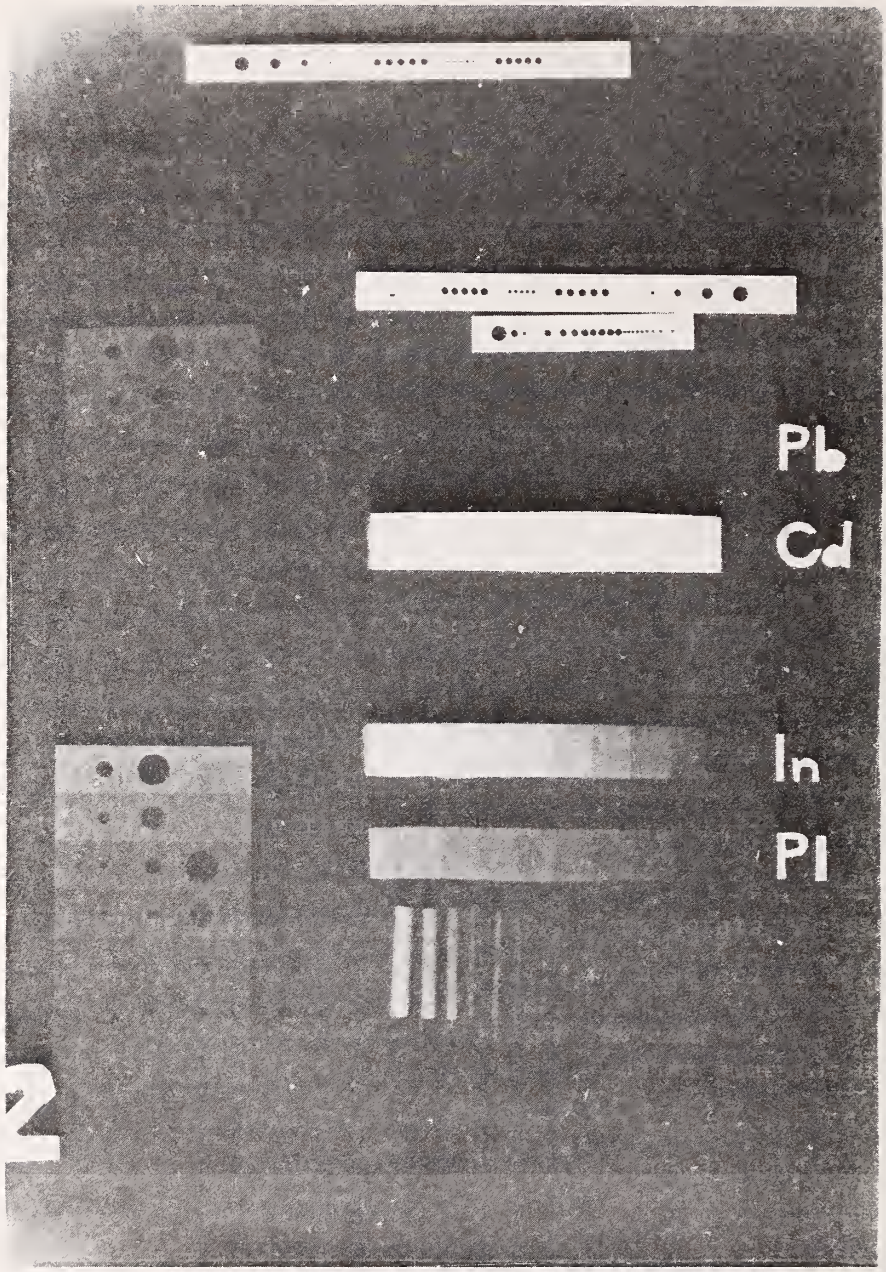

Fig. 2. A neutron radiograph of a test piece, obtained on radiographic paper. The high contrast rectangular images are of cadmium, hole sizes vary from 2 mm to 0.25 mm dia. Closest hole spacing is 25 μm. The stepped wedges on the right are of lead, cadmium indium and plastic (as marked from top to bottom). Stepped objects on the left are steel (upper) and plastic (lower) each varying in thickness from 2 mm to 0.25 mm.

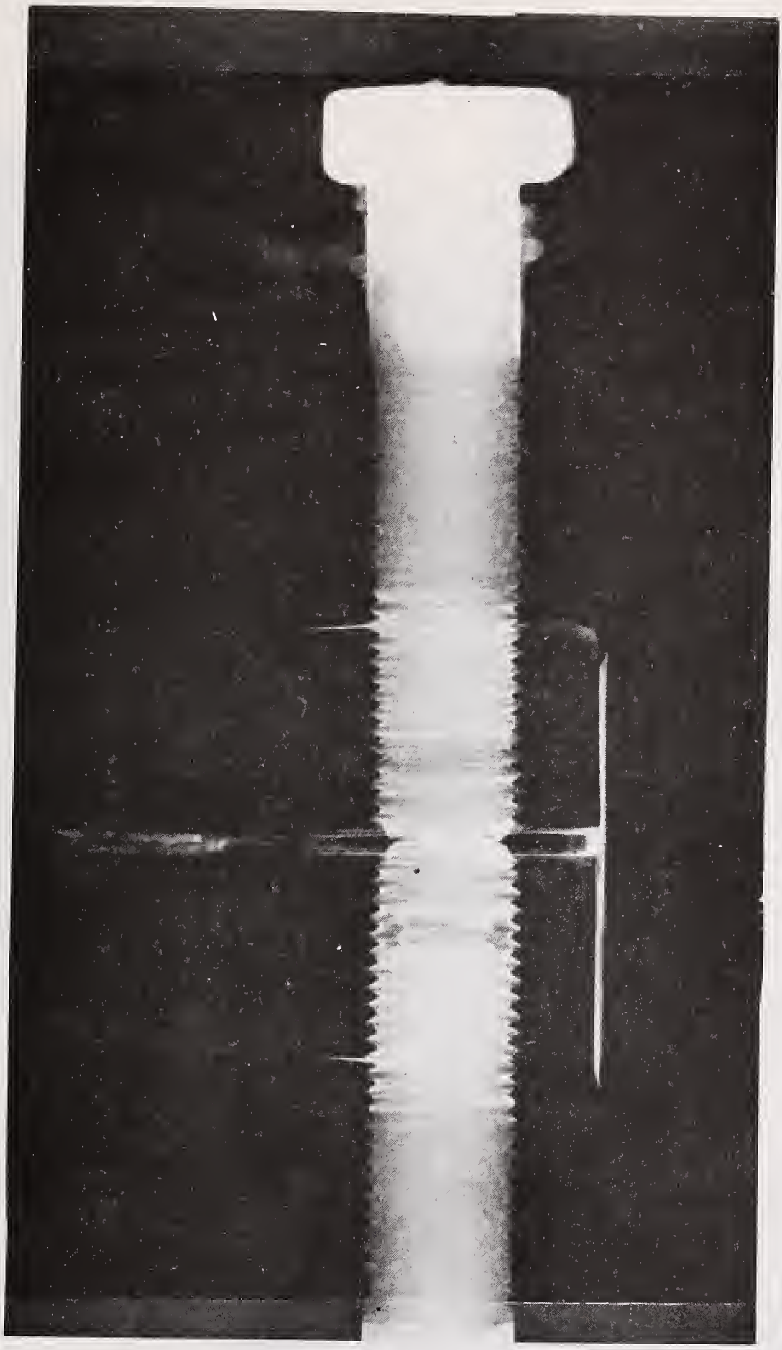

Fig. 3. A neutron radiograph of an aluminum sample. The sample was pre-cracked and cathodically polarized in HCl. The area of attenuation around the double cantilever beam specimen crack is thought to be due to hydrogen. Sample from the Naval Air Development Center, Worminster, Pa.

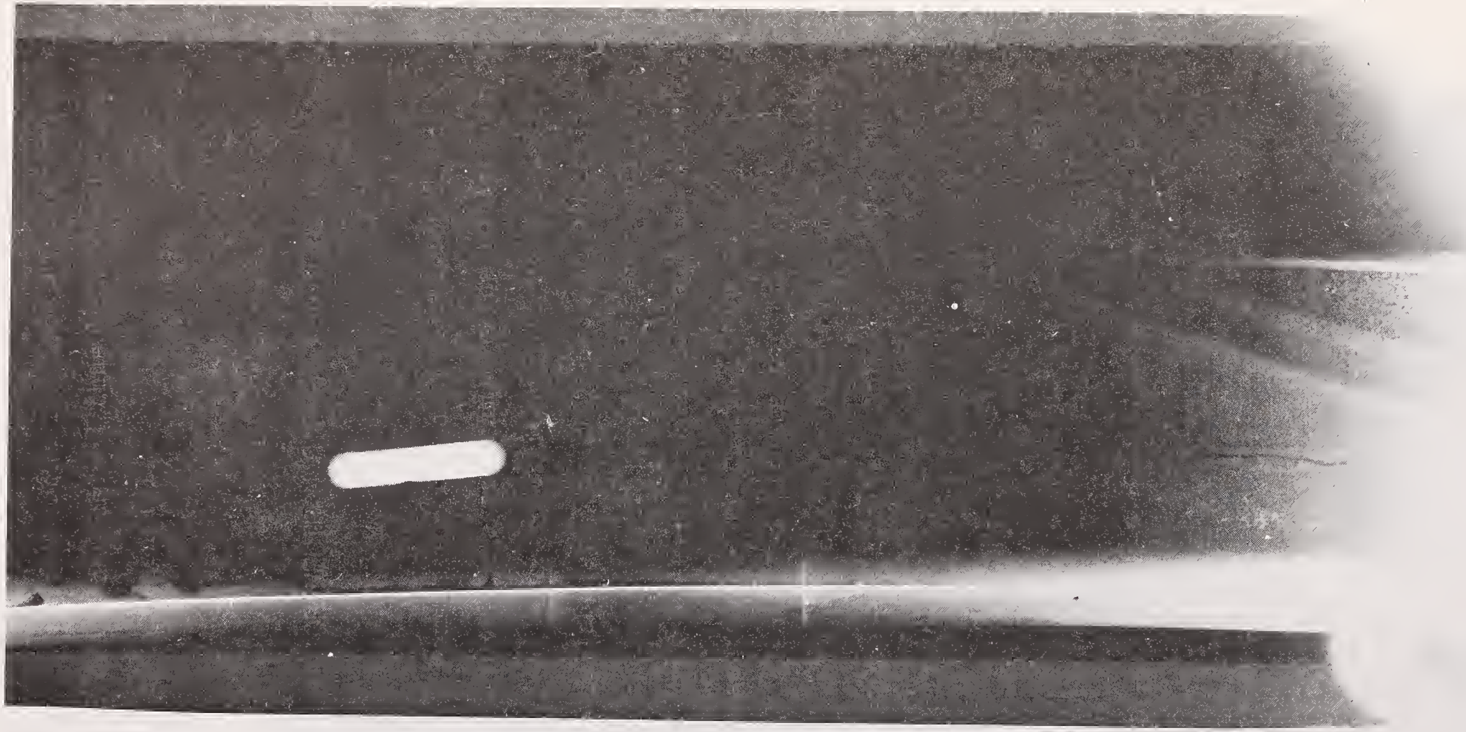

Fig. 4. A neutron radiograph taken by placing a detector inside a cylindrical landing gear strut. The cylinder is aluminum, a brass bushing at each end is believed to trap moisture resulting in corrosion. The neutron radiograph shows the image of the bushing and areas of transmitting and attenuating spots under it. These salt and pepper indications (see area at left in particular) are thought to result from corrosion and the trapped hydrogen associated with it. Samples from the Naval Air Systems Command.

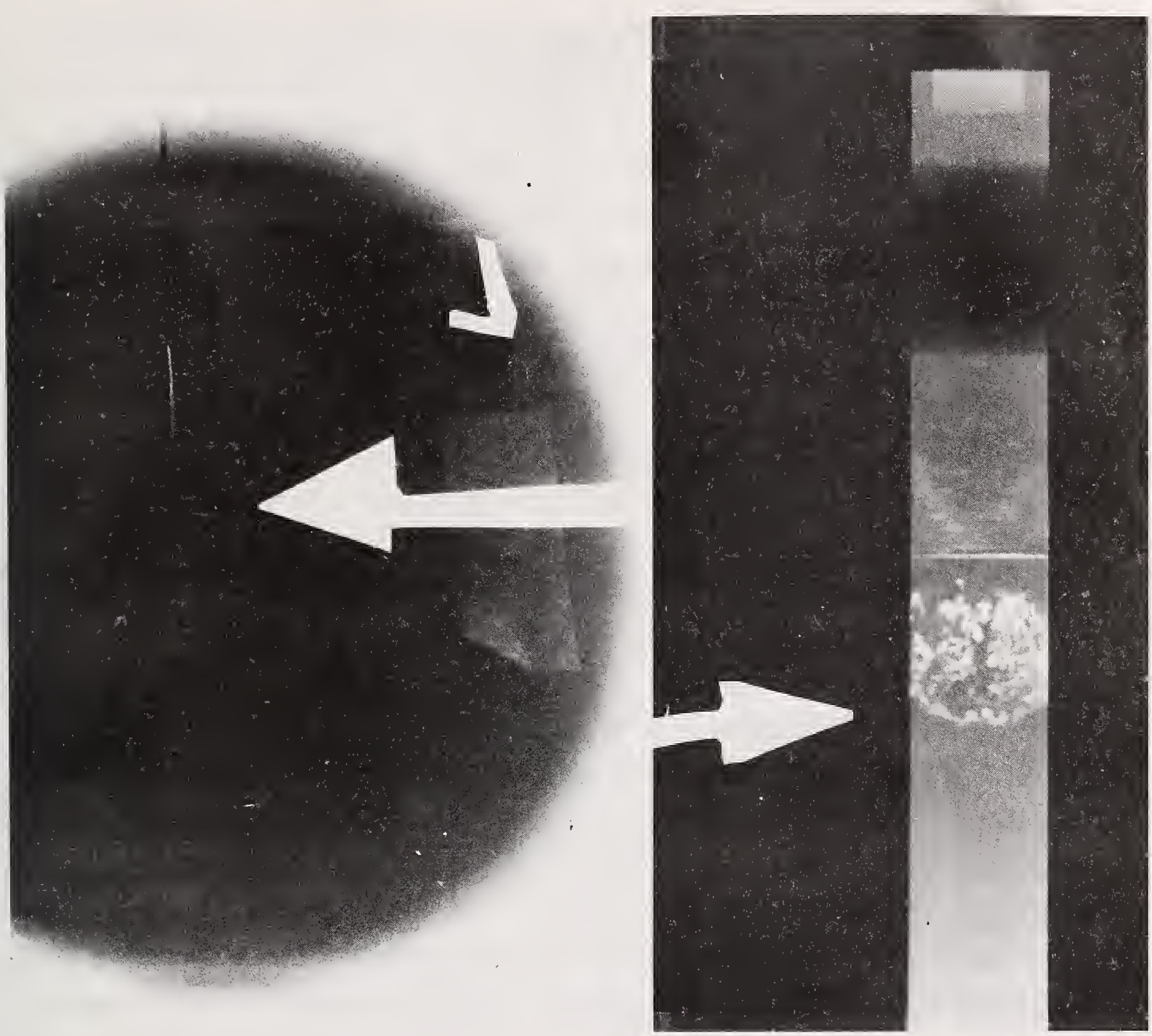

Fig. 5. Two neutron radiographic views of a liquid-filled crack in an aluminum fatigue sample. In each case the arrow points to the bottom area of the crack. In view A (left), the neutron beam passes through almost 2 cm of penetrant; a high contrast image results. In view B, the neutron beam passes through only the small thickness of the crack and contrast is less. In the case of radiograph B, however, contrast of the crack front has been enhanced by filling the crack with a slurry of GdO in alcohol. The radiograph shows high contrast of the GdO and indicates that it has not uniformly distributed.

required; at 6×10^4 n/cm$^2\cdot$s the plastic thickness had to be increased to 1 mm to provide detection. Both these latter thermal neutron intensities represent values that can be achieved easily with non-reactor neutron sources. The tests, therefore, may have impact on possible users in industry. All the contrast and resolution results at the lower neutron intensities were improved if the neutron image was integrated for several frames. A complete report on these tests is in preparation.

Materials for normal photographic detection of thermal neutron images, particularly gadolinium, indium, and dysprosium metal foils, are also available and have been used for application investigations for NBS and other agency programs. Application studies have involved a variety of samples from many agencies. Most have been concerned with the detection of hydrogenous material in a metal matrix. Materials have included potting foam, adhesives and hydrides. Anomalies to be detected included voids, cracks, inclusions and variations caused by hydriding and corrosion. An example of a neutron radiograph showing excessive hydrogen concentration charged in an aluminum sample under stress corrosion is shown in figure 3. Figure 4 shows a neutron radiograph of an aluminum landing strut in which corrosion under a brass bushing has been detected.

At NBS, the major use of neutron radiography has been the characterization of fatigue cracks in aluminum. These cracks, fabricated in the Mechanics Division, have been filled with penetrant and other hydrogenous liquids, which act as contrast agents for thermal neutron radiography. Experiments with several liquids containing boron, cadmium, and gadolinium have been conducted in an attempt to enhance contrast so that reliable visualization of the crack front can be achieved. Examples of some early neutron radiographs of filled cracks are shown in figure 5.

The neutron radiography program is just beginning to address the problem of standards. NBS is represented on the new ASTM subcommittee E07.05, Neutron Radiography. Plans are also under way to put in operation at the reactor, a second more intense, lower cadmium ratio beam for neutron radiography. The beam will be brought out of a vertical thimble.

---

1. H. Berger, "Neutron Radiography," *Annual Rev. Nucl. Science*, E. Segré, editor. 21, 335-364 (1971).
2. H. Berger, "The Present State of Neutron Radiography and its Potential," *Materials Evaluation*, 30, 55-65 (1972).
3. A. Klem, "Decalix With Isocon," *Odelca Mirror*, 9, 2-4 (June, 1971).
4. K. A. Wickersheim, R. V. Alvers, and R. A. Buchanan, "Rare Earth Oxysulfide X-Ray Phosphors," *IEEE Trans. Nuclear Science*, NS-17, 57-60 (1970).

GAUGE THEORIES

R. C. Casella

The experimental discovery of neutral weak currents in neutrino-hadron scattering and neutrino-electron scattering has given added impetus to Weinberg-type theories which have as their basis invariance under a nonabelion local gauge group. We have begun a study of Yang-Mills fields with a view towards understanding the Higgs mechanism for acquiring mass under spontaneous symmetry breaking and mechanisms for inducing time-reversal violation in K° meson decays. Quite apart from the question of degenerate vacua, we also wish to understand the relative importance of local gauge invariance *per se* and the associated imposed supplementary condition in maintaining masslessness of the associated gauge boson (e.g., vanishing of the commutator of $\partial^\mu A_\mu(x)$ at different space-time points in QED). We believe this question is relevant to an earlier remark of Lee and Yang that the (abelion) baryon gauge group cannot be local since it would give rise to a long range force proportional to baryon (nucleon) number which would be observable in Etvös-type gravitational experiments.

B. RRD-NBS COLLABORATIVE PROGRAMS

SCATTERING OF NEUTRONS FROM ^{4}HE NEAR THE CRITICAL TEMPERATURE

B. Mozer
(Inorganic Materials Division)

We have measured the diffraction of neutrons from ^{4}He at the critical temperature. In this experiment we were able to use the same sample cell that was used in a similar experiment on neon. Temperature control was harder to maintain for this experiment but manual operation of the system would allow 1-2 milli-Kelvin control near the critical temperature. Diffraction data was obtained for two reduced temperatures $8\text{x}10^{-4}$ and $2\text{-}3\text{x}10^{-3}$ above T_c, - $4\text{x}10^{-4}$ below T_c, and at 14K. The raw data was corrected for background, short range correlations, and collimation effects as explained for neon. Theromdynamic data was obtained to determine the critical density and critical temperature relative to our sensors, dielectric measurements using the capacitor in the cell and resistance measurements of the germanium sensor on a temperature controlled copper block to which the sample cell was attached. The thermodynamic data can yield a value of β for helium but this has not been determined with great accuracy. The corrected diffraction data yields a value of $\eta = 0.100 \pm 0.015$ somewhat smaller than neon but with less accuracy. Analysis of the helium data for coefficients of series expansions or assumed forms of the scattering function have not been attempted.

NEUTRON DIFFRACTION MEASUREMENTS OF NEON NEAR ITS CRITICAL TEMPERATURE

B. Mozer
(Inorganic Materials Division)

In a brief note[1] we reported preliminary neutron diffraction measurements of neon very close to T_c, the critical temperature. In that note we described our observation of the deviation from Ornstein-Zernike theory in the critical scattering of neutrons from neon. We were able to extract the critical exponent $\eta = 0.11\pm^{0.03}_{0.02}$ which is a measure of the deviation from Ornstein-Zernike theory.

We have extended the measurements on neon verifying the earlier results and obtaining data over a large range of temperatures in the critical region. The temperature difference from T_c varies from $7x10^{-5}$ to $3.17x10^{-2}$ in units of the reduced temperature. Angular measurements were taken from 1 to 20 degrees in the scattering angle corresponding to roughly 0.022 to $0.436\mathring{A}^{-1}$ momentum transfer for a $5\mathring{A}$ beam of neutrons. The wave length of the primary beam was varied from 4.5 to $7.5\mathring{A}$ to obtain information on wave length dependence of the scattering. Collimation of the incoming beam was restricted by Soller slit collimators and cadmium masks. Divergence of the incoming beam was less than 4 minutes of arc in the vertical direction and 8 minutes of arc in the horizontal direction. The scattered beam was collimated to 10 minutes of arc in the horizontal direction with Soller slits. For most of the measurements the vertical collimation was left open and was determined by the divergence at the detector which corresponds to 4/3 degrees of arc. We calculated the resolution correction factors using an Orstein-Zernike form for the scattering law and then smearing this scattering behavior by taking into account the various horizontal and vertical divergences with triangular distribution functions. We then placed a Soller slit collimator in the scattered beam with 20 minutes of arc vertical divergence. The correction factors for the diffraction data in the latter case are essentially unity over the angular range greater than 2.5 degrees. Taking the ratio of the corrected data for 4/3 degree vertical divergence to the data for 20 minutes vertical divergence provided an experimentally determined correction factor to check our calculations.

The resultant data was corrected for background, collimation and short range correlations as determined from the structure factors measured over a κ range of 0.2 to $9.0\mathring{A}^{-1}$. A constant multiple scattering correction and small incoherent scattering correction were also applied to the data.

From the corrected diffraction data and thermodynamic measurements we found the following values for the critical exponents of neon exhibited in table 1. We also found that our diffraction data could be presented on a universal curve[2] over the temperature range by plotting $I\epsilon^{\gamma}$ versus $(\kappa\xi)^2$ where I is the corrected intensity $\epsilon = (T-T_c)/Tc$, κ is the momentum transfer, and ξ the correlation length. Preliminary analysis indicates a universal curve for $\gamma = 1.18\pm.01$ and $\nu = 0.630\pm.004$. Thus static scaling concepts seem to apply to our diffraction data at this stage in the analysis and seem to agree with the values determined in a straightforward way as quoted in table I.

Additional analysis of our data was undertaken to obtain estimates for various coefficients in the series approximations to the scattering function for large and small $\kappa\xi$. Our estimates for these coefficients are much larger than estimates calculated from the lattice-gas model using the renormalization group approach[2].

Table I. Several critical exponents for neon

β	γ	ν	η	α
0.360±0.005	1.18±0.01	0.630±0.004	0.125±0.005	0.14±0.04

---

[1] V. W. Warkulwiz, B. Mozer, and M. S. Green, Phys. *Rev. Lett.* 32, 1410 (1974).

[2] M. E. Fisher and A. Aharony, *Phys. Rev. Lett.* 31, 1238 (1973).

CRYSTALLOGRAPHIC METHODS FOR THE STUDY OF PHASE TRANSFORMATIONS

A. Santoro
and
A. D. Mighell
(Inorganic Materials Division)

In the automatic determination of a unit cell from powder diffraction data, often a powder pattern can be indexed on more than one lattice (de Wolff, 1961; 1968; Visser, 1969; Ishide and Watanabe, 1967, 1971). In most cases the ambiguities in the indexing are due to accidental causes such as errors in the measurements of the angular positions of the diffraction lines, extinctions that are either related or unrelated to the space group symmetry of the crystalline species under investigation, and the presence of reflections produced by impurities. When ambiguities of this type occur, it is not possible to assess the correctness or incorrectness of a unit cell with certainty, but procedures can be used for estimating the reliability of a particular indexing (de Wolff, 1961; 1968).

Recently in the course of a neutron diffraction study of phase transitions in rubidium and sodium hydrosulfides, it was observed that two different lattices, one of rhombohedral symmetry and the other of monoclinic symmetry, give calculated powder patterns with the identical number of distinct lines in identical 2θ angular positions. The number of planes (hkl) contributing to each reflection is not the same in the two cases, however. These two lattices are related to each other by a transformation matrix whose elements are simple rational numbers.

An ambiguity of this type is geometrical in nature rather than accidental and has not been recognized previously. It has to be expected that cases similar to that encountered in the study of the hydrosulfides play an important role in the automatic determination of unit cells from powder data. Therefore, it is useful to analyze the conditions under which these ambiguities occur. This analysis has been carried out and some of the results are shown in table 1.

Geometrical ambiguities in the indexing of powder patterns do occur in high-symmetry lattices. One of the main conclusions of our study is that these ambiguities, where they exist, are systematic. For example, any powder pattern consistent with a body-centered cubic cell (see case 1 in Table I) can also be indexed in terms of a tetragonal cell with a volume 1/4 that of the cubic cell, or in terms of orthorhombic P and F cells having volumes 1/8 and 2/3 that of the original cubic cell, respectively.

There are cases of geometrical ambiguities in which it is not possible to decide on the reliability of the indexing on the basis of the angular positions of the diffraction lines. For example, the low temperature phases of sodium and rubidium hydrosulfides (Rush, Livingston and Rosasco, 1973) give neutron powder patterns which can be indexed in terms of a monoclinic and a rhombhedral cell (case 5 in table 1). Both lattices are equally valid and the choice of one or of the other depends exclusively on how the hydrogen atoms are ordered in the structure. Similar situations may well exist in analogous order-disorder transformations.

The indexing of the pattern of α-$Li_4B_2O_5$ (de Wolff, 1968) represents an example of the occurrence of geometrical ambiguities in the automatic determination of unit cells from powder data. The pattern of this compound can be indexed as orthorhombic and as hexagonal. The two lattices are not the same (transformation matrix from orthorhombic to hexagonal: $1\bar{1}0/110/001$, case 4 in table 1). The true orthorhombic symmetry of the structure was established in this case by single-crystal work rather than from powder data.

The lattices of all the examples given in table 1 are related by transformation matrices with simple rational elements, i.e. lattice II is in all cases a derivative lattice of lattice I (Santoro and Mighell, 1972; 1973). This relationship between lattice I and II seems to be a necessary, but certainly not a sufficient, condition that the lattices have to satisfy to be consistent with the same set of calculated lines.

Table 1. Examples of lattices giving geometrical ambiguities in the indexing of powder patterns

Lattice I	Lattice II	Transformation I→II
1) Cubic P	Tetragonal P	$0\overline{\tfrac{1}{2}}\tfrac{1}{2}/0\tfrac{1}{2}\tfrac{1}{2}/\bar{1}00$
2) Cubic I	Tetragonal P	$0\overline{\tfrac{1}{2}}\tfrac{1}{2}/0\overline{\tfrac{1}{2}}\overline{\tfrac{1}{2}}/\tfrac{1}{2}00$
	Orthorhombic F	$\overline{\tfrac{1}{3}}\overline{\tfrac{1}{3}}0/00\bar{1}/\bar{1}10$
	Orthorhombic P	$\tfrac{1}{4}\overline{\tfrac{1}{4}}0/00\tfrac{1}{2}/\tfrac{1}{2}\tfrac{1}{2}0$
3) Cubic F	Orthorhombic C	$\overline{\tfrac{1}{2}}0\tfrac{1}{2}/010/\overline{\tfrac{1}{4}}0\overline{\tfrac{1}{4}}$
	Orthorhombic I	$\overline{\tfrac{1}{6}}0\overline{\tfrac{1}{6}}/\tfrac{1}{2}0\overline{\tfrac{1}{2}}/0\bar{1}0$
4) Hexagonal	Orthorhombic P	$\tfrac{1}{2}\tfrac{1}{2}0/\tfrac{1}{2}\overline{\tfrac{1}{2}}0/00\bar{1}$
5) Rhombohedral	Monoclinic P	$\overline{\tfrac{1}{2}}0\overline{\tfrac{1}{2}}/\tfrac{1}{2}0\overline{\tfrac{1}{2}}/0\bar{1}0$

T. Ishida, and Y. Watanabe, *J. Phys. Soc. Japan* 23, 556-565 (1967).

T. Ishida and Y. Watanabe, *J. Appl. Cryst.* 4, 311-316 (1971).

J. J. Rush, R. C. Livingston, and G. J. Rosasco, *Solid State Comm.* 13, 159-162 (1973).

A. Santoro and A. D. Mighell, *Acta Cryst.* A28, 284-287 (1972).

A. Santoro and A. D. Mighell, *Acta Cryst.* A29, 169-175 (1973).

J. W. Visser, *J. Appl. Cryst.* 2, 89-95 (1969).

P. M. Wolff, *Acta Cryst.* 14, 579-582 DE(1961).

P. M. Wolff, *Acta Cryst.* 1, 108-113 DE(1968).

DETERMINATION OF LATTICE DISTORTIONS FROM SIMULTANEOUS DIFFRACTION EFFECTS

A. Santoro
A. D. Mighell
(Inorganic Material Division)
and
M. Zocchi
(Politecnico di Milano, Italy)

Phase transformations are not infrequently associated with symmetry changes resulting in slight distortions of the crystal lattice. It is therefore of interest to devise procedures not only for detecting changes in symmetry, but also for determining uniquely which of the possible distortions of a lattice has occurred in any particular case. Simultaneous diffraction offers an ideal method for analyzing phase transitions of this type when single crystals are available.

Multiple, or simultaneous, diffraction of X-rays and neutrons occurs when two or more reflections satisfy the Bragg condition simultaneously. Its effect is a more or less pronounced perturbation in the intensities diffracted by each of the reflections involved. A pattern of these perturbations (Renninger pattern) can be obtained for any desired reflection HKL (primary reflection) by measuring the intensity diffracted by the reflection while the crystal is being rotated about the scattering vector.

The sensitivity of the lattice parameters to the angular positions of the Renninger peaks is greater than that of the conventional single-crystal and powder methods. In the case of cubic crystals, for example, we have

$$da^*/a = \cos^2\theta \, tg\psi d\psi \qquad (1)$$

where a^* is the reciprocal parameter, θ is the Bragg angle of the primary reflection HKL and $\psi=(\psi_1-\psi_2)/_2$, where ψ_1 and ψ_2 are the angles at which a second reflection $hk\ell$ diffracts simultaneously with HKL during a 360° rotation about the scattering vector corresponding to HKL. Equation (1) compared quite favorably with the corresponding expression valid for the powder method, i.e.

$$\frac{da^*}{a^*} = c\alpha \tan \theta d\theta \tag{2}$$

A further advantage offered by simultaneous diffraction over the conventional methods is that the Renninger peaks are far less affected by systematic errors and far sharper than single-crystal and powder diffraction effects.

The peculiar geometry of simultaneous diffraction confers to the Renninger patterns particular properties which can be used for the detection of lattice distortions. Our method makes use of the fact that in the absence of distortions certain peaks are superposed in the Renninger pattern of particular primary reflections, and they are split if the distortions are present. Without entering into the details of the derivation, we have summarized in tables 1 and 2 the conditions under which the distortions can be detected. The main conclusion of our study is that each of the possible distortions can be uniquely determined from the splittings characteristic of that distortion.

Experimental work intended to verify the theoretical results is planned in the near future.

Table I. Primary and Secondary Reflections Showing Distortions of the Interaxial Angles

Primary Reflection	Split Reflections	Distortions
H 0 0	$h_i\ 0\ l_i$, $H-h_i\ 0\ l_i$	$\beta^* \neq 90°$
	$h_i\ k_i\ 0$, $H-h_i\ k_i\ 0$	$\gamma^* \neq 90°$
0 K 0	$0\ k_i\ l_i$, $0\ K-k_i\ l_i$	$\alpha^* \neq 90°$
	$h_i\ k_i\ 0$, $h_i\ K-k_i\ 0$	$\gamma^* \neq 90°$
0 0 L	$0\ k_i\ l_i$, $0\ k_i\ L-l_i$	$\alpha^* \neq 90°$
	$h_i\ 0\ l_i$, $h_i\ 0\ L-l_i$	$\beta^* \neq 90°$

Table II. Primary and Secondary Reflections Showing Distortions of the Interaxial Angles

Primary Reflection	Split Reflections	Distortion
$h_i+h_j, -h_i+h_j, 0$	$h_i\bar{h}0$; $h_jh_j\ 0$	$a^* \neq b^*$
$h_i+h_j, h_i-h_j, 0$	$h_ih_i0_j$; h_jh_j0	
$h_i+h_j, 0, -h_i+h_j$	$h_i0\bar{h}_i$; h_j0h_j	$a^* \neq c^*$
$h_i+h_j, 0, h_i-h_j$	$h_i0\bar{h}_i$; $h_j0\bar{h}_j$	
$0, k_i+k_j, -k_i+k_j$	$0k_i\bar{k}_i$; $0k_jk_j$	$b^* \neq c^*$
$0, k_i+k_j, k_i-k_j$	$0k_ik_i$; $0k_j\bar{k}_j$	

HYDROGEN BONDED DIMERS IN $SnHPO_4$

L. W. Schroeder
(Polymers Division)
and
E. Prince

A previous x-ray determination, although of limited accuracy, of the crystal structure of $SnHPO_4$ indicated the presence of hydrogen-bonded HPO_4^{-2} dimers. The length of the hydrogen bond as obtained in the previous study is 2.50Å indicative of a strong hydrogen bond. This suggests that dimeric HPO_4^{-2} may be a component of phosphate solutions at higher pH values.

Recently, we have obtained extensive single crystal Raman and infrared data on $SnHPO_4$ in an effort to characterize the dimers in terms of their vibrational spectrum. It is necessary to know the details of the hydrogen bonding in order to place the interpretation of the spectrum on a firm basis. We have collected 1724 neutron data from a crystal of $SnHPO_4$. Structure refinements will begin after the data have been corrected for the effect of incoherent scattering by hydrogen.

ATOMIC ORDERING IN A-15 COMPOUNDS OF THE V-NI AND V-CO SYSTEMS

R. M. Waterstrat and B. Dickens
(Polymers Division)

and

J. J. Rhyne
(Naval Ordnance Laboratory, White Oak, MD)

Neutron scattering has been used to determine the relative site occupancy of V atoms on the "A" and "B" sites in compounds of V_3-Co and $V_{77.5}Ni_{22.5}$. In the latter off-stoichiometric compound the atomic order was maximized while in the Co compound the order parameter was found to be 0.9±0.1. These compounds are isomorphic with the high temperature super-conductor Nb_3Sn.

The neutron technique is particularly valuable for determining site order in these compounds due to the nearly identical values of the x-ray scattering amplitudes of V and Ni (or Co). In the neutron case these amplitudes are widely different and are not related to the atomic number which allows the superlattice ordering Bragg lines (e.g. the [110]) to be strongly visible as shown in the accompanying comparison of x-ray and neutron diffraction intensities on the nickel compound.

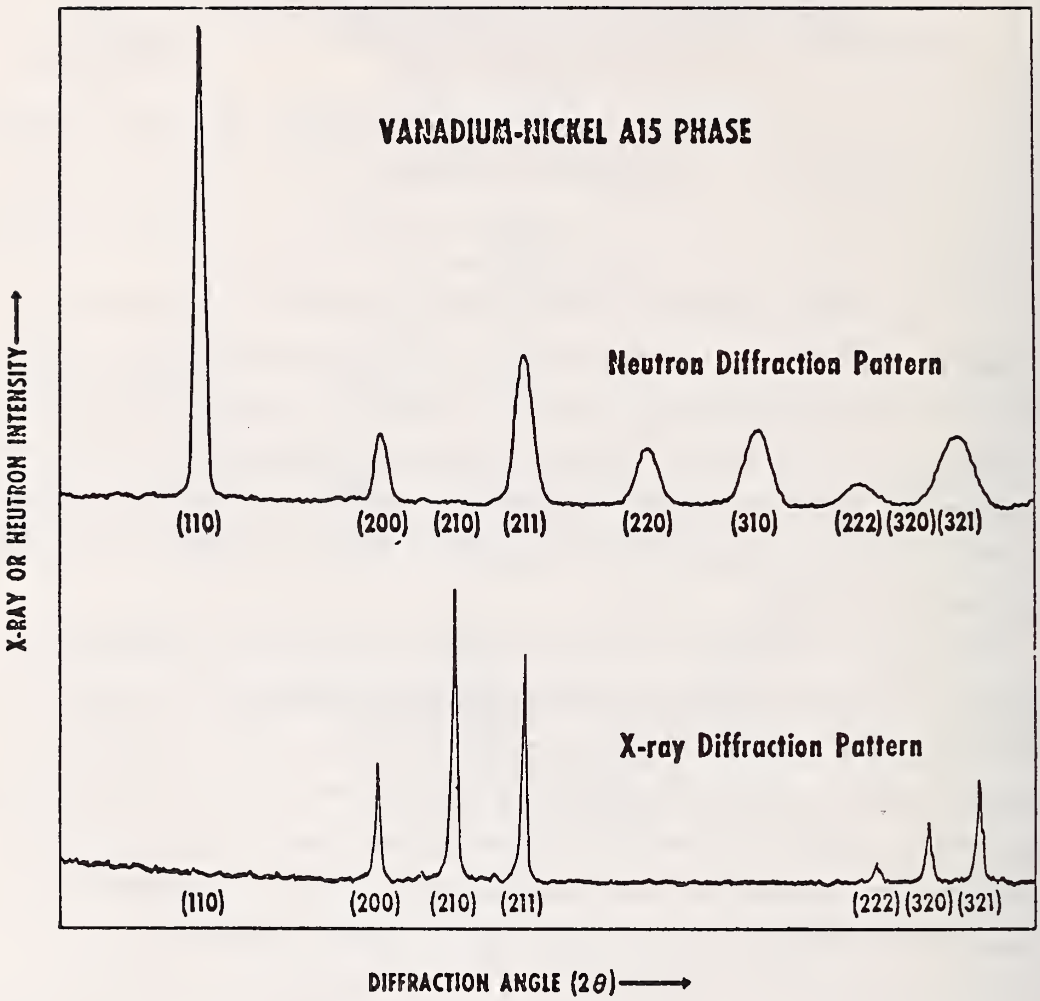

Fig. 1. X-ray and neutron scattering intensity from a $V_{77.5}Ni_{22.5}$ A15 compound. The superlattice order peaks ([111] etc.) are clearly visible in the neutron scattering which allowed the determination of the order parameter.

THE CRYSTAL STRUCTURE OF LEAD DEUTERIUM ORTHOPHOSPHATE

C. S. Brickenkamp
(Inorganic Materials Division and Office of Weights and Measures)
and
E. Prince

Preliminary refinement of the structure of lead deuterium orthophosphate was reported in the summary of activities for 1972-73. After refining the structure to an R of 0.10 with isotropic temperature factors, a refinement with anisotropic temperature factors was attempted, but the initial cycles did not converge. While R was reduced slightly, parameter shifts remained large, and the temperature factor matrices for several atoms went non positive-definite. In order to reduce the number of parameters while keeping a more appropriate model than the isotropic temperature factor model, the thermal parameters of the phosphate group were constrained to be those appropriate to a rigid body, and the components of $\underline{T}$ and $\underline{L}$ (but not $\underline{S}$) for the rigid body motion were refined. With these constraints, and with an extinction parameter included, the refinement proceeded to an R of 0.049 (R_w=0.063). A conventional refinement with anisotropic temperature factors then gave a final R of 0.036 (R_w=0.051).

The crystal structure consists of phosphate groups bound into chains by strong asymmetric hydrogen bonds. The O-O distance is 2.514 (5)Å, the two O-D distances are 1.032(6)Å and 1.484(6), and the O-D-O angle is 175.9(5)°. The phosphate group is a slightly distorted tetrahedron, with O-P-O bond angles ranging from 106.5(4)° to 112.5(3)°. The P-O bond angles ranging from 1.515(5)Å to 1.573(6)Å, with the long bond being to the hydrogen bond donor, as expected.

Table 1 summarizes the crystal data and table 2 gives a list of the final atom parameters.

Table 1. Crystal Data for $PbHPO_4$

a = 4.6855(5)Å
b = 6.6911(7)Å
c = 5.7867(8)Å
β =97.10(1)°

Space group Pc
Z = 2

Table 2. Atomic Parameters for $PbDPO_4$. The temperature factor expression used is: $\mathrm{Exp}\ [-(\beta_{11}h^2+\beta_{22}k^2+\beta_{33}\ell^2+2\beta_{12}hk+2\beta_{13}h\ell+2\beta_{23}k\ell)]$. Numbers in paranthesses are estimated standard deviations.

Atom	X	y	z	β_{11}	β_{22}	β_{33}	β_{12}	β_{13}	β_{23}
Pb	0	.1992(3)	1/4	.0136(9)	.0063(4)	.0082(6)	-.0012(6)	-.0009(5)	.0008(4)
P	.5094(12)	-.2046(4)	.2239(8)	.0119(13)	.0059(7)	.0052(10)	-.0013(11)	-.0018(9)	-.0014(8)
O(1)	.3830(10)	-.3406(7)	.4085(8)	.0154(18)	.0053(7)	.0162(11)	.0027(10)	.0048(11)	.0029(9)
O(2)	.2630(10)	-.0764(6)	.1132(8)	.0066(16)	.0076(10)	.0086(11)	.0022(10)	-.0013(9)	.0007(8)
O(3)	.6260(10)	-.3374(7)	.0420(8)	.0245(22)	.0082(9)	.0130(11)	-.0018(11)	.0064(13)	-.0040(9)
O(4)	.7509(10)	-.0794(6)	.3580(7)	.0152(19)	.0084(10)	.0053(11)	-.0017(12)	-.0022(9)	-.0013(7)
D	.4885(11)	.5280(5)	.4578(7)	.0210(14)	.0099(9)	.0149(11)	-.0006(12)	.0017(10)	-.0005(9)

THE LOW TEMPERATURE PHASE OF TANTALUM OXIDE

R. S. Roth
(Inorganic Materials Division)
and
E. Prince

Tantalum oxide, To_2O_5, is an end member of a series of tantalum-tungsten oxides studied previously by x-ray diffraction by Stephenson and Roth[1]. The structure of these oxides are based on a framework of various numbers of octahedral and pentagonal bipyramidal subunits. The low temperature phase of Ta_2O_5 is difficult to prepare in single crystal of any size, but the addition of small amounts of lithium oxide stabilizes the crystal structure so that large, good-quality crystals can be grown. The unit cell is orthorhombic, $\underline{a}$=6.198, $\underline{b}$=40.29, $\underline{c}$=3.888 Å, and the structure conforms approximately to space group Pbmm. However, an ideal structure in this space group must have the composition $Ta_{22}O_{58}$, whereas the stoichiometry provides only 55 oxygen atoms, and the addition of lithium, at least if the lithium replaces tantalum, reduces the oxygen content even further below the ideal value. X-ray diffraction studies are dominated by the tantalum, because of its high atomic number. A neutron diffraction study was undertaken in an attempt to determine the roles of the light atoms in the crystal.

Because of the very long $\underline{b}$ axis reflections are very close together, and if the usual scanning techniques were used there would be a tendency for peaks to overlap. To get around this problem the data collection program was altered to scan through reciprocal space along a line approximately perpendicular to the short reciprocal lattice spacing resulting in the use of a θ-2θ scan for h00 reflections, an ω scan for 0k0 reflections, and a hybrid of the two for other reflections in the hk0 zone. All of the atomic positions lie in either the z=0 plane or the z=1/2 plane, so there is little information in upper level reflections. Furthermore a very large fraction of the ℓ=0 reflections is below the threshold of observability.

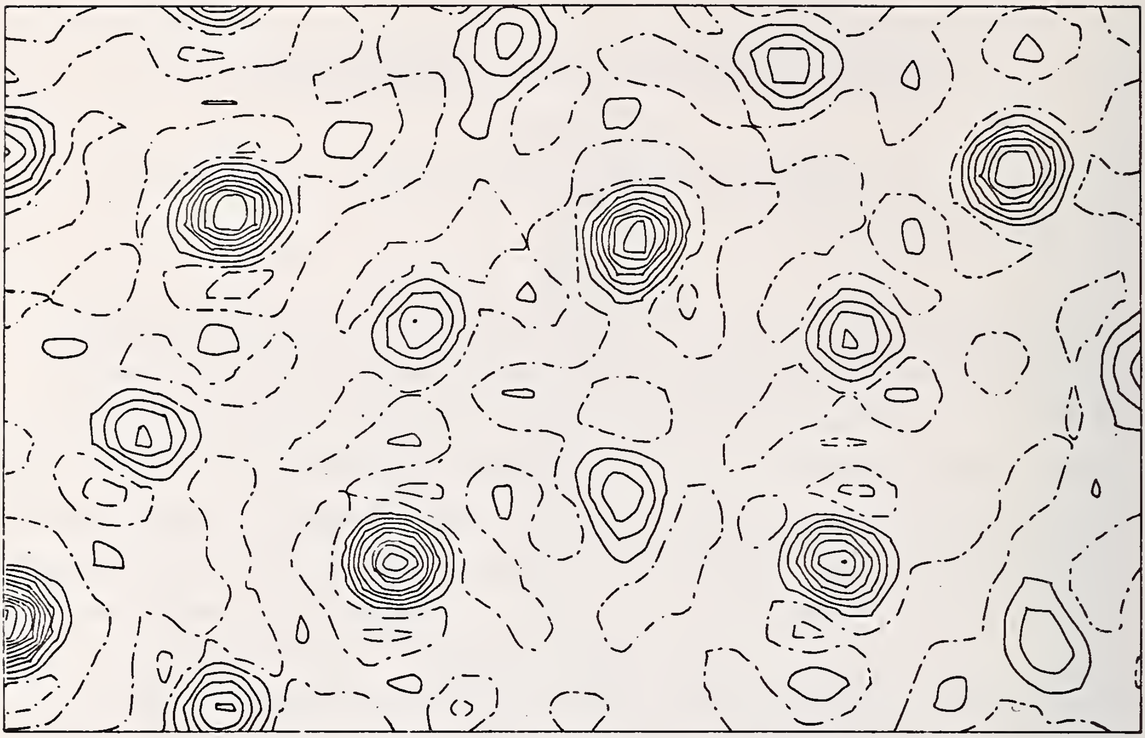

Fig. 1. Fourier projection of the structure of L-To_2O_5, as viewed looking down the C axis. 1/4 of the unit cell is shown. Large peaks are O and Ta superposed. Smaller peaks are O alone. Dot-dash lines represent the O contour.

A Fourier projection along the c axis (figure 1) shows all of the features of the ideal structure, but no significant additional features, either as negative peaks that would indicate that the lithium was occupying "interstitial" sites or as positive peaks indicating alternative positions for some oxygen atoms in accordance with the scheme proposed by Stephenson and Roth. It appears that the structure contains so many M-O-M linkages that a few can be missing here and there without any effect on the stability of the crystal.

---

[1] N. C. Stephenson and R. S. Roth, *Acta Cryst.*, B27, 1037 (1971).

C. INTERAGENCY AND UNIVERSITY COLLABORATIVE PROGRAMS

CRYSTAL STRUCTURE OF DIACETO-PENTAMETHYLENE-TETRAMINE

C. S. Choi
(Picatinny Arsenal, Dover, NJ)

and

A. Santoro

Diaceto-pentamethylene-tetramine, $C_9H_{16}N_4O_2$, (hereafter referred to DAPT) is one of the several intermediates in the manufacture of HMX (cyclo-tetramethylene-tetranitramine). Preliminary investigation by precession photographs revealed the space group to be monoclinic $P2_{1/c}$. The unit cell dimensions are a=6.183(2), b=10.101(2), c=17.037(4), β=101.78(2)°, and contains 4 molecules per unit cell. A total of 1708 independent reflection intensities were measured within the limiting sphere of 60° in 2θ angle by using an automated x-ray diffractometer with MoKα radiation. The structure was solved by the direct method using the XRAY72 system and the hydrogen positions were located from the difference map. The full matrix least squares refinements with anisotropic temperature factors for the heavy atoms and isotropic temperature factors for the hydrogen atoms reduced the R-index to wR=0.041 and R=0.051.

The DAPT molecule is isostructural with the DPT (dinitro-pentamethylene-tetramine molecule which has been described previously in NBS Technical Note 813, 1973). Fig. 1 is the ORTEP drawing of the DAPT molecule. The molecule possesses a pseudo 2-fold rotation symmetry, which is comparable to the pseudo mirror symmetry of the DPT molecule. The two acetamide groups are both essentially planar. The bond lengths and angles of the DAPT generally agree well with those of HMX and its derivatives. Both oxygen atoms in the molecule are involved in C-H...O type hydrogen bonding. The molecules in the crystal are linked together mainly by two weak hydrogen bonds, C(2)-H(3)...O(2) and C(5)-H(9)...O(2), where the C...O distances are 3.28Å and 3.39Å respectively.

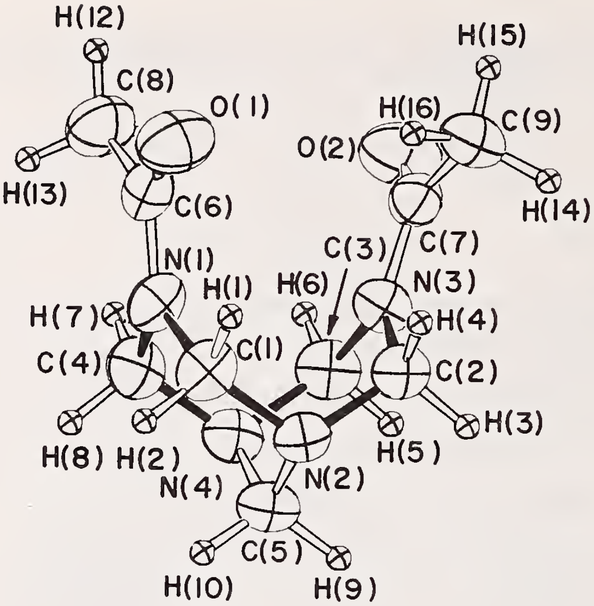

Fig. 1. A molecule of DAPT with thermal ellipsoids to enclose 50% probability. The isotropic hydrogen atoms are scaled down to an arbitrary small size.

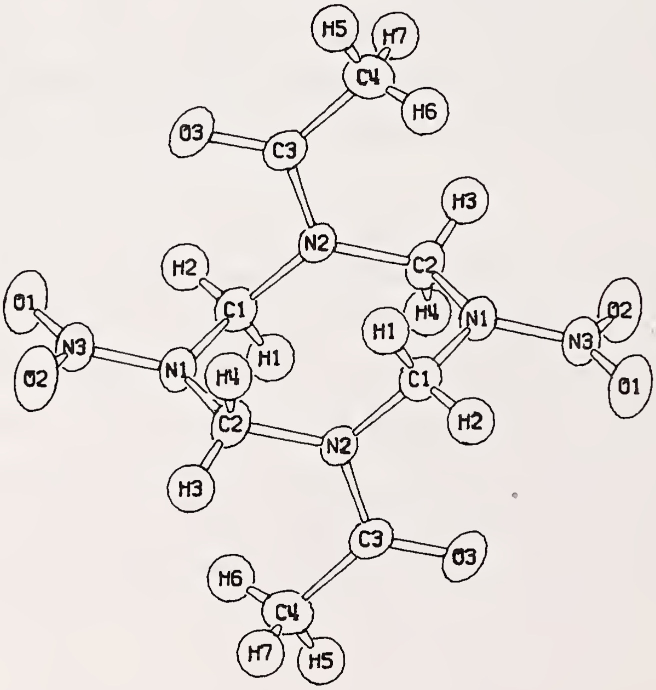

Fig. 2. DADN molecule.

CRYSTAL STRUCTURE OF 1,5 DIACETO-3,7 DINITRO-1,3,5,7, TETRAZACYCLO-OCTANE

C. S. Choi
(Picatinny Arsenal, Dover, NJ)

and

A. Santoro

The compound, 1,5 diaceto-3,7, dinitro-1,3,5,7, tetracyclo-octane, $C_8H_{14}N_6O_6$, (hereafter referred to DADN), is also a derivative of HMX. Preliminary investigation by precession photograph with MσKα radiation indicated that the space group is monoclinic $P2_{1/c}$ with two molecules per unit cell. The cell dimensions are a=7.422(1) b=13.253(2) c=6.156(1) and β=103.38(1)°. Using an automated 3-circle x-ray diffractometer with MσKα, a total of 1342 independent reflections were measured within the limiting sphere of 90° in 2θ angle, of which 1149 reflections were recorded as observable. The structure was solved by the direct method using the program X-RAY72 system, and the hydrogen atoms were located by difference synthesis. The structure was further refined by the full matrix least squares method to the final R-index, WR=0.05 and R=0.04. The DADN molecule shown in figure 2 possesses a center of symmetry and is isostructural with the β-HMX molecule, which is an interesting contrast to the TAT (1,3,5,7, tetraceto-1,3,5,7, tetrazacydo-octane, NBS Technical Note 758, 1972) molecule which has a conformation similar to the α-HMX with 2-fold rotation symmetry. The acetamide groups and the $N\text{-}NO_2$ groups are both planar. The bond lengths and angles agree well with those of the HMX and its derivatives.

REFINEMENT OF THE CRYSTAL STRUCTURE OF MONOVALENT METAL AZIDES

C. S. Choi
(Picatinny Arsenal, Dover, N.J.)
and
E. Prince

Monovalent metal azides are ionic crystals, consisting of spherical metal cations and linear N_3 anions. Both cations and anions always occupy centrosymmetric sites in the crystal. Hence the thermal motions of an azide anion may be treated as a rigid body motion if we neglect the comparatively small amplitude of the N-N stretching vibrations.

KN_3:

The crystal structure of KN_3, known to be I4/mcm, was refined to wR=0.022 R=0.020 by the constrained rigid body method using 166 reflections. The observed N-N distance, 1.174Å, becomes 1.184(1)Å when corrected for libration. The rigid body parameters for N_3 anion obtained from the neutron data refinement were fitted to a set of 145 x-ray reflections (obtained by Müller). In this fit the scale factor, a secondary extinction parameter, and the thermal parameters of the potassium cations were adjusted. The fit was extremely good, with wR=0.026 R=0.022. The fit is far better than Müller's results, which were wR=0.042 and R=0.038.

β-NaN_3:

A total of 94 independent reflections were collected, using 0.983Å wavelength neutrons. The structure was refined by the rigid N_3 group model to the final R-index wR=0.024 and R=0.026. The observed N-N distance, 1.162Å, becomes 1.180(1)Å when it is corrected for libration. It is interesting to notice that the libration amplitude of the N_3 anion in β-NaN_3 (approximately 14°) is much larger than that in KN_3 (approximately 8°), although the temperature of the β-NaN_3 sample (room temperature) is only a few degrees above the phase transition temperature.

$T\ell N_3$:

The reflections in an entire hemisphere of reciprocal space were investigated at room temperature out to a maximum 2θ of 100° (λ=0.983Å). Of 169 independent reflections within range, only 77 had observable intensity. The structure was also investigated at lower temperature, 260 K, which is approximately 12°C above the transition point. Using 1.23Å wavelength neutrons, 84 observed reflections were collected. At both temperatures least squares refinements were not successful because of the so-called false minimum catastrophe. This difficulty in the refinement was resolved when a lower symmetry space group, I4cm, was used as the initial space group. The correct space group, I4/mcm, was used only at the final stage of the refinement. The final R-indices were, wR=0.018 R=0.016 for the 260 K data and wR=0.027 R=0.039 for the room temperature data. The N-N distances of the azide anions, after correction for libration, were 1.184(1)Å for the 260 K structure and 1.181(4)Å for the room temperature structure.

The librational motions and the N-N bond lengths of β-NaN_3, KN_3, $T\ell N_3$ (260 K) and $T\ell N_3$ (300 K), are summarized in table 1. It is clear that the N-N bond lengths of the N_3 anions of the monovalent metal azides are essentially the same, probably 1.182±0.002Å.

Table 1. Libration tensor elements ($radian^2$) and N-N bond lengths of the azide anions

Libration Tensor	β-NaN_3	KN_3	$T\ell N_3$(260K)	$T\ell N_3$ (300K)
L_{11}	.0150	.0110	.0270	.0274
L_{22}	.0150	.0063	.0069	.0097
L_{33}	.0000	.0000	.0000	.0000
N-N bond length (Å)				
Corrected :	1.180(8)	1.184(6)	1.184(1)	1.181(4)
Uncorrected:	1.162	1.174	1.164	1.159

THE STRUCTURE OF DEUTERIUM PEROXIDE

E. Prince

S. F. Trevino and C. S. Choi
(Picatinny Arsenal, Dover, NJ)

The crystal and molecular structure of H_2O_2 were determined in the early 1960s by Busing and Levy[1]. Extensive Raman and IR studies by Armen, *et al.*[2] on both H_2O_2 and D_2O_2 have shown some interesting differences resulting from the isotope substitution. The O-D stretch frequency shows that the corresponding force constant is larger for the deuterated compound. Also the O-O stretch frequency is the same for D_2O_2 and for H_2O_2, although the increased mass might be expected to result in a lower frequency. Because these effects suggest differences in molecular structure, we undertook a neutron diffraction study of the deuterated compound.

A single crystal of D_2O_2 was grown in a quartz tube approximately 2 mm inside diameter with one end drawn down to a fine capillary. A seed nucleus was formed by dipping the end of the capillary in liquid nitrogen, after which the entire sample was cooled to -14°C. When viewed between crossed polarizers the resulting solid showed sharp extinction. The crystal was mounted in a temperature-controlled cryostat, and was maintained at -15°C throughout the experiment.

The structure is tetragonal, space group P4, 2, 2 (or $P4_3 2, 2$). The constants were determined on the diffractometer. The cell constants, determined on the diffractometer, were $\underline{a}$=4.035(5), b=7.97(1). There are four D_2O_2 molecules in the unit cell. Of 113 independent reflections within the sphere defined by λ=1.230Å and 2 max-106° 107 had observable intensity. The structure quickly refined to R-.027, Rw=.038, using anisotropic temperature factors and an isotopic extinction parameter.'

The O-O distance, uncorrected for thermal motion, is 1.453Å, in exact agreement with the Busing and Levy result for H_2O_2. The O-D distance, however, is 0.995Å (with a riding model correction) as compared with 1.008Å in H_2O_2. This is consistent with the observation of a stronger force constant. The dihedral angle is 91.1° which is significantly different from 90.2° in H_2O_2. The O-O-H bond angle is 101.9°, compared with 102.7°. These results do not suggest an explanation for the fact that the O-O stretching frequency is not reduced, although the more compact molecule may have stronger O-D and D-D repulsions.

The data are further analyzed using a restricted rigid body constrained refinement.

---

[1] W. R. Busing and H. A. Levy, J. *Chem. Phys.*, 42, 3054 (1965).

[2] Jose L. Arrau, Paul A. Giguere, Motoko Abe and Robert C. Taylor, Spectrochimica Acta, 30A, 777 (1974).

THE LATTICE DYNAMICS OF DEUTERIUM PEROXIDE

S. F. Trevino and M. K. Farr
(Picatinny Arsenal, Dover, NJ)

and

J. L. Arrau and P. A. Giguere
(Laval University, Quebec, Canada)

The energy and momentum of phonons propogating along the crystallographic c direction in D_2O_2 have been measured. A single crystal (volume 5cc) of 99.5% D_2O_2 was grown by the Stockbarger method. The crystal was maintained at -30°C during the measurements which were performed on a triple axis spectrometer.

Deuterium peroxide crystallizes in an ordered tetragonal cell of symmetry $P4_12_12$ with four molecules in the primitive cell. There are 24 phonon branches of rigid body motion, all with energies below 300 cm^{-1} with the exception of the four librational modes corresponding to rotations about the low moment of inertia O-O axis. The classification of observed phonon resonances to symmetry species was accomplished by the use of group theoretical selection rules. Figure 1 shows the results of

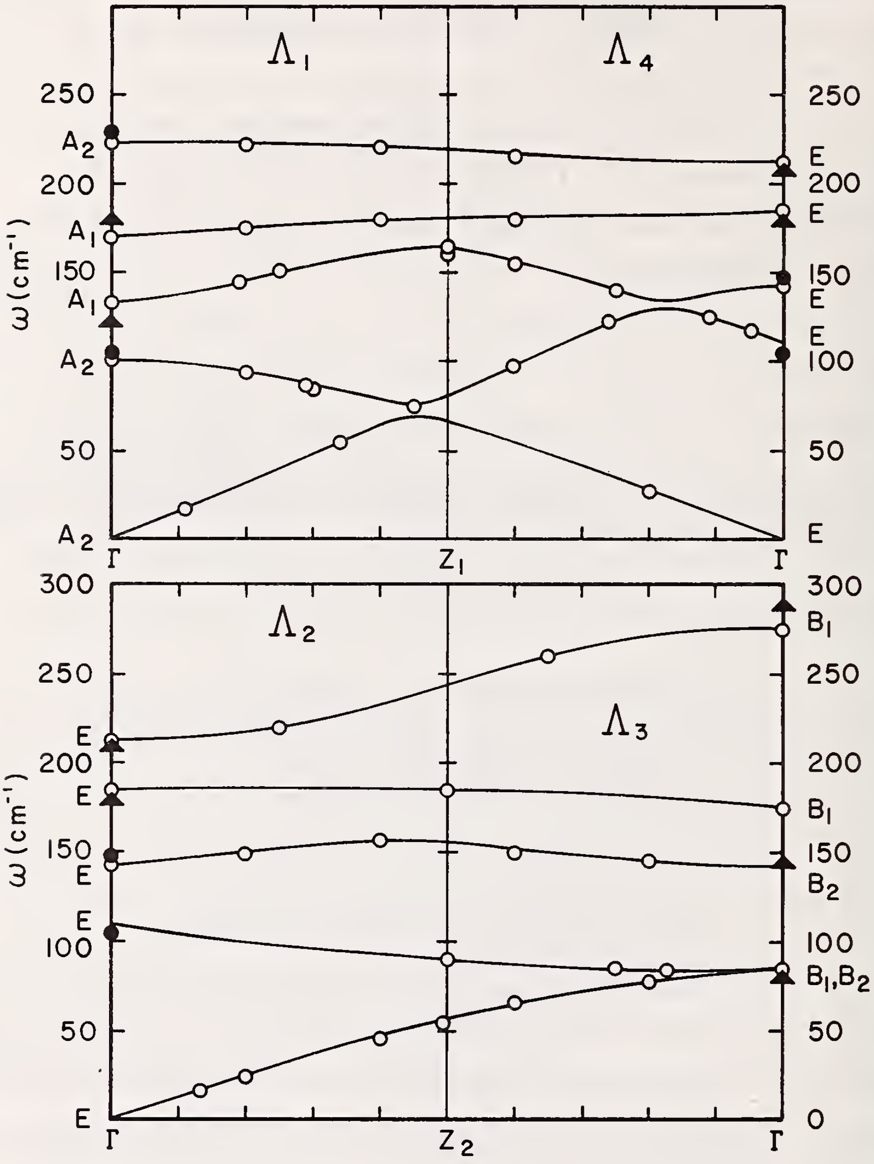

Fig. 1. Phonon dispersion curves in D_2O_2 along the [00ζ] direction. Open circles indicate present neutron measurements at 244K, solid triangles represent Raman data of Arnau *et al.*[1] at 190K, and solid circles are from the infrared measurements of Giguère *et al.*[2] at 90K.

the measurements of the 20 low energy branches and Γ point data from infrared and Raman studies[1,2]. The branches are plotted in pairs corresponding to those symmetry species which stick together at the Z-point (zone boundary). The solid lines are drawn as guides to the data. A model is under development for fitting the data and should result in valuable information concerning the hydrogen bonds and other forces which constitute the crystal potential.

---

1. J. L. Arnau, P. A. Giguère, M. Abe, and R. C. Taylor, *Spectrochim. Acta* 30A, 777 (1974).
2. P. A. Giguère and C. Chapados, *Spectrochim. Acta* 22, 1131 (1966).

LATTICE DYNAMICS OF KN_3 AT 298K

S. Trevino, M. Farr and H. Prask
(Picatinny Arsenal, Dover, NJ)

The metal azides are a class of compounds, the chemical properties of which range from quite stable to highly unstable. In comparison with other "energetic" materials, they also have relatively simple crystal structures and appear to offer the best prospects for a quantitative description of the lattice dynamics of a homologous series of explosive substances. KN_3, with two formula units per primitive cell and D_{4h}^{18} space group, is among the simpler of the metal-azide salts and has been the subject of considerable spectroscopic study, including very limited dispersion curve measurements[1].

The dispersion curves of KN_3 have now been measured much more completely with the primary emphasis placed on the highest symmetry direction [00μ]. Characterization of observed modes was greatly facilitated by the use of group-theoretical selection rules for neutron scattering[2]. Preliminary results are shown for the [00μ] direction in figure 1. A rigid ion force model calculation to fit all observed spectroscopic frequencies is in progress.

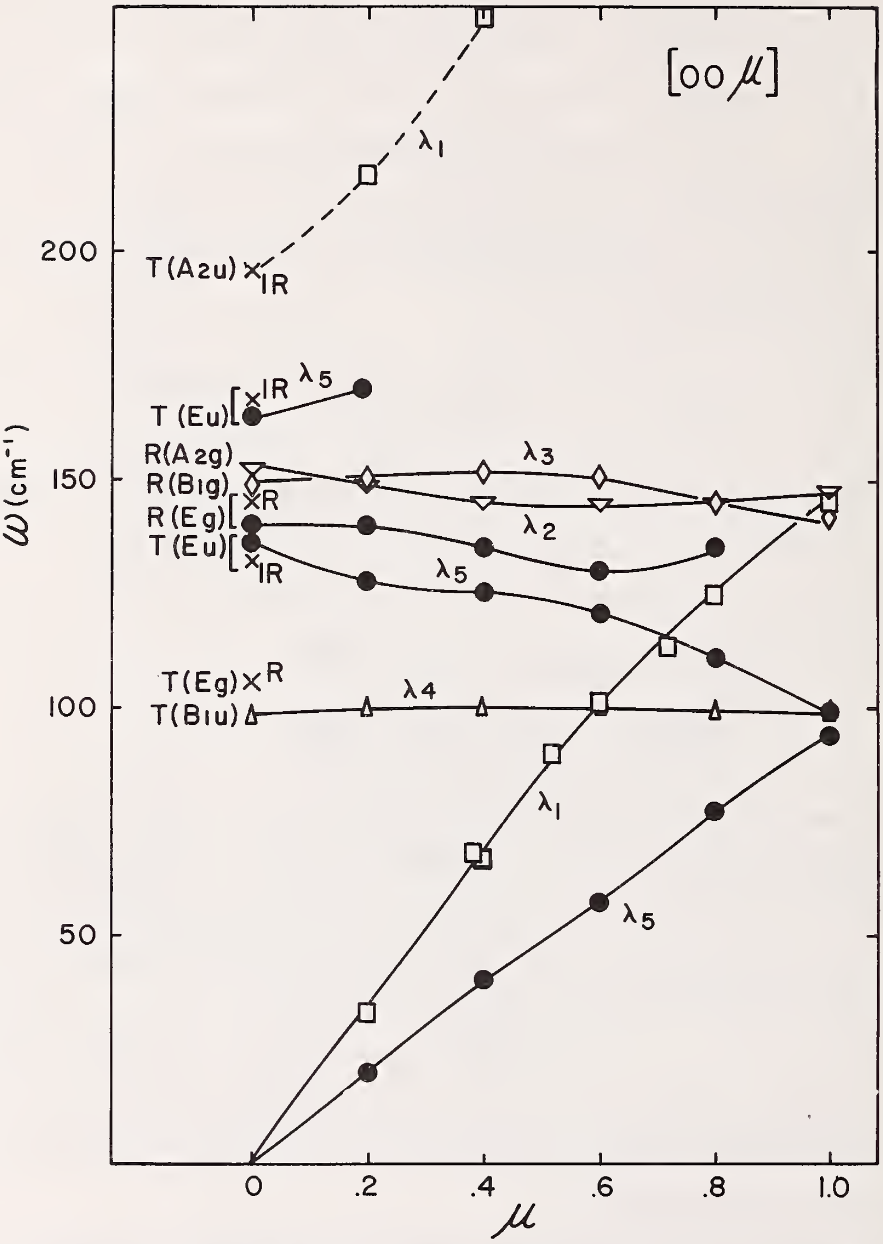

Fig. 1. Measured dispersion curves (various symbols), infrared (X,IR) and Raman (X,R) spectroscopic results and irreducible representations of [00μ] lattice modes in KN_3 at 298K ($33cm^{-1} \simeq 1$ THz).

---

1. K. R. Rao, S. F. Trevino, H. Prask and R. D. Miscal, *Phys. Rev.* B4, 4551 (1971).
2. R. C. Casella and S. F. Trevino, *Phys. Rev.* B6, 4533 (1972).

POLARIZED RAMAN STUDY OF AMMONIUM PERCHLORATE AT LOW TEMPERATURES

H. J. Prask
(Picatinny Arsenal, Dover, NJ)
and
G. J. Rosasco
(Inorganic Materials Division)

The dynamical behavior of NH_4^+ groups in NH_4ClO_4 (referred to hereafter as AP) has been the subject of considerable measurement and speculation because of the very low barrier to NH_4^+ rotation in this salt. However, it is only very recently that the structure has been determined at low temperature[1]. Following the structure determination, we have made a direct examination of Raman-active vibrational modes at low temperature (12 to 297K) in oriented single crystal AP and d-AP

The Raman spectrum of AP can be ascribed to three characteristic types of modes: the "external" lattice phonons, the "internal" modes of ClO_4^- group, and the "internal" modes of NH_4^+ group. The ClO_4^-iinternal modes are relatively temperature insensitive and correlate with the C_s site splittings of a tetrahedral ion in the D_{2h}^{16} space group at all temperatures. The NH_4^+ internal mode spectra show large temperature effects in going from 297K to 12K. At room temperature these spectra exhibit extremely broad unresolved bands in the characteristics NH_4^+ stretching and bending regions whereas at the lowest temperatures these bands are sharp and the site group splittings well resolved. The low temperature splittings and symmetries are compatible with the C_s site in D_{2h}^{16}. The external lattice mode region also shows dramatic temperature effects; in particular, the lowest frequency modes of B_{1g} and B_{3g} show anomalous damping with increasing temperature as shown in figure 1.

To characterize these modes as to rotational or translational nature, high resolution spectra were measured for AP at 18, 49 and 82K, and d-AP at 18K. The shift upon deuteration shows that the modes are predominantly translational in character. It is believed that the damping arises from anharmonic coupling of the large amplitude NH_4^+ rotatory motions with the B_{1g} and B_{3g} translations. Correlation of these results with changes observed in the internal mode spectra is in progress.

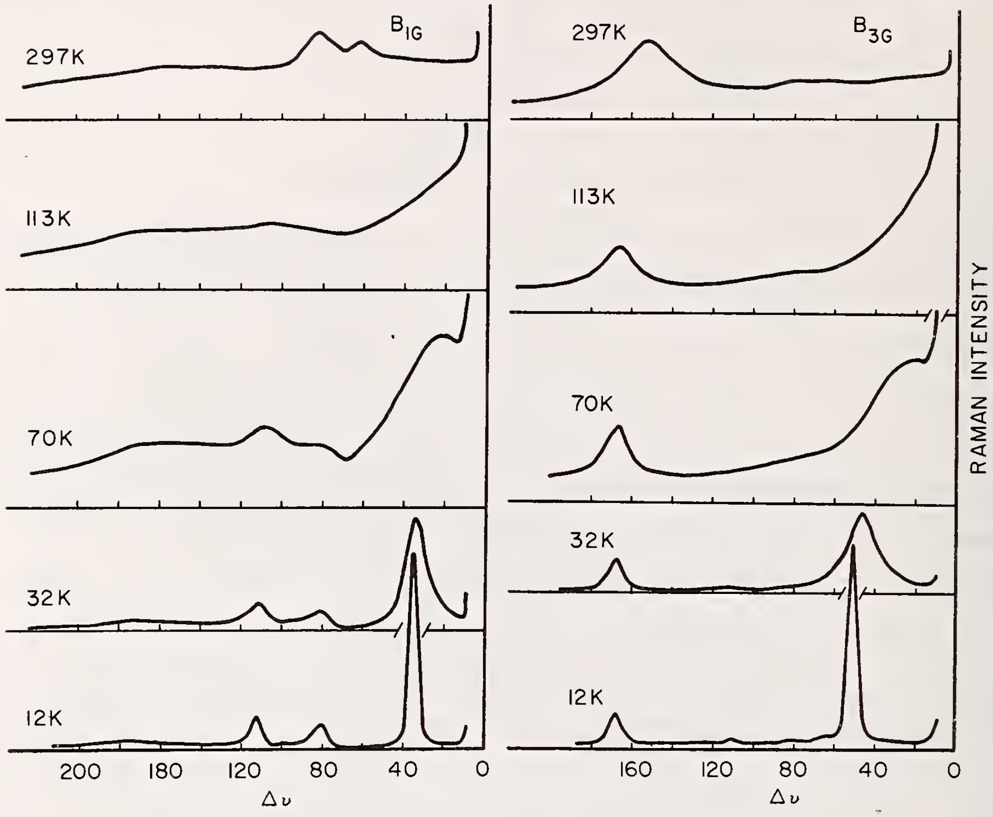

Fig. 1. Smoothed Raman Spectra as a function of temperature for the B_{1g} and B_{3g} modes in NH_4ClO_4. Relative intensities are arbitrary.

---

[1] C. S. Choi, H. J. Prask and E. Prince, *J. Phys. Rev.*, in press.

SUBLATTICE MAGNETIZATION OF RARE EARTH LAVES PHASE COMPOUNDS

J. J. Rhyne
(Naval Ordnance Laboratory, White Oak, MD)

Neutron diffraction provides a unique method for determining the magnetic sublattice magnetization in materials which have more than one magnetic site, for example the series RT_2 where R is a rare earth atom and T is either Fe, Ni or Co. We have continued work on the RFe_2 series compounds to obtain the temperature dependence of rare earth and Fe sublattice magnetization in the ordered range from 4K to the Curie temperature, typically 650-700 K. In the Laves phase materials, the rare earth-iron exchange is significantly weaker than the iron-iron exchange and results in a different temperature dependence for the magnetization of the two atom sites. At 0K, the rare earth element exhibits the free ion value for the magnetic moment, while the iron moment is significantly reduced to 1.6 - 1.8 μ_B (Bohr Magnetons) by band structure effects from the 2.2 μ_B observed in elemental iron. A theoretical model to explain the observed sublattice magnetization and its temperature dependence is being developed.

ANNEALED AMORPHOUS $TbFe_2$

J. J. Rhyne, H. Alperin and S. Pickart
(Naval Ordnance Laboratory, White Oak, MD)

One facet of the investigations of amorphous rare-earth transition metal compounds has been the nature of the recrystallization process and its effect on the magnetic properties. We have recently studied the effect of annealing on the coercive force and structure of initially amorphous $TbFe_2$. As the material became crystalline the coercive field abruptly increased from 100 Oe in the amorphous state to 3.75 kOe in the recrystallized state after a 525°C anneal. An analysis of the broadening of the magnetic and nuclear components of the Bragg lines

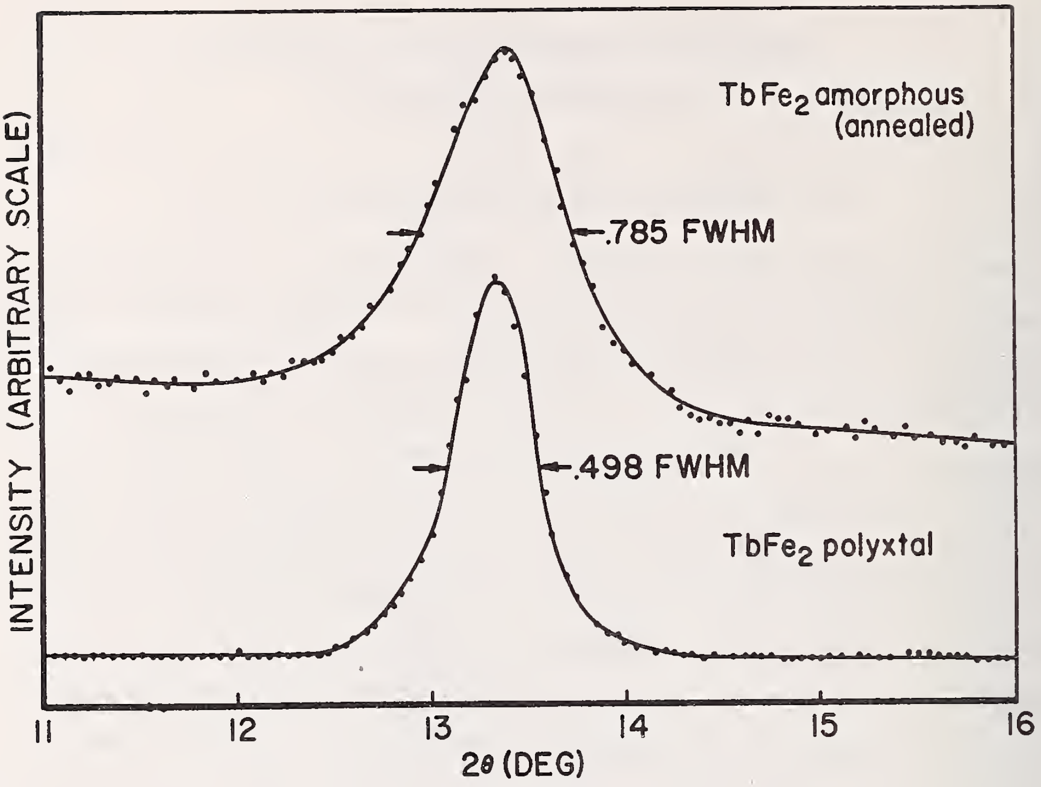

Fig. 1. Fine particle broadening of (111) reflection in recrystallized inititally amorphous $TbFe_2$.

(see figure 1) in the annealed specimen indicates that the amorphous structure is completely replaced by Laves phase microcrystallites of average size 100±10A after a 415°C anneal. Further annealing to 525°C increased the particle size to 150±10A, much smaller than the critical size for single magnetic domains.

Feasibility of this method for fabricating fine particle, high coercive force permanent magnets has thus been demonstrated; indeed, the resultant materials have a respectable energy product of 8.7 MGO (1 MGO = 10^6 ergs/cm^3), compared to 20 MGO obtained for the best commercially processed $SmCo_5$ magnets.

This large value of the energy product, achieved without optimization, means that the annealed cubic rare earth-Fe_2 compounds show considerable promise for permanent magnet material that do not require grinding, orientation and sintering.

STRUCTURAL STUDIES ON AMORPHOUS MAGNETIC ALLOYS

J. Rhyne, S. Pickart and H. Alperin
(Naval Ordnance Laboratory, White Oak, MD)

Our previously reported diffraction data[1] on amorphous $TbFe_2$ and new data on YFe_2 have been analyzed by Fourier transformation to give the atom correlation functions. This requires the separation of the magnetic component of the scattering and was accomplished by elastic diffraction methods above T_c in $TbFe_2$, whereas in YFe_2 it is negligible because there is no rare-earth moment.

Figure 1 shows this correlation function obtained for $TbFe_2$. A series of peaks is observed that correspond closely to combinations of rare-earth and iron metallic radii, as indicated. The height of the peaks agrees well with a model that predicts probabilities solely on the number of ways of achieving the various combinations--the so called dense random packing (DRP) model. The result for YFe_2 can almost be superimposed on Figure 1, as expected since the radii and neutron scattering amplitudes are approximately equal. These results lend considerable confidence to the model, and the next step will be to construct spin models, based on DRP positions, for comparison with our observed spin correlation functions from magnetic scattering.

We have also completed neutron diffraction studies on a series of Tb_xFe_{1-x} with x = .12, .45 and .75 (in addition to x = .33 described above). All the compositions were found to be amorphous, demonstrating one of the potential advantages of these amorphous alloys, namely that

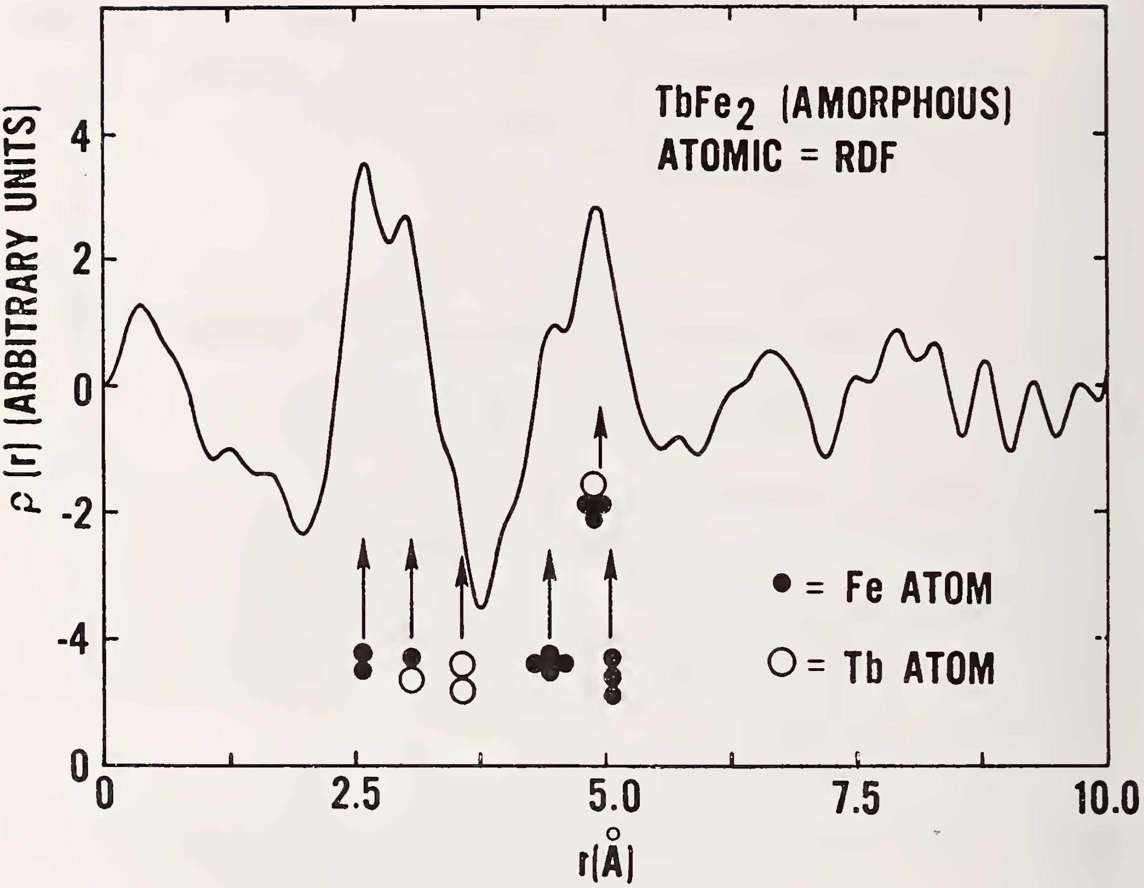

Fig. 1. Multiple Atomic Pair Correlation Function for TbFe$_2$. The arrows indicate combinations of Fe and Tb atoms in contact at their Goldschmidt radii (see text).

they can be fabricated over a wide composition range with no restriction to definite compounds, as are crystalline alloys.

---

[1] J. J. Rhyne, S. J. Pickart and H. A. Alperin, *Phys. Rev. Letters*, 29 1562 (1972).

DYNAMIC SPIN BEHAVIOR IN AN AMORPHOUS MAGNET

H. Alperin, J. Rhyne, and S. Pickart
(Naval Ordnance Laboratory, White Oak, MD)

and

D. L Price
(Argonne National Laboratory, Argonne, IL)

We have previously shown that the magnetic spin distributions in atomically amorphous materials are themselves also amorphous in nature. A second fundamental question to be answered regarding this new class of materials is, how do the magnetic moments fluctuate in time in response to some disordering influence? In particular, what are the nature of the excitations, what is the relation between their energies and momenta and how do these quantities for an amorphous magnet compare to the crystalline form? These questions have now been answered by means of neutron inelastic time-of-flight scattering measurements on an amorphous $TbFe_2$ sample prepared by sputtering and a polycrystalline sample of the same composition. Representative data (almost entirely of magnetic origin) are summerized in Figure 1. The most striking result is that at 295K (which is below the Curie point), in contrast to the crystalline ferrimagnet which exhibits the usual discrete, well-defined spin wave excitations, the spectrum of the amorphous magnet is smeared out and shifted to lower energies. This can be understood as due to the inability of the shorter wavelength (higher energy) excitations to propagate in a disordered structure. The occurrence of localized modes, the lack of atomic order and finite lifetime effects contribute to the smearing out of well-defined excitations.

Above the Curie temperature (443K) the peak at $\Delta E = 0$ is considerably broadened, indicative of paramagnetism.

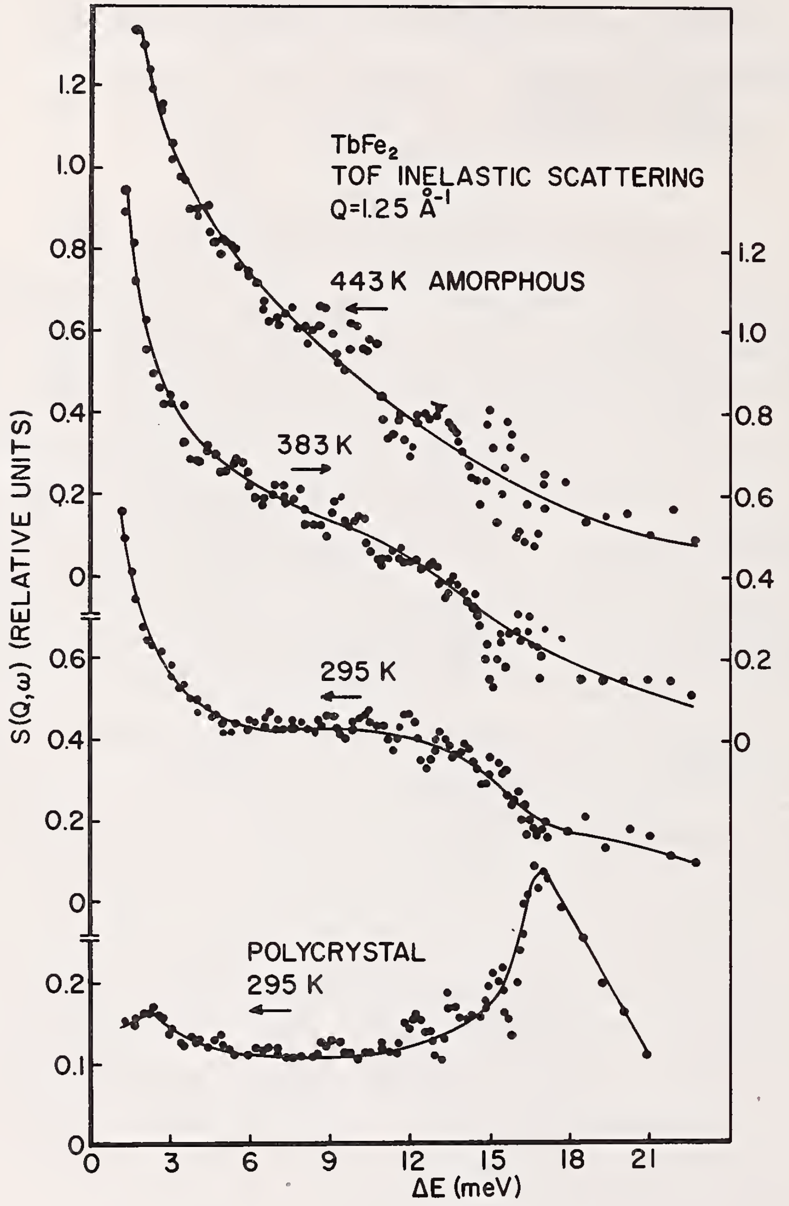

Fig. 1. Time-of-flight, neutron inelastic scattering spectrum of amorphous and crystalline $TbFe_2$ for a momentum transfer of q = 1.25$Å^{-1}$. The Curie temperature of amorphous material is ∿385 K.

SMALL ANGLE NEUTRON SCATTERING FROM AMORPHOUS MAGNETS

S. Pickart, H. Alperin and J. Rhyne
(Naval Ordnance Laboratory, White Oak, MD)

In addition to spin and atom correlations and excitation spectra, neutron scattering can provide information about long-wavelength static fluctuations in the magnetization density from amorphous magnets by the method of small-angle, quasielastic scattering. We have obtained striking new results by this method on the compounds $TbFe_2$ and YFe_2 that provide insight into the nature of the magnetic transition and the spontaneously ordered state in these materials.

Data for $TbFe_2$ are shown in figure 1. Two features are apparent in this figure: a weak "critical" anomaly near T_c and a giant, temperature dependent component below T_c. The scattering above T_c behaves like the critical scattering normally observed in a ferromagnet, but the spin correlation length remains finite at T_c instead of diverging. The hitherto unobserved component below T_c can be analyzed on a model analogous to particle-size broadening and yields a cluster size comparable to the correlation length at T_c. We have therefore proposed a new model for the amorphous magnetic transition in which the critical spatial fluctuations are "frozen-in" at T_c and survive as a sort of magnetic "graininess" below T_c of $\sim 10^2$ Å dimensions (not related to any structural inhomogeneities). The origin of this effect is as yet unknown but depends on the presence of a magnetic rare-earth since YFe_2 showed only scattering similar to that above T_c. However, the correlation length is much smaller in YFe_2, never reaching more than 10Å even at low temperatures, consistent with the fact that it does not order magnetically.

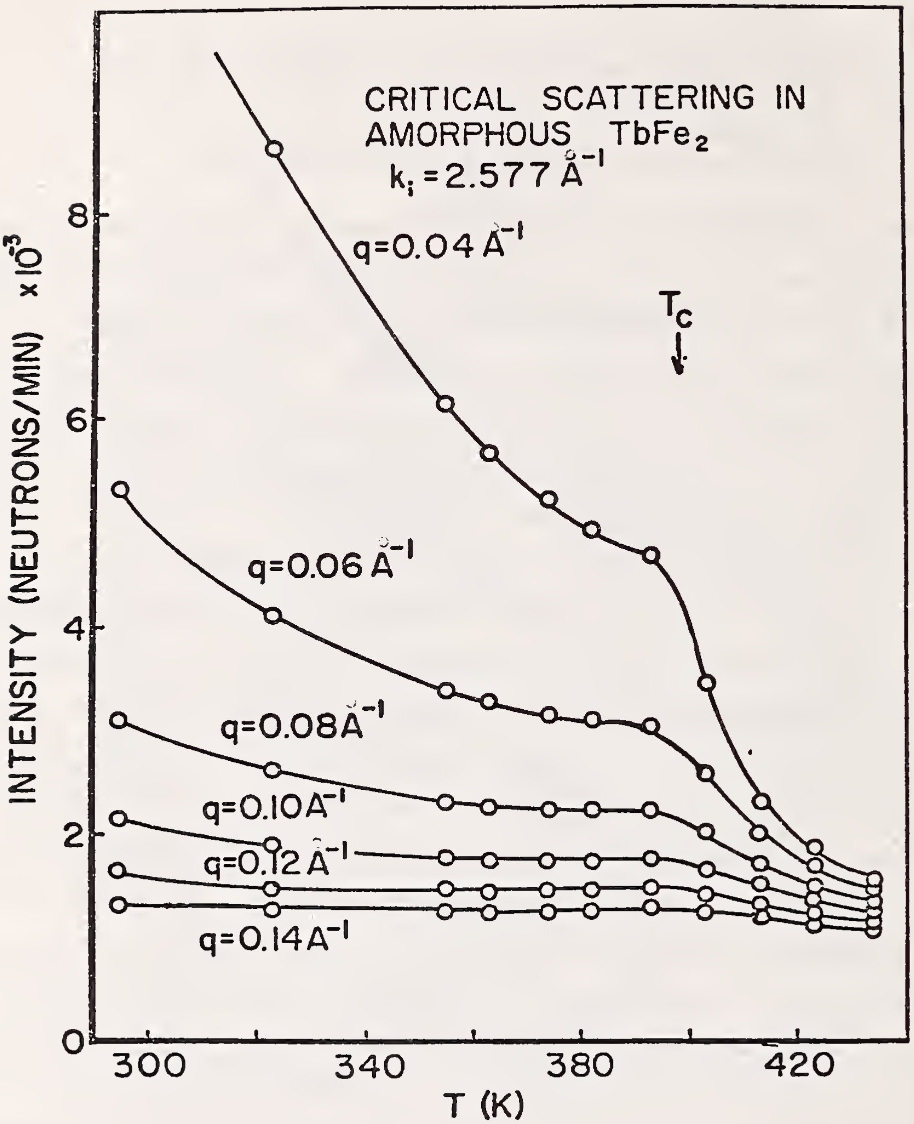

Fig. 1. Small angle neutron scattering from amorphous $TbFe_2$ in the critical region, corrected for absorption and instrumental background. (Data taken for q = $.02\text{Å}^{-1}$ would be off scale and are not plotted for convenience, while data at higher q continue to decrease slightly and are essentially flat with T.)

LATTICE DYNAMICAL STUDIES OF BERYLLIUM AT ELEVATED TEMPERATURES

H. Alperin, J. Rhyne, S. Pickart
(Naval Ordnance Laboratory, White Oak, MD)

Measurements of the phonon dispersion of beryllium have been extended to higher temperatures (778°C) in order to look for changes with temperature that could be correlated with the ductility anomaly. Measurements have also been taken in the $[10\bar{1}0]$ propagation direction, thus completing all three principal directions. A general fall-off of phonon energies with increasing temperature is noticed but there is no obvious indication of any anomaly. However, at room temperature, at the zone boundary of the $[11\bar{2}0]$ direction it is noticed that the LA(//) mode is degenerate with the TA(//) mode and not with the LO(//) mode. This is opposite to the situation in zinc and magnesium but similar to that in brittle holmium. It is now planned to carefully follow these mode orderings to see if there is a reversal at a higher temperature.

NEUTRON SCATTERING FROM AMORPHOUS SELENIUM

L. Rauber and V. Minkiewicz
(University of Maryland, College Park, MD)

The scattering function $S(\underline{Q},\omega)$ for amorphous selenium has been studied for a wide range of temperature, energy transfer, and momentum transfer. The measurements have established that the dominant features of $S(\underline{Q},\omega)$ consist of a sheet of scattering at zero energy transfer along with low energy phonon side bands. The sheet of scattering at zero energy transfer is the counter part of the Bragg scattering in the ordered phase. This zero energy component has a strong temperature dependence, and increases with decreasing temperature. This temperature dependence reflects the dependence of the Debye-Waller factor on temperature. A Debye model was used to fit this temperature dependence, and was found to be very satisfactory, yielding a Debye temperature of 94K. This value should be contrasted with that found for the ordered phase of 123K. This decrease in the Debye temperature in going from the system with long-range order to the amorphous state could be a general feature of all disordered lattices, and indicates an increase in the low energy part of the phonon density of states in the disordered state.

The phonon contribution to $S(\underline{Q},\omega)$ was then compared with the theory of multiple phonon scattering developed by Sjölanden. Using the same Debye temperature that was obtained from the elastic component (i.e. θ_D=94 K), the theory satisfactorily reproduces the observed spectra.

SCATTERING AMPLITUDES - SMALL ANGLE SCATTERING

C. S. Schneider
(U.S. Naval Academy, Annapolis, MD)

Prism refraction experiments using Ge, Cu and SiO_2 single crystal 90° prisms have been carried out. This work completes for the present our program of precise measurements of neutron scattering amplitudes. The refracted angles Δ can be fit to a trigonometrically exact equation for the refractive index deviation from unity: $\delta=\frac{1}{2}[\sin^2\phi-\sin^2(\phi-\Delta)]=\frac{N\lambda^2 b}{2\pi}$ where ϕ is the glancing angle of the beam from the first prism surface and Δ has been corrected for the small attenuation-dispersion and second order collimation effects. Thus the nuclear scattering amplitude for silicon becomes b_{Si}= 4.1478(16) fm while the new results are b_{Ge}=8.1898(16) fm and b_{Cu}= 7.646(6) fm. The quartz results are being analyzed.

Design and fabrication of the raised double-crystal small angle scattering (SAS) neutron diffractometer have proceded, with final assembly due late this year. The first pair of crystals used to raise the beam is mosaic copper and they serve to lower background nicely. The SAS diffractometer will initially use Bonse-Hart multiple reflection crystals in order that the low angles of diffraction (seconds of arc) from low density defects in the micron size range may be observed. This is the limit of application of SAS instruments so that all other size distributions will be more easily extracted from the diffraction intensities. This instrument can have a number of applications in the study of particle and defect size and density distributions, etc. in solutions and in solid state and polymer physics and metallurgy.

THREE AXIS NEUTRON SPECTROMETER

A. Cinquepalma, W. Rymes, J. M. Rowe, J. J. Rush, and R. S. Carter
and
H. Prask and S. Trevino
(Picatinny Arsenal, Dover, NJ)

The fabrication of this high-efficiency, high-versatility three axis neutron spectrometer has been completed. The two complete analyzer systems, which will be employed in order to increase the rate of data taking, have been constructed and tested. All shielding necessary to interface the spectrometer to the NBSR beam port has been designed and fabricated. This includes a pneumatically operated shutter located in the saddle between the spectrometer and the beam port which serves to close off the main neutron beam. The shutters insert can be replaced with an insert housing an LN_2 cooled beryllium filter, should this be desirable. Installation of the facility should be completed this coming fall.

ACTIVATION ANALYSIS SECTION: SUMMARY OF ACTIVITIES

D. A. Becker and P. D. LaFleur
(Analytical Chemistry Division)

The Activation Analysis Section of the Analytical Chemistry Division is physically located in the NBS Reactor Building. It has at present eleven full time members, and has programs in the areas of reactor neutron activation analysis, isotopic source neutron activation analysis, photon activation analysis, and polarography. These programs include both research projects and analytical programs on a wide variety of real sample matrices. Summaries of the work in these areas are included below.

1. Research Projects

a. Water Sampling and Sample Handling for Trace Element Analysis

S. H. Harrison, and P. D. LaFleur

The study of natural water systems to determine their trace and ultratrace element profiles is now of great interest to environmental chemists. The validity of the data being produced is directly related to the validity of the sampling procedures used. In the Analytical Chemistry Division there is a continuing project to study and develop water sampling and pre-analysis handling procedures for trace element profile determinations.

In order to investigate sampling protocols, an analysis technique capable of multielement determinations on a single sample was needed. Nondestructive neutron activation analysis of freeze-dried water was chosen for this purpose. This technique was used to evaluate a Teflon water sampler developed in our Division. This evaluation consists of replicate sampling studies and a comparison of results with those from a popular commercial water sampler. To demonstrate that the sampling, treatment and analysis procedure developed is applicable to environmental problems, a study of two waterways, suspected of abnormal trace element content, was initiated.

During this evaluation, the sampling, storage and handling techniques used are reevaluated, and changed if necessary in order to provide a convenient, workable and scientifically valid water sampling system.

Radioactive tracer studies for determining the trace element retention of 21 elements during the freeze-drying process have been completed. The results show that all but the most volatile elements (e.g. Hg,) are quantitatively retained in a residue resulting from the freeze-drying of 100 g of filtered river water. Talks presenting this data have been given at the 8th (1973) MARM of the ACS (American Chemical Society) and the Fall 1973 Meeting of the ANS (American Nuclear Society). A manuscript for publication in *Analytical Chemistry* is in preparation.

b. Forensic Activation Analysis - T. E. Gills, L. T. McClendon and D. A. Becker

In cooperation with the NBS Law Enforcement Standards Laboratory (LESL), the Activation Analysis Section of the Analytical Chemistry Division has a program for the examination and evaluation of the neutron activation analysis technique for the determination of gunshot residues (GSR). This technique analyzes for minute quantities of the elements barium and antimony, which are components of the primer material and are deposited on certain areas of the hand during discharge of a firearm.

Various methods for residue collection as well as the neutron activation technique for barium and antimony analysis, have already been examined and evaluated, and recommended procedures for both these areas are presently being written. The activation analysis procedure involves irradiating the residues in a nuclear reactor to make them radioactive, chemically separating the elements of interest (i.e., barium and antimony), and then quantitating them on a radioactivity detection system.

In addition to the procedures, information on the stability of residues on the hand as a function of time after firing, and on the evaluation of background levels of barium and antimony to be found in the general population is being obtained and evaluated. This program is contributing significantly to the scientific basis for the GSR technique, and will greatly assist law enforcement officers in their criminal investigations.

In another cooperative program with LESL, the Activation Analysis Section is evaluating the use of trace element profiles (TEP) for the unique identification of automobile headlight glass. The TEP technique entails the measurement of many trace elements in a specific piece of headlamp glass, and compares the concentrations of these trace elements to another piece of glass thought to come from the same source. This TEP technique has been used before in forensic analysis, and has been shown to be extremely useful in a number of areas.

c. The Application of a Mass Separator to Activation Analysis -

H. L. Rook, J. E. Suddueth and D. A. Becker

Iodine-129 is an isotopic species of considerable interest. It is produced in trace quantities by natural processes and has a half life of 1.59×10^{7} years. Thus, a steady state concentration of ^{129}I had been established in the biosphere prior to the advent of the nuclear age. Since that time, its concentration is believed to be steadily increasing. Thus, for health and safety reasons, a reliable method for determining ^{129}I concentrations in biological and ecological matrices is of great interest.

Due to the long half life of ^{129}I, low level counting techniques are not normally sensitive enough to enable its direct determination at natural levels.

A unique procedure has been developed for the determination of ^{129}I which couples neutron activation with mass separation. The procedure results in a significant improvement in sensitivity, thus allowing analyses to be performed on a variety of matrices which heretofore had not been investigated.

Mass separation is an extremely important tool as it offers the only means of separating ^{130}I from ^{126}I in the irradiation products.

This fact, plus the virtual elimination of other radioactive contaminants accounts for the improved sensitivity.

Method development and analytical procedures have been completed and analytical results at the 10^{-13} to 10^{-14} gram ^{129}I level have been demonstrated on real samples.

d. Radiochemical Separation of Selenium, Arsenic, Zinc, Cadmium, and Mercury in Environmental Matrices by Neutron Activation Analysis - E. Orvini, T. E. Gills, and P. D. LaFleur

Recently, heavy metal contamination of the environment has been recognized as serious pollution problem. Among these metals, particular attention is being given to Se, As, Zn, Cd, and Hg.

Neutron activation analysis is capable of high sensitivity for the determination of these elements. However, the most sensitive and useful (n,γ) reactions involve short halflived isotopes of As, Zn, Cd, and Hg, thus requiring chemical separation of these elements from the activated matrix.

A procedure has been developed for the simultaneous determination of selenium, arsenic, zinc, cadmium, and mercury in different environmental matrices. The radiochemical separation method involves the combustion of the samples, followed by reduction with carbon monoxide and volatilization of the metals at high temperature. The method was initially tested with radiotracer experiments; then by analyzing some NBS Standard Reference Materials. The procedure has been used to determine the Se, As, Zn, Cd and Hg concentration of some new Standard Reference Materials being prepared by the National Bureau of Standards.

e. Selective Radiochemical Separation of Chromium in Biological and Environmental Matrices - L. T. McClendon

Chromium has now been identified as an essential trace element in human nutrition. At high concentrations, or in different chemical states, it can also cause deleterious or toxic effects. There is thus a definite need for reliable methods of analysis for chromium at the trace level. A recent laboratory intercomparison on fossil fuels (coal, fly ash, fuel oil), which was conducted jointly by the Environmental Protection Agency (EPA) and the National Bureau of Standards (NBS), pointed up the sad state of chromium determinations as performed by most of the analytical community. Three standard analytical techniques were used--atomic absorption, emission spectrometry, and activation analysis. Of the twenty-two laboratories which reported results for chromium in fly ash--an environmental matrix in the process of being certified for a number of elements, including chromium, at NBS--only two were within the NBS recommended value of 131 ± 2 μg/g. The others ranged from 21 μg/g to 289 μg/g, with no discernible pattern. As a result of these round robin analyses, and other considerations, it became evident that more biological and environmental materials needed to be analyzed and certified for their chromium content.

When the chromium concentration is less than one microgram/gram, a radiochemical separation is almost obligatory to optimize the sensitivity and to eliminate interferences and the long time delay for analysis.

An efficient chemical separation for chromium is certainly advantageous for biological and environmental materials. A destructive NAA technique, using a tribenzylamine-chloroform solution to extract chromium, has been developed at NBS to determine the chromium content in five materials-fly ash, coal, orchard leaves, urine, and bovine liver. The results using this radiochemical separation technique have been good, and have agreed closely with those which were able to be analyzed nondestructively by NAA.

f. Activation Analysis Using an Isotopic Californium-252 Source - P. D. LaFleur and J. E. Suddueth

Previous research efforts in the area of Cf-252 activation analysis have included the determination of specific elements in metal organic Standard Reference Materials, the evaluation of lead analysis for paint samples, and the production of an experimental set of sensitivity tables for Cf-252 activation. During the past year, a new set of eight (8) larger size Cf-252 sources were obtained, and subsequently evaluated as to neutron flux variation and absolute neutron flux obtainable. The absolute flux value obtained was $4.6 \times 10^{7} \text{n} \cdot \text{cm}^{-2} \text{sec}^{-2}$ at the maximum thermal neutron flux position. These measurements were made on a copper foil, using the $Cu^{63}(n,\gamma)Cu^{64}$ nuclear reaction.

An effort is currently underway to evaluate the best possible precision and accuracy obtainable with these sources. To date the results indicate that a precision of ±0.3% is obtainable, with an accuracy slightly greater than this. These procedures are presently being evaluated in the analysis of sodium and chlorine in a clinical blood serum reference material.

g. Photon Activation Analysis Using the NBS LINAC - R. Lindstrom and D. Becker

With George Lutz on a leave of absence in West Berlin, the Activation Analysis Section had need for someone to take over the LINAC activation facility. We were fortunate in having Richard Lindstrom agree to take over this responsibility, and he is in the process of evaluating a number of photon activation analysis systems for the determinations of elements not readily analyzed by neutron activation techniques. The elements of primary interest include nickel, lead, calcium, and magnesium. Several light elements are determinable in a variety of matrices through the use of short-lived radionuclides. These include carbon, nitrogen, oxygen, and silicon. In addition, some effort is being made to develop analytical capabilities for several elements which are determinable by neutron activation techniques but not easily determined by other trace element analytical techniques, such as arsenic and antimony.

h. High Sensitivity Activation Analysis - D. A. Becker and J. E. Suddueth

Activation Analysis has progressed from its comparatively recent beginnings into one of the most versatile and useful trace element analytical methods currently available. It has the capability of analyzing almost any matrix, for many different elements, either destructively or non-destructively. At the National Bureau of Standards, activation analysis must compete with the other trace element techniques which are available, and must consistently provide analytical results which are both accurate and precise in order to remain competitive.

These requirements for high accuracy and precision have evolved into an active program of critical evaluation of those variables and factors which affect all aspects of the technique. This had led to a systems analysis approach to evaluation, in which the technique has been divided into four specific areas of involvement. The first is Sampling and Sample Handling, and includes obtaining the sample as well as all manipulations up until irradiation. Area 2 is called Irradiation Parameters, and includes all aspects of irradiation. This irradiation may be by nuclear reactor, LINAC, or by any other irradiation source. This aspect was discussed in last year's Progress Report, concerning the neutron flux characterization of the NBS Nuclear Reactor. Area 3 is Radiochemical Separations and is the only area which is not absolutely necessary for each analysis. Of interest in this area would be dissolution and separation procedures. Area 4 is Detection Systems, and is the subject that was investigated this past year, namely, the evaluation of accuracy and precision in conventional gamma-ray counting systems.

It should be mentioned at this point that some of the factors to be discussed may seem relatively minor to some analysts, with magnitudes of one or a few percent each. Their significance to an organization like NBS is obvious. In addition, however, if such variables are left uncontrolled and two or more should sum, they may very well adversely affect even routine analytical results. It is important, therefore, that any good analyst be at least aware of such potential problems.

Basically, most activation analysis detection systems consist of a single gamma-ray detector [Ge(Li), Ge, or NaI(Tl)] and associated electronics, with a sample positioning device of some sort. With such a system, a variety of sample radioactivity levels and sizes can be counted rather easily. What is often not realized is that even relatively small differences between sample and standard, or from sample to sample, in any one of many variables can often result in a significant bias in the resulting count rates.

In an attempt to experimentally evaluate the systematic biases associated with gamma-ray counting, they were separated into eight (8) sub-groups as follows: Configuration, Positioning, Density, Homogeneity, Intensity, Radioisotopic Purity, Peak Integration, and Nuclear Constants. These sub-groups were then individually examined and investigated, and the results will be published in the open literature.

i. The Determination of Oxygen in Human Tissue Using the Nuclear Track Technique - B. S. Carpenter

While the reactor is being used to analyze materials that touch our everyday lives, chemists in the Activation Analysis Section are also using it to expand the frontiers of medicine. Several lines of evidence suggest that the amount and distribution of oxygen in human tissues may be critical for certain diseases. A low level of oxygen in the brain, for instance, has been linked with mental disorders. And certain types of tumors are characterized by either too much or too little oxygen.

But until the "Nuclear Track Technique," it was difficult for "in situ" measurement and location of oxygen in tissues. It happens that ordinary oxygen (oxygen16) is not easily measurable at the trace level, but oxygen-17 is. Therefore, the first step is to replace a fraction of the oxygen in the body by oxygen-17 (which is not as difficult as it sounds) and the samples, say from the brain, are put into the reactor mounted on a film of plastic. When the oxygen-17 is irradiated, it ejects alpha particles that produce tracks in the film, tracks that appear similar, though of course smaller, to the tail of a comet. By measuring and analyzing these tracks, and counting them, one can accurately tell the amount and location of the oxygen-1 in the tissue being studied. This is a method used in a collaborative program with the Weizmann Institute of Science in Israel. This work is continuing in an attempt to evaluate and use the information thus gained for medical diagnostic and research purposes.

j. Effect of Progressive Etching on Fission Track Ages - G. M Reimer

Fission track ages of some minerals are often interpreted as cooling ages not related to any discrete thermal event. This is particularly true of apatite, for which fission track ages are usually younger than those determined by other radiometric methods using the same rock sample. These younger ages are the result of annealing the spontaneous fission tracks which, in effect, reduces the track etching rate. This lower etching rate, with respect to the bulk etching rate of the material, samples in fewer fission tracks being revealed than if the sample were unannealed.

Special consideration must be given to the etching of samples so that ages obtained can be related on a common basis. As a phenomenon of subjective optical counting criteria and etching, the observed number of tracks increases as the etching proceeds. Ultimately, an "etching plateau" is reached where the track density remains constant. An annealed sample would have a lower plateau than an unannealed equivalent. In practice, it is usually convenient to etch to a degree short of the plateau because of increasing interference from enlarged crystal defects and overetched tracks. It is also difficult to know exactly when the plateau has been reached.

An experiment with apatite shows that the etching plateau is reached at different times for an annealed sample and an unannealed sample. Apatite was annealed so that no spontaneous tracks were revealed even by prolonged etching. This annealing was done because the spontaneous tracks may have already been partially annealed and the maximum plateau might not be reached. The apatite was irradiated to induce fission. One portion of this sample was annealed again, but this time only partially. The average true track length equaled 77% of the average true track length of the other portion (measured after a 30-sec etch). Etching was with 5% HNO_3, 20 °C, in five-sec intervals. The results indicate that the spontaneous-to-induced ratio changes as a function of etching time.

If fission track ages of the same mineral are to be compared or related in any way on an absolute basis, particularly for a study of a localized geologic area, it is critical that the samples be etched identically. This is especially important when the spontaneous tracks of some samples appear to be underetched, since they may be, in fact, partially annealed. Only then can meaningful interpretations of the thermal effects be made.

k. Polarographic Analysis - E. J. Maienthal

During the past year the emphasis in the polarographic laboratory has been largely on the analysis and development of methods for the analysis of a large number of both essential and hazardous trace elements in a variety of biological and environmental materials. The methods usually involve wet or dry ashing of the sample, sometimes a simple chemical separation (such as solvent extraction or ion exchange) and polarographic determination. Trace quantities of aluminum, antimony, arsenic, cadmium, copper, iron, lead, nickel, titanium, zinc and zirconium have been determined in matrices such as orchard leaves, spinach, freeze-dried urine, blood, river bottom sediments, fossil fuels, and borosilicate glass.

2. Standard Reference Materials (SRM) Analyses

Much of the Section's efforts during the past year have directed towards the development of high precision and accuracy in neutron activation analysis, with the primary aim being the analysis and certification of NBS Standard Reference Materials.

In total, the Activation Analysis Section during the past year has analyzed 185 SRM samples, while determining 463 elemental concentrations. These analyses encompassed a variety of materials, including coal, fly ash, fuel oil, glasses, urine, orchard leaves, sediments, cholesterol, and steels. For a number of the above mentioned SRM's, the Activation Analysis Section was responsible for a large fraction of the total effort applied towards their production and certification. These materials are discussed further below.

a. Biological SRM's - P. D. LaFleur and D. A. Becker

Biological SRM's already issued include Orchard Leaves (SRM 1571) and Bovine Liver (SRM 1577). At present, SRM 1571 has 20 elements certified and information values for 9 additional elements. Of these 29 elements, over half were determined by activation analysis or the nuclear track technique. SRM 1577 presently has 11 elements certified, with information values on 12 additional elements. Again, over half of these elements were determined by nuclear techniques. Several additional biological materials are under development at present, including a Tuna Fish research material, a Spinach SRM, and several additional botanical Standard Reference Materials.

b. Fossil Fuel SRM's - P. D. LaFleur and D. A. Becker

Emissions from the burning of fossil fuels is a possible major source of contamination for some trace elements. A joint program between the Environmental Protection Agency and NBS has resulted in a characterization of samples of coal and coal fly ash as well as fuel oil for use as Standard Reference Materials. These materials were analyzed using a number of different analytical techniques, with a major role being provided by the nuclear techniques.

The approach that has been used was to obtain samples of the required materials for processing and issuance as Standard Reference Materials.

This processing included insuring the material had a limited particle size range, proving homogeneity on the final bottles of samples, and finally analyzing and certifying these materials for trace element content content.

At present, the Trace Elements in Fly Ash (SRM 1633) is ready to be issued. The certificate has been completed and is ready for printing. The Fly Ash will be certified for 12 trace elements, with information numbers on 7 additional trace elements. This material will be available for sale in the very near future.

The Trace Elements in Coal (SRM 1632) is also ready to be issued. The analyses have been completed and the certificate is ready for printing. This material will be certified for 14 trace elements with information numbers on 5 additional trace elements. This Standard Reference Material will also be available for sale in the very near future.

The Trace Elements in Residual Fuel Oil (SRM 1634) is undergoing final analyses. At present 13 trace elements have been determined in this material. Four of these elements are currently able to be certified, while many of the others are undergoing analysis by the second analytical techniques. This material should be finished late in 1974.

c. Trace Elements in Water SRM - H. L. Rook and J. Moody

The National Bureau of Standards is currently developing two mercury in water standards. One standard is in the ppm concentration range, to be used as a spike with natural water samples. The second is in the ppb concentration range and will be used as a benchmark standard. The most important criteria in developing these standards, as with all SRM's issued by NBS, are homogeneity and stability of the certified species. For mercury in water, homogeneity is no problem. Stability, however, has been a constant problem for anyone storing solutions containing trace mercury. Mineral acids have been employed as stabilizing agents and are usually successful in the ppm range and above. However, in the ppb concentration range, significant mercury is often lost to the container walls, even when large amounts of acids are added. In an attempt to solve this problem, a study of various mechanisms to stabilize trace mercury solutions was undertaken.

After several attempts, a successful method has been developed for stabilizing part-per-billion ionic mercury in water. Tracer studies using carrier-free mercury-203 were conducted in order to evaluate the various methods. Finally, a method using ionic gold to inactivate the active sites on pre-cleaned quartz containers was found to be successful. Analytical methods for the determination of mercury at the ppb level have been developed using neutron activation analysis, isotope dilution spark source mass spectroscopy, and atomic absorption spectroscopy. The neutron activation method used a modification of the combustion separation developed for the determination of mercury in biological materials. Blank levels were kept low by the use of ultra-pure reagents and by isolating all work to a class 100 clean room. Precision of the method was estimated to be ±6% based on replicate analyses.

A second program for Trace Element in Water SRM's has been initiated. This program is to develop a standard containing 8 trace elements, at these levels, which are stable in solution together. Preliminary research on this problem has just begun.

d. Environmental SRM's - H. L. Rook and J. K. Taylor

In addition to the above mentioned biological, fossil fuel, and water SRM's, all of which could be considered environmental standards, the Analytical Chemistry Division, in cooperation with the Office of Standard Reference Materials, is presently in the process of obtaining and preparing two additional SRM's specifically for environmental standards. These are a fresh water sediment material, and an urban air particulate material. The sediment Standard Reference Material is in the process of being gathered near Chicago, and it will then be freeze-dried, pulverized, and particle sized before bottling as a Standard Reference Material. When this has been completed, analysis for homogeneity and certification will begin.

Procedures for the gathering of a large quantity of air particulate from the St. Louis area have been initiated. However, a number of difficulties have been encountered which have delayed the project significantly.

As soon as a sufficient quantity of urban air particulate has been gathered, the material will also be thoroughly mixed and bottled, measured for trace element homogeneity, and then if suitable, analyzed for trace element content and certification.

3. Cooperative and Service Analyses

In addition to the many Standard Reference Materials, a large number of additional analyses were made on non-SRM materials. These include both the cooperative analyses, where the analysis is made on samples of mutual interest to NBS and some other organization, and also service analyses, where the technical expertise of the Activation Analysis Section is required by NBS or another Government agency.

During the past year the Activation Analysis Section has had a total of nine different cooperative and service analytical projects, resulting in the analysis of 58 different samples and 251 elemental determinations. These samples were obtained from four other NBS laboratories, and a number of other Government agencies, including the National Institutes of Health, the National Institute of Occupational Safety and Health, Environmental Protection Agency, Philadelphia Veteran's Administration Hospital, the Federal Highway Administration, Naval Research Laboratory, and the Department of Transportation. Determinations included 29 different elements, in matrices ranging from biological materials such as urine and thyroid granules, to brake fluid, concrete, clays, and a tungsten-aluminum alloy. In particular, two extended programs of analyses were undertaken in cooperation with another NBS laboratory and the National Institute of Occupational Safety and Health. There are described further below.

a. Clay and Clay-based Papers Study - S. H. Harrison

The cooperative analytical program initiated last year with the Fiberous Systems Section at NBS has continued. This laboratory is concerned with the trace element profiles of a variety of clays and clay-based papers.

The analyses were performed for both short-lived and long-lived radionuclides. Eight short-lived elements were determined after irradiation in the thermal column pneumatic tube facility (RT-5), while 19 longer-lived radionuclides were determined after irradiation in RT-3. The results to date include the analysis of 14 samples for as many as 27 trace elements. This program should be completed in the near future.

b. Determination of Toxic Trace Elements in Body Fluid Reference Sample - T. E. Gills, L. T. McClendon, E. J. Maienthal, D. A. Becker

The measurement of elemental concentrations in body fluids has been widely used to give indication of exposure to certain toxic materials and/or a measure of body burden. To understand fully the toxicological affect of these trace elements on our physiological system, meaningful analytical data is required along with accurate standards or reference samples. The National Bureau of Standards has prepared for the National Institute for Occupational Safety and Health (NIOSH) a number of reference samples containing selected toxic trace elements in body fluids. The reference samples produced include mercury in urine at three concentration levels, five elements (Se, Cu, As, Ni, and Cr) in freeze-dried urine at two levels, fluorine in freeze-dired urine at two levels, and lead in blood at two concentration levels. These reference samples have been found to be extremely useful for the evaluation of field and laboratory analytical methods for the analysis of toxic trace elements. In particular, the use of at least two calibration points (i.e., "normal" and "elevated" levels) for a given matrix provides a more positive calibration for most analytical techniques over the range of interest for occupational toxicological levels of exposure.

Neutron activation analysis was used to determine the mercury in urine, and the five trace elements in freeze-dried urine. For the mercury in urine reference material, mercury-203 tracer was used to establish suitable storage conditions for stability. The analysis was made using mercury-197, with a chemical separation of the mercury before counting. For the selected trace metals in freeze-dried urine, they were all analyzed using a radiochemical separation after neutron irradiation. The arsenic, copper, and selenium were separated together as the sulfides, while nickel was determined as the dimethylglyoxine and chromium by the solvent extraction procedure described earlier in this report. Copper and nickel were also determined polarographically in the samples, with good agreement to the neutron activation results.

4. Facilities

During this past year, there were two particular facilities projects in the Activation Analysis Section which may be of interest and are included here. The first concerns our irradiation capability, namely, the installation and evaluation of RT-6 pneumatic tube facility. The second concerns the re-evaluation and improvement of our radioactivity detection capabilities. These two projects are described below.

a. Pneumatic Tube Facility RT-6 - J. E. Suddueth and D. A. Becker

The RT-6 pneumatic tube facility has been completed and was inserted during the past year. This facility is located in the vertical tube location VT-3 in the reactor reflector area. It uses the small size polyethylene rabbit (7/8" dia.) as the irradiation container, and should have irradiation characteristics somewhere between RT-3 and RT-4. The prime advantage of these facility is the location of the send-receive terminals which are located in two of the B-wing hot laboratories. These locations will allow the use of RT-6 for very short-lived radionuclides, with counting on the germanium-lithium detector systems, also located in the B-wing.

Initial testing of this facility revealed that there was a small tritium leak somewhere in the outer containment shell of the terminal. Thus, the tube was shut down until the leak could be located and repaired. This repair is scheduled to take place during the heat-exchanger replacement shut-down, in the fall of 1974.

b. Evaluation and Modernization of Radioactivity Detection Systems - R. W. Shideler and D. A. Becker

Evaluation of the existing radiation detection systems in this Section reveal two serious shortcomings. First of all, there was a severe lack of large-memory pulse height analyzer systems available for use. Second, an automatic sample changer was urgently required to automate the counting of large numbers of samples for certain of our projects. Both of these problems are well on their way toward solution at the present time. Two 4096-channel pulse height analyzers of modern design, each with their own computer compatible magnetic tape deck, have been obtained and should be received shortly. In addition, an automatic sample changer has been designed in conjunction with the Special Analytical Instrumentation Section of the Analytical Chemistry Division, and is currently being constructed. This device should provide jam-free operation with multiple sample capabilities for the counting of up to 20 samples without stopping. The acquisition of these instruments should materially assist the Section in the completion of its projects.

5. Conclusions

The Activation Analysis Section of the Analytical Chemistry Division has been active in a large number of significant research areas. During the past year, they have analyzed for a total of 39 different elements, in 243 samples, for a total of 713 elemental determinations. They have also made significant progress in a number of very difficult research areas. Work is continuing on many of these projects, as well as in several additional projects recently initiated.

STANDARD NEUTRON FIELDS AND INTEGRAL REACTION RATES

J. A. Grundl, D. M. Gilliam, V. Spiegel, Jr., and I. G. Schroeder
(Neutron Standards Section)

Efforts this year continue to be centered around the reactor thermal column facility. Preparing NBS double fission chambers for operation at laboratories around the world, performing fissionable deposit mass assays and carrying out preliminary thermal fission yield determinations were prominent activities during the period covered by this report. Once again interaction with reactor technology via the Interlaboratory LMFBR Reactor Rate Program (ILRR) was the strongest motivation behind much of the work undertaken. Preparations for the new Intermediate-Energy Standard Neutron Field (ISNF) was carried forward: final construction, hazards evaluation, and operational proof-testing are complete. A brief outline of these activities follows.

1. Fission Chambers for Off-Site Operation.

The NBS double fission chamber is a high-resolution double ionization chamber of minimized volume and mass designed to measure absolute fission rates in a wide variety of neutron environments. The assembled fission chamber, internal pieces, and two fissionable deposits are shown in figure 1. Performance characteristics, summarized in last year's Reactor Radiation Division Report, were investigated more systematically this year: The linearity of chamber dead time was established to random pulse rates of up to $2x10^4$ sec, and was observed to be proportional to pulse width over that range. The absolute efficiency of the chamber was found to be nearly linear for fissionable deposit thickness from ∿500 $\mu g/cm^2$ down to ∿5 $\mu g/cm^2$. The results of this latter investigation are shown in figure 2. During the year fission chambers were constructed and checked out for operation in the following programs: (1) continuation of international comparisons of absolute fission rate measurement scales; (2) interlaboratory flux measurements sponsored by the Bureau Intenational des Poids et Mesures, Paris (Intercomparison of 14 MeV neutron fluxes at Van de Graaff accelerators); (3) absolute fission rate determinations in the CFRMF Reactor, at Aerojet Nuclear Corp., and the Big Ten critical assembly at the Los Alamos Scientific Laboratory. Each of these neutron environments presented unique operational requirements for the fission chamber, and each requirement was met by means of beam measurements at the NBS Reactor thermal column.

2. Mass Assay of the NBS Fissionable Deposits

At the present time the National Bureau of Standards set of fissionable deposits includes five major isotopes, ^{239}Pu, ^{235}U, ^{238}U, ^{237}Np, and ^{233}U, from more than a dozen batches of fissionable materials. Masses of the fissionable deposits are based on interrelated measurements of specific alpha activities, isotopic concentrations, and fission fragment emission rates. When completed each fissionable deposit will have associated with it an absolute alpha disintegration rate, and a fission rate ratio which will establish the mass relative to one or more reference fissionable deposits of the same type. The reference deposits are kept aside from the normal course of programmatic fission rate measurements.

Fission rate ratios obtained at the reactor thermal column from back-to-back fission counting of fissile deposit pairs are used to derive certain principal isotope mass ratios: (1) a mass ratio of ^{238}U in natural uranium deposits to ^{235}U in an enriched uranium deposit based on the well-established isotopic concentration of ^{235}U in natural uranium;* (2) an isotopic mass ratio between ^{235}U and ^{239}Pu deposits based on the thermal cross section ratio $\sigma_f(^{235}\mathrm{U})/\sigma_f(^{239}\mathrm{Pu})$; and (3) mass transfer ratios among deposits of the same principal isotope, in particular ratios for very light 5 μg/gcm^2 ^{235}U deposits required for monitoring high-flux fast-neutron irradiations. These thermal fission comparison

---

*The ^{235}U atom fraction in natural uranium, $7.201 \pm 0.0010 \times 10^{-3}$ for NBS Standard Reference Material ("Belgium Congo" pitchblende), is not observed to vary by more than ±0.1% for uranium processed from other geological formations.

measurements are carried out in a 5 cm diameter thermal-neutron beam emerging from the thermal column. Proper averages are taken for fission chamber rotation and electronic interchange. In order to circumvent errors associated with non-1/v and epithermal response differences of ^{235}U and ^{239}Pu, auxiliary ratio measurements were performed in a monoenergetic 0.025 eV beam. The agreement between the monoenergetic and the Maxwelliam-averaged results obtained at the thermal column was better than 1%.

3. Thermal Fission Yields for Long-Lived Fission Products.

Fission products with half-lives in the range of a few weeks to a few decades and including stable end products like ^{148}Nd are important for monitoring fission rates in large-scale reactor fuel tests and in the design of reactor core reloadings. Two unique capabilities at NBS make it possible to undertake with relative ease, new and entirely independent measurements of these fission yields: (1) intense thermal fluxes at the NBS reactor thermal column; and (2) the capability to measure absolute fission rates over a large dynamic range. Preliminary experiments involving ^{235}U are complete and fission yields for five long-lived fission products have been reported. These measurements were carried out in collaboration with Hanford Engineering Development Laboratory, Aerojet Nuclear Corp., and Argonne National Laboratory.

4. The Intermediate-Energy Standard Neutron Field.

Intermediate-energy Standard Neutron Field (ISNF) represents an advanced effort to create a primary standard neutron field with a smoothly varying energy spectrum between 1 keV and 5 MeV. This energy range is just that of core neutrons in presently conceived U.S. fast breeder reactors. The ISNF design is fundamentally simple: a fission spectrum source driving a one-dimensional geometry of graphite and boron-10. The spherically-symmetric ISNF cavity arrangement, is assembled at the center of the reactor thermal column where it will be driven by fission source disks operating at a total fission rate of up to 10 watts. Construction of the ISNF is essentially finished with the exception of the

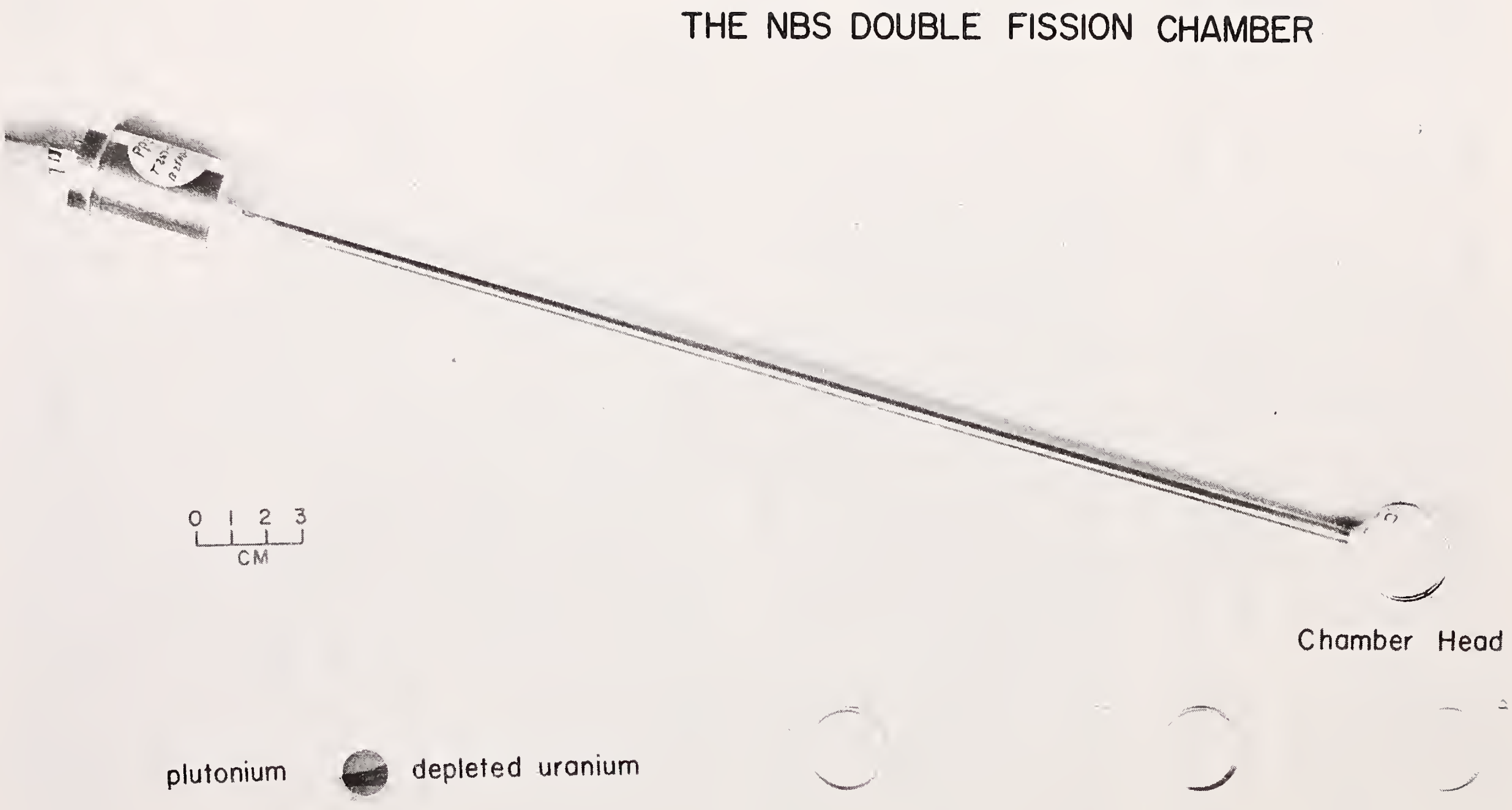

Fig. 1. The NBS Double Fission Chamber.

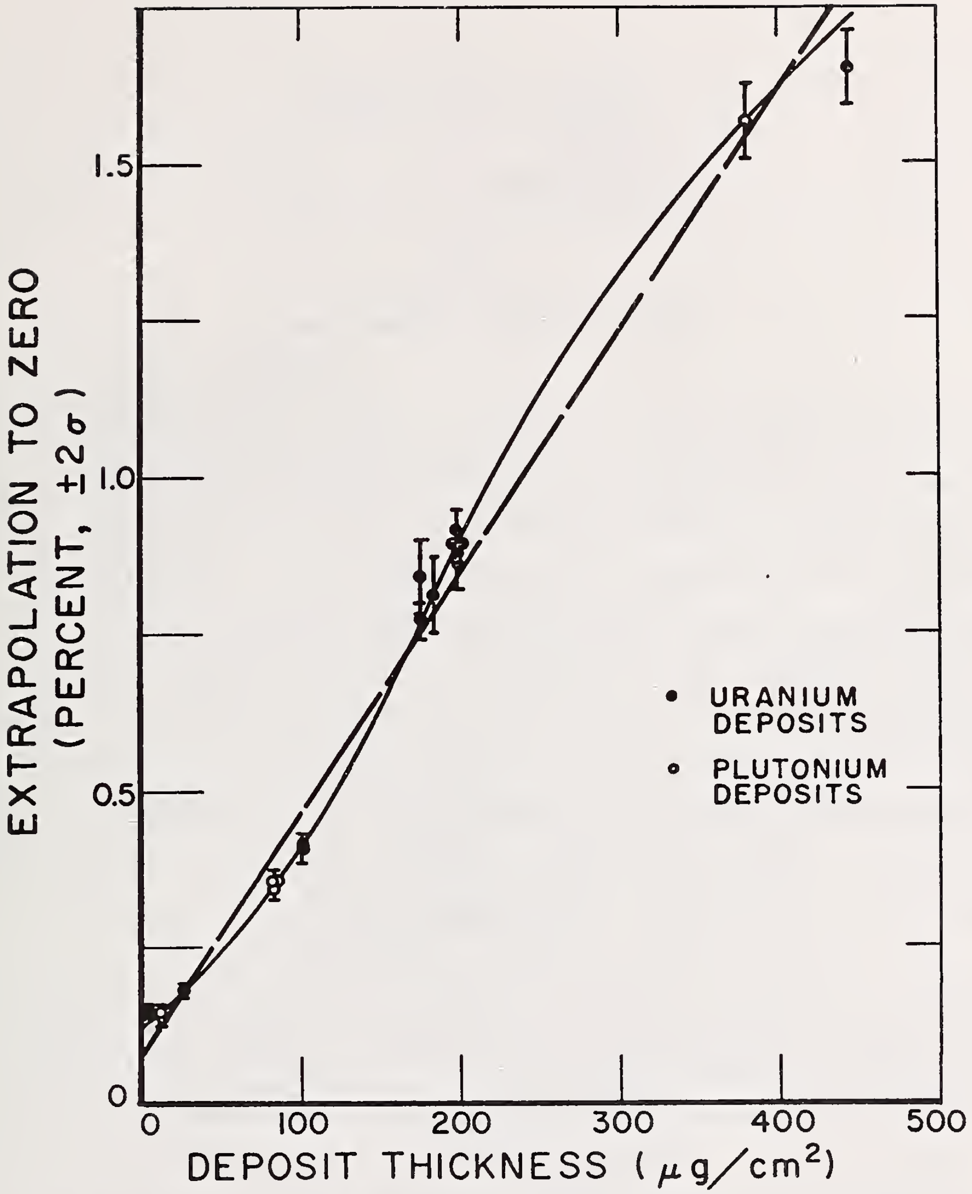

Fig. 2. The extrapolation-to-zero pulse height for the NBS Double Fission Chamber versus thickness of fissionable deposit. Error bars on data points are given as ±2σ for better display.

thin shell of boron-10. Facilities for insertion and removal of the system from the thermal column with the reactor at full power are also complete and have received final approval of the Reactor Division Hazards Evaluation Committee. Brief operational proof-tests of the ISNF were carried out just before the extended reactor shutdown in August, 1974.

TWO-keV FILTERED BEAM

R. B. Schwartz and I. G. Schroder
(Nuclear Sciences Division)

and

E. D. McGarry
(Harry Diamond Laboratory)

The existence of "neutron windows" in the total cross section has permitted the development of a series of neutron filters which transmit neutrons in a narrow energy band from a reactor spectrum. Thus, high intensity beams have been obtained at 2 keV, 24.5 keV and 144 keV using scandium, iron, and silicon filters respectively. The existence of other energy windows in these filters reduce the purity of such beams. This has proved up to now to be a major problem in the development of a monoenergetic filtered beams. The production of such high intensity filtered beams was pioneered at the Materials Testing Reactor[1], but unfortunately the MTR was phased out before the development of these beams could be completed. The filters themselves were subsequently transferred to NBS for use in the neutron standards program.

The 2-keV window in scandium results from overlap of the interference minima from the s-wave resonances at 3.24 and 4.27 keV, producing a cross section with a minimum value of only 50 mb.[2] Unfortunately, there are also many other windows in scandium at higher energies. These windows are responsible for a neutron background in the energy region between 7 keV and 800 keV. In the work of Simpson, et al.,[1] this background flux was equal to ∿2/3 of the 2 keV flux. The problem is inevitable in any facility in which a scandium filter looks at a reactor core. The higher energy neutron background severely limits the utility of this filter and constitutes a major source of uncertainty.

The problem is solved in the NBS reactor by the use of a through tube in conjunction with a resonant scatterer. The through tube passes 10 cm outside of the edge of the reactor core, and the collimating system containing the filter only sees a scatterer at the center of the tube.

(See figure 1). This design eliminates unwanted core neutrons and core gammas. To scatter the neutrons, we make use of the 2.375 keV resonance in manganese. Although the resonant energy does not exactly match the energy of the 2 keV window, the Mn resonance is sufficiently broad ($\Gamma = 400$ eV) that at 2 keV the scattering cross section is still >100 barns.[3] Physically, the scatterer is a 3 mm thick Mn-Al alloy, containing 57 atomic percent manganese.

The advantage of this design may be seen in the spectra shown in figure 2. (These data were taken with a 1 atm hydrogen photon-recoil counter.) The solid line shows the spectrum obtained with the 110 cm Sc filter; the dashed curve shows the effect of adding one cm of Ti to the Sc. It can be seen that even without the Ti, the main secondary peak at 29 keV has an area of only 3% of the 2 keV peak. The addition of the Ti reduces this peak (as well as the ones at 7, 15, and 40 keV) by a factor of about 2-1/2, at the cost of only 17% of the 2 keV peak. There were no peaks observed at energies higher than 144 keV. The measurements with the Ti have not yet been extended above 50 keV. Since the Ti cross section is ∿10 b at 60 keV and decreases with energy[3] we do not, however, expect the Ti to have a significant effect at higher energies.

In terms of total flux (i.e., the area under the peaks), the higher energy contaminants amount to approximately 6% of the 2 keV flux without the titanium; the addition of the titanium reduces their contribution to ∿3% of the 2 keV flux.

---

[1] O. D. Simpson, J. R. Smith and J. W. Rogers, *Proc Symp. Neutron Standards and Flux Normalization;* CONF-701002, U.S. Atomic Energy Commission, 362 (1971); also, *Proc. Third Conf. Neutron Cross Sections and Technology*, CONF-71031, 598 (1971).

[2] W.L. Wilson, "Neutron Cross Section Measurements and Gamma Ray Studies of ^{45}Sc," M.S. Thesis, University of Idaho Graduate School, Dec. 1966 (unpublished).

[3] M. D. Goldberg, S. F. Mughabghab, B. A. Magurno, and V. M. May; "Neutron Cross Sections, Vol. IIA, Z=21 to 40;" BNL 325, Second Edition, Supplement No. 2 (Physics-TID-4500) Feb. 1966.

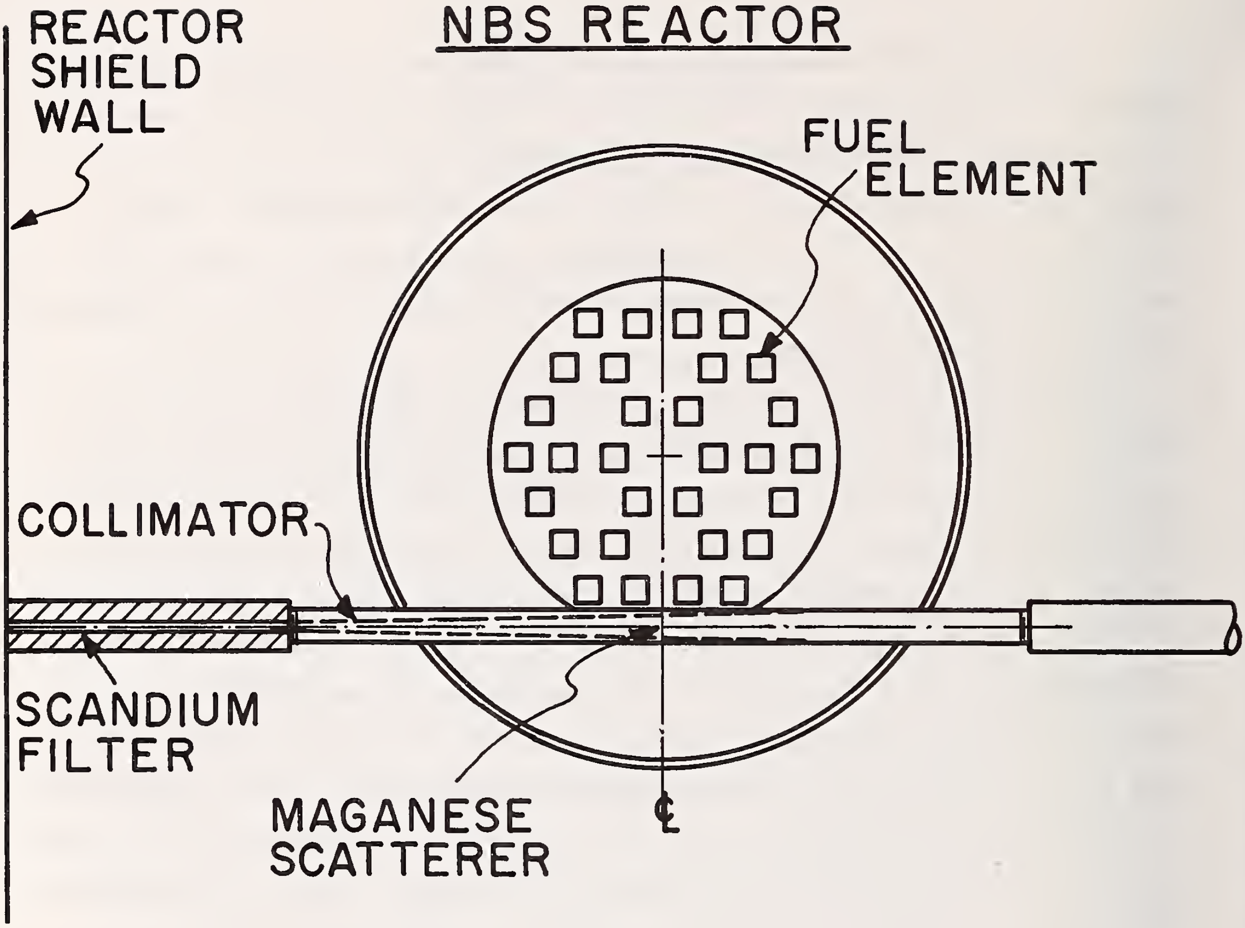

Fig. 1. Schematic representation of the NBS Reactor showing the filter, collimator and scatterer in the through tube. (Not to scale.)

The neutron intensity is ∿5×10^5 neutrons/s , in a 2 cm diameter beam. The gamma ray background is ∿1 Mr/hr.

Further studies are now being conducted to optimize the thickness of the scandium and the titanium.

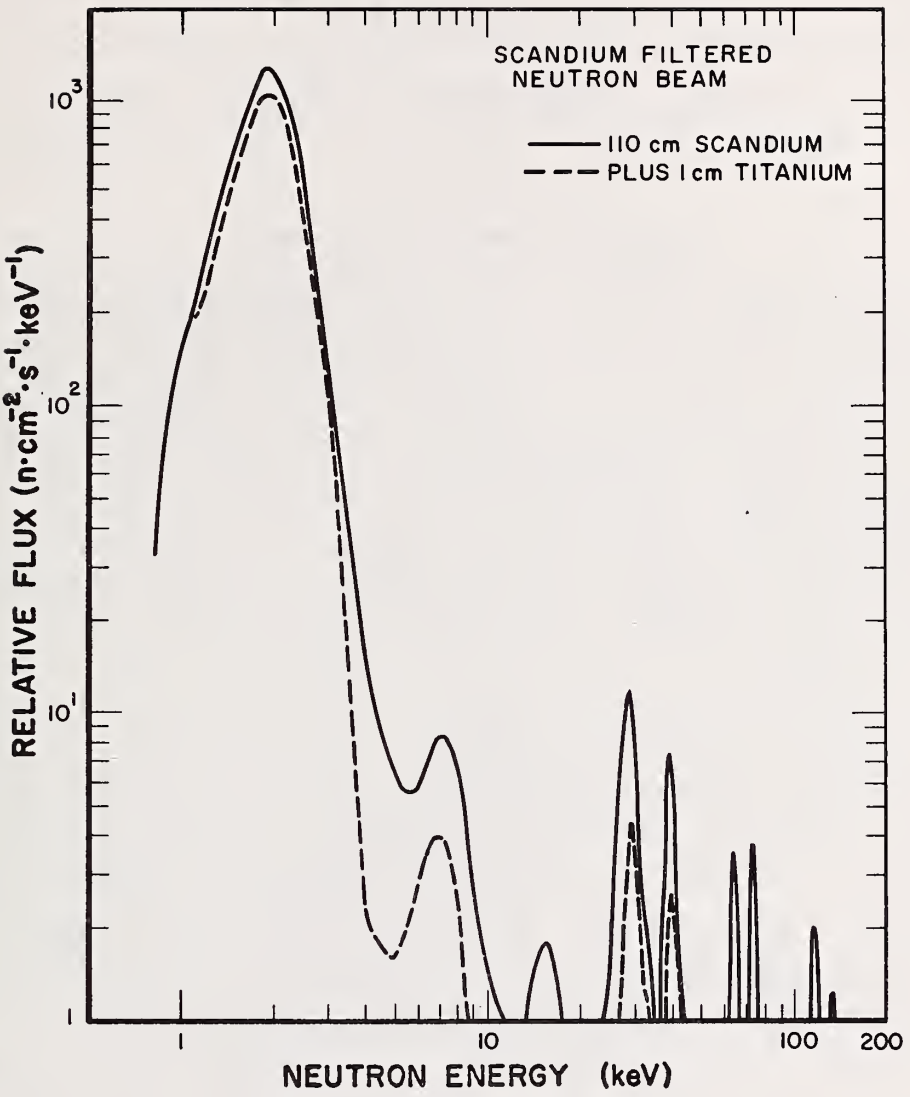

Fig. 2. Neutron spectrum through scandium filter. The solid curve represents the spectrum with a 110 cm scandium filter alone, and the dashed curve the spectrum observed with the addition of 1 cm of titanium.

25-keV FILTERED BEAM

E. D. McGarry and C. R. Heimbach
(Harry Diamond Laboratories, Washington, DC)

and

I. G. Schroder
(Nuclear Sciences Division)

An iron-filtered, neutron-beam facility that provides a well-collimated source of 25-keV neutrons has been installed in a vertical, 2.5-inch diameter thimble of the National Bureau of Standards (NBS) Reactor. For selected physics experiments and monoenergetic calibration of neutron dosimeters, the beam flux may be tailored to provide $5 \times 10^5 n/cm^2 \cdot s$ with 99 percent 25-keV neutrons. For other experiments, such as calibration of fast-neutron spectrometers, fluxes of $10^6 n/cm^2 . s$ may be obtained with as many as 13 identifiable peaks in the range 25 keV to 1.5 MeV.

The 25-keV, filtered-beam facility is shown in Fig. 1. It consists of four principal parts: (1) the collimating system; (2) the iron filter; (3) a secondary filter of aluminum; (4) a titanium neutron scatterer. The facility is a completely assembled and gas-sealed tubular configuration 5.4 meters long. The bottom section of the assembly is a 3.4 meter aluminum tube filled with one atmosphere of helium to minimize air scattering and to provide a low-scattering path through the D_2O reactor coolant. This aluminum tubing also positions a 4.5 centimeter by 0.64 centimeter titanium neutron-scattering element in the immediate vicinity of the reactor fuel. The titanium preferentially scatters 25-keV neutrons into the iron filter. The use of a resonance scatter between the fuel elements, as opposed to aiming the collimating system directly at the fuel, eliminates substantial quantities of core neutrons and core gammas. For a neutron intensity of $5 \times 10^5 n/cm^2 \cdot s$, in the one-centimeter diameter beam, the gamma ray background is less than 2 mR/hr.

There are two collimator sections in the assembly. The lower collimator is composed of a carbon-steel pipe, one centimeter inside diameter, through 1.2 meters of lead shielding. The upper collimator is a titanium tube, also one centimeter in diameter, through 1 meter of lead.

Between the collimators is the principal neutron filter; 30 centimeters of Armco electromagnet iron. This iron is relatively impurity free (99.99% iron) and has a measured[1] resonance-interference minimum of 0.41 barns in the total cross section at 24.5 ± 0.3 keV. There are other less pronounced minima in the iron cross section between 50 keV and 1 MeV. The principal contributions are at 82 keV, 137 keV, and 270 keV. However, these peaks are quite effectively removed by the secondary aluminum filter. Figure 2 shows a spectrum filtered through 30 centimeters of iron and 35 centimeters of aluminum. By an analysis of the areas under the peaks, shown in figure 2, 99 percent of the neutrons are in the 25-keV peak and the remaining one percent is primarily in the 137-keV peak and 270-keV peak. We have compared this distribution with that filtered through 30 centimeters of iron and no aluminum. The spectrum, suitable for energy calibration[2] of a neutron spectrometer in the range 25 keV to 650 keV, is shown in figure 3. Here, only 83 percent of the total flux is in the 25-keV peak. The second most intense peak is that at 137 keV; however, without the aluminum, many other peaks are evident. A study is being made of the spectral content of the beam with a range of filtering materials.

The spectra were measured with a hydrogen-gas, proton-recoil spectrometer. The hydrogen, at five atmospheres, is contained in a 2.5 centimeter diameter stainless-steel tube. Because of the extremely low gamma background, the spectra can be obtained without the use of gamma-discrimination techniques. For example, figure 4 shows the raw proton-recoil pulse-height distribution from which the spectrum of figure 3 was obtained. The quality of the data are to a large extent attributable to the excellent low-noise qualities of the charge-sensitive

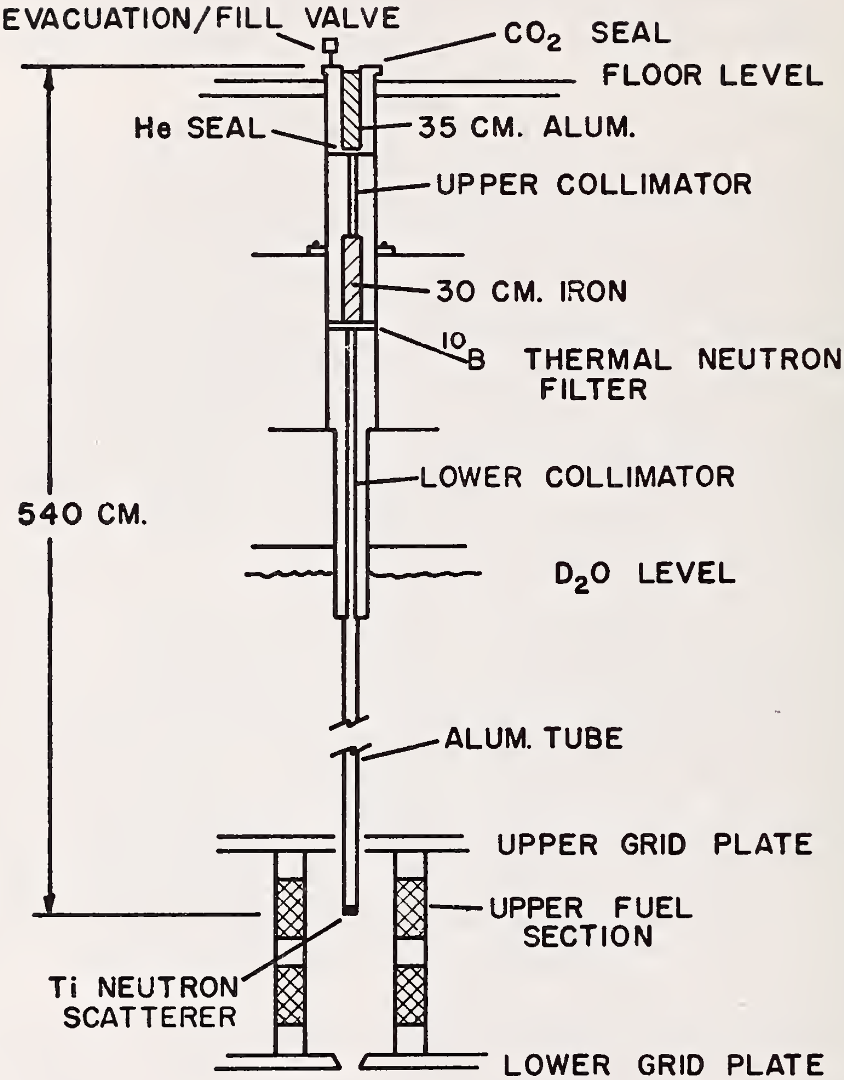

Fig. 1. The facility.

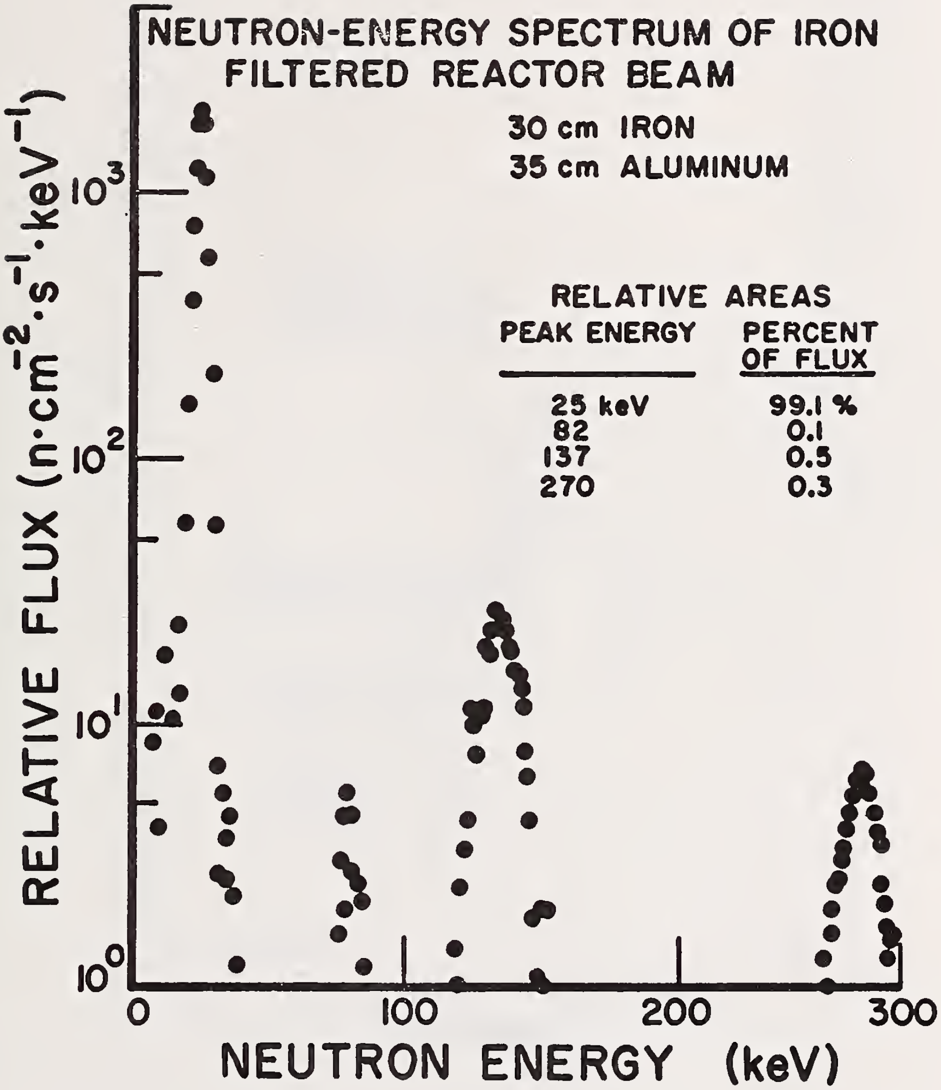

Fig. 2. Neutron-energy spectrum of iron filtered reactor beam.

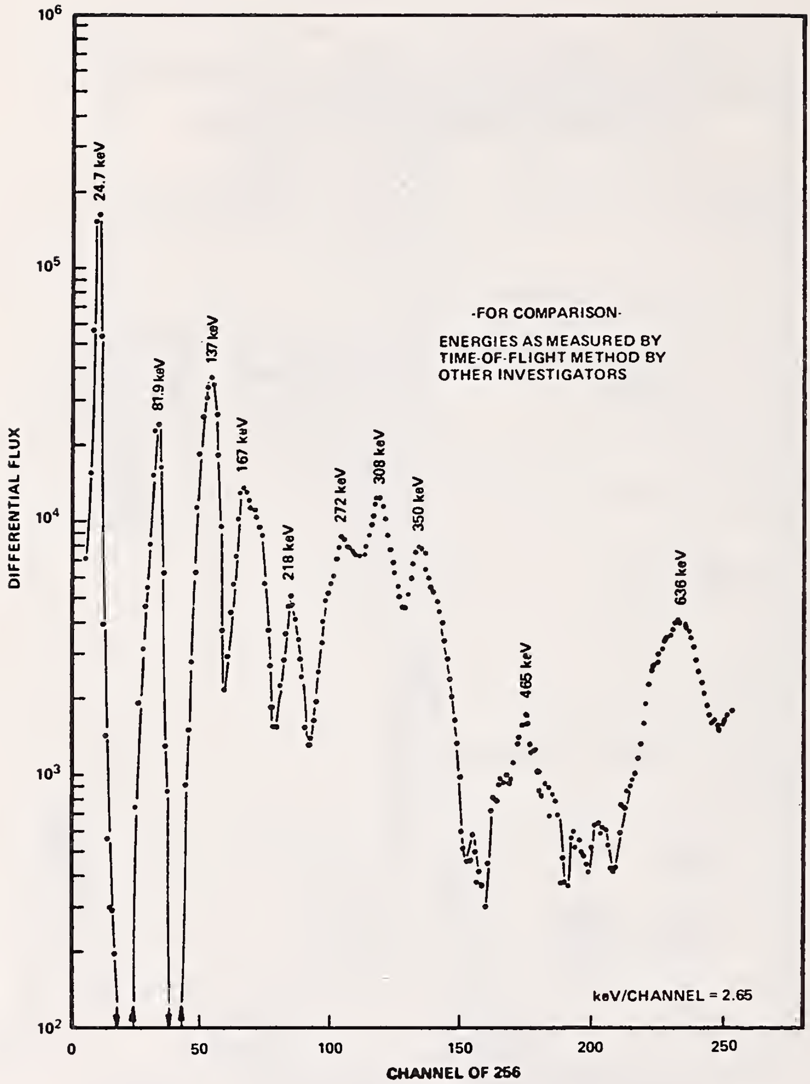

Fig. 3. Flux as a function of energy from a beam scattered from the NBS reactor core by titanium and filtered through 30 cm of iron.

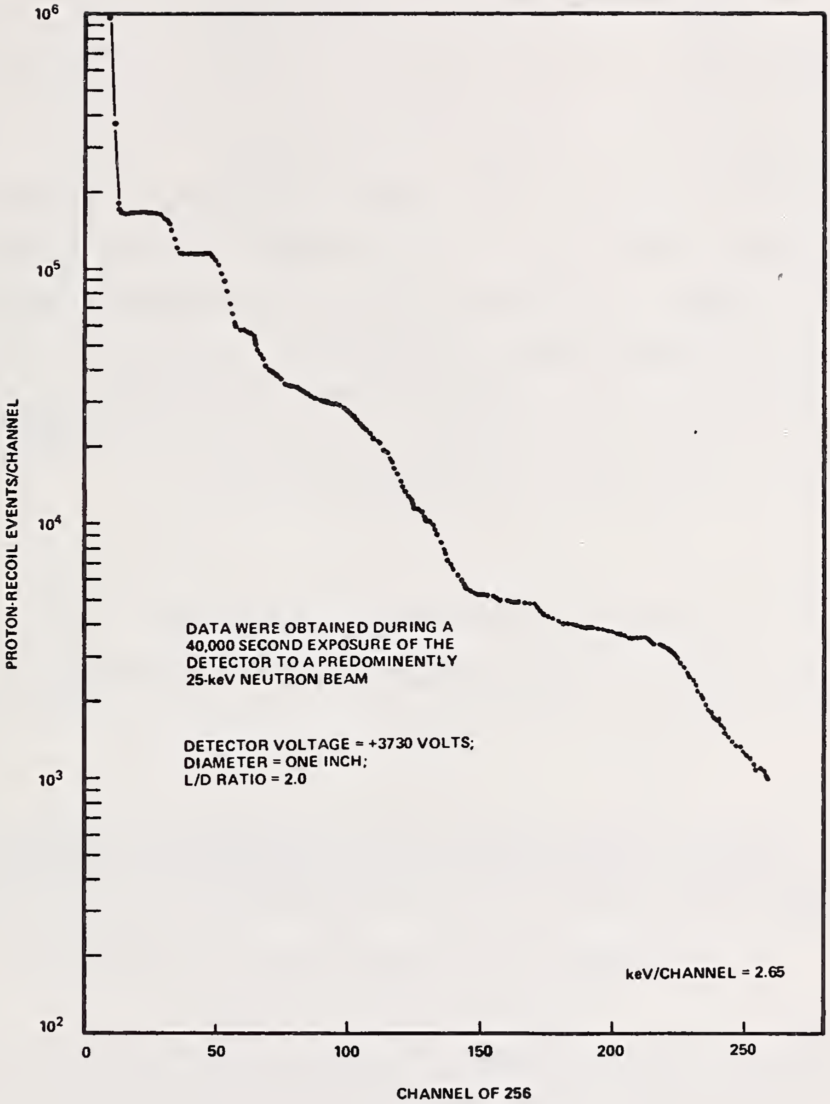

Fig. 4. Proton pulse-height distribution as collected on a multichannel analyzer from a 5-atmosphere hydrogen protein-recoil detector.

preamplifier used. The major contribution to the resolution, which varies inversely with energy from 5.3 percent at 600 keV to 9 percent at 25 keV, is the relative absence of wall and end effects on proton-recoil track lengths. This is because the one-centimeter beam can be directed at the center of the hydrogen-filled tube oriented with the anode perpendicular to the beam. Very few protons interact with the distorted electric field near the ends of the tube. Furthermore, the ionization-track lengths in the 1.25 centimeter radius around the anode are 0.03 centimeters for 25-keV protons and 1.0 centimeter for 700-keV protons. Accordingly, greater than 85 percent of the observed pulses will correspond to protons that are completely stopped in the gas.

A new design is being considered to minimize the number of neutrons scattered by the D_2O below the titanium scatterer.

---

[1] R. C. Block, et al., *Trans. Am. Nucl. Soc.* 15, 531 (1972).

[2] J. E. Powell and J. W. Rogers, *Nucl. Instr. and Meth.* 87, 1, 29 (1970).

PRECISION MEASUREMENT OF THE WAVELENGTHS OF NUCLEAR GAMMA LINES AND THE COMPTON WAVELENGTH OF THE ELECTRON

W. C. Sauder, E. G. Kessler and R. D. Deslattes
(Optical Physics Division)

The goals of this experiment are precise measurements of the wavelengths of nuclear gamma lines and the Compton wavelength of the electron. The measurements are performed on a two-axis, Laue case transmission crystal diffraction spectrometer. The instrument has an angular range of 2.5 degrees and an angular sensitivity of better than 10^{-4} arc seconds.

Some of the gamma lines that will be measured are the 412 keV line of ^{198}Au, the 100 keV line of ^{182}Ta, the 84 keV line of ^{170}Tm, and several lines of ^{169}Yb. The source of the Compton wavelength radiation is two-photon annihilation of positronium. The positron emitter, a multi-kilocurie ^{64}Cu source, will be housed in a cryostat which provides a 7 K environment in a 0.2 T magnetic field for the annihilating positronium.

The spectrometer, the source and detector positioning apparatus, the container for the γ sources, and the annihilation cryostat have been completed and tested. During the past year motor drive and fringe counting circuitry has been designed and constructed. Equipment for calibrating the crystal axes via a 72 sided optical polygon has been constructed and the calibration procedure has begun. Germinatium crystals have been cut and mounted. A data acquisition system has been assembled and tested. Measurement of the 412 keV line of ^{198}Au should be completed before the end of the year.

E. SUMMARY OF REACTOR OPERATIONS

Operating productivity continued at a very high level. Outstanding among these are 75% on-line time and a 54% burnup rate. A summary of operating statistics for this and previous years is presented in the following table.

NBSR Operating Summary

	1971	1972	1973	1974
Reactor Operations to date, MWh	124,000	175,000	229,000	290,000
Reactor Operations for year, MWh	51,000	51,000	67,000	61,000
Hours Reactor Critical	5,400	5,200	7,000	6,600
Number of Days at 10 MW	213	214	279	254
On-line Time at 10 MW	58%	58%	77%	70%
Number of fuel elements used	24	26	28	24
Average U-235 Burnup	48%	45%	52%	54%
Number of Refueling Operations	6	6	7	6
Number of Unscheduled Shutdowns	10	11	14	6
Number of Irradiations	3,000	4,000	4,300	3,000
Number of Visitors	4,000	3,400	3,000	5,000

No additional problems were experienced with the main heat exchanger this year. However, operation at reduced power was continued during hot weather periods. The main heat exchanger, which is made of aluminum, will be replaced by stainless steel units during the next few months.

F. SERVICE PROGRAMS

There was a major shift in the manner in which service irradiations were performed this year. While the total number of irradiations decreased, irradiations times increased substantially to the point where some of the facilities were overloaded a good fraction of the time. Discontinued use of neutron activation in the analysis of most gunshot residue samples also contributed to the reduction in the total number of irradiations. Highlights of some of the major service programs are presented in the following sections.

THE NEUTRON ACTIVATION ANALYSIS PROGRAM OF THE FOOD AND DRUG ADMINISTRATION AT THE NBSR

J. T. Tanner and M. H. Friedman
(Food and Drug Administration, Washington, DC)

The activation analysis unit of the Food and Drug Administration (FDA) is located at the National Bureau of Standards in the Reactor Building. Neutron activation analysis (NAA) has been used by the FDA for trace metal analysis of foods, drugs, hair, laundry aids, and cosmetics. The service of this group is available to anyone within the FDA both in the headquarters laboratory and in the field. The program described below accounts for the main effort of NAA at the FDA.

1. Multielement Analysis of Total Diet Samples

The "Total Diet" program of the Food and Drug Administration (FDA) is a continuing market basket study in which 117 food items are collected, prepared in a "table-ready" fashion, and composited into 12 commodity groups for analysis for selected metals, pesticides, and certain industrial chemicals to determine the average daily intake of these contaminants in the diet. The sampling is intended to represent the 2-week diet of a 15- to 20- year old male in each of four regions of the country in which the samples are collected: Northeastern, Southeastern, Central, and

Western. The details of the selection, collection, preparation, and compositing of the samples are described elsewhere[1]. The homogenized, slurried composites of each commodity group are divided into 100 gram portions. The different commodities are: Dairy products; meat, fish and poultry; grain and cereal products; potatoes; leafy vegetables; legume vegetables; root vegetables; garden fruits; fruits; oils and fats; beverages; and sugars.

The FDA Kansas City District Laboratory has the main responsibility for analysis of the Total Diet samples. In addition to pesticides, these composites are routinely analyzed for Hg, As, Se, Pb, Cd, Zn, Ca, Fe, P, and I. At various times the Neutron Activation Analysis (NAA) group of the FDA has aided the Kansas City Laboratory when improved limit of detection was required. Mercury was determined in Total Diet composites for one year by NAA. These results have been reported elsewhere[2].

During the past year the FDA has been testing and evaluating NAA methodology for the surveillance of a number of trace elements in foods. Elements which are of interest to FDA include Fe, Co, Sb, Rb, Cs, Zn, Se, Cr, Sc, Hg, Ag, K, Mg, Na, Dy, Mn, Ni, V, Al, In, Cl, Br, I, Pb, Cd, As, and Ca. Some of these elements produce long lived radionuclides on neutron irradiation and therefore offer the possibility of determination by instrumental NAA (INAA). These include Fe, Co, Sb, Rb, Cs, Zn, Se, Cr, Sc, Hg, and Ag. Others are short lived and may also be determined by INAA. These are K, Mg, Na, Dy, Mn, Ni, V, Al, In, Cl, Br, I, Ca, and As. While it may not be possible or practicable to determine all of these elemnents by INAA at least some of them possibly can be determined (Fe, Co, Zn, Sb, Rb, Se, K, Mg, Na, Mn, Al, and Br) and upper limits established for other elements. The purpose will be to provide additional information for elements not determined by the Kansas City Laboratory, provide an interlaboratory comparison within FDA, and provide greater sensitivity for some elements where only upper limits are now obtained.

Our initial survey will consist of a one year Total Diet sampling. These are the same samples which have been analyzed for mercury[1] earlier. Based on the results obtained, the time required per analysis, and the total work load, the use of INAA for routine surveillance will be evaluated.

In addition to INAA, group separation methodology for multielement analysis is being developed for FDA by researchers at the Washington State University. This will provide improved sensitivities for some elements.

2. MULTELMT: A Computer Language For the Reduction of Neutron Activation Analysis Data.

To carry out the program of the Food and Drug Administration outlined above, many γ-ray spectra have to be recorded by a multi-channel analyzer and then reduced. Since each spectrum typically consists of 2048 channels with many γ-ray photopeaks, it is expedient to reduce the data with a large computer. It was desirable, however, to maintain the flexibility inherent in a manual calculation. This was done by constructing a specialized language called MULTELMT. In this language the user "talks" to the computer in a language resembling English and tells it how to reduce the data.

MULTELMT consists of a number of interacting subroutines written in FORTRAN V and has been run on the UNIVAC 1108 computer at the National Bureau of Standards. It is used to reduce gamma or x-ray spectra for either a single element or combination of elements. The analysis calculation is done by comparing a sample with a standard. It computes the micrograms or ppm of the element(s) present, the uncertainty of the measurement, and for those cases where the amount of the element is below the sensitivity of the measurement, calculates an upper limit. In addition, the language can be used to: 1) automatically search a spectrum, find the peaks and output the energies and areas of the peaks, 2) make linear or semi-logarithmic plots and 3) provide an accurate energy calibration.

The data reduction system has worked well to date, even when the elements of interest are present at very low levels.

---

[1] Duggan, R.E., and F. J. McFairland, "Residues in Food and Feed." Pesticides Monitoring Journal, Vol. 1, pp 1-5 (1967).

[2] Tanner, J. T., and W. S. Forbes, "Determination of Mercury in Total Diet Samples by Neutron Activation," Anal. Chim. Acta, (in press).

U.S. POSTAL SERVICE ACTIVATION ANALYSIS PROGRAMS

J. B. Upton
(Crime Laboratory, Washington, DC)

During the past fiscal year, the U.S. Postal Service Crime Laboratory used neutron activation analysis routinely to compare questionable and known samples of evidentiary value such as paint, safe insulation, paper, plastics and metals. While there was a considerable reduction in the number of burglaries directed toward postal property due to improved security measures, the use of neutron activation for the analysis of particles of evidence in this type case which related suspects to the crime scene further contributed to curtailment of this activity through successful prosecutions.

NAA was also used in the analysis of components of bombs sent through the mails. In one important bomb case resulting in court conviction, NAA was used to compare insulation from the wire used in the construction of the explosive device to that recovered from the suspect's home. Results obtained regarding the trace elemental composition of the two insulation samples, along with additional physical property data, demonstrated the wires were associated by both manufacture and batch production.

NAA has proved to be a very useful and necessary tool in the field of forensic chemistry and efforts to obtain analytical research data regarding different types of materials are continuing.

ACTIVATION ANALYSIS PROGRAM OF THE U.S. GEOLOGICAL SURVEY

J. J. Rowe
(U.S. Geological Survey, Reston, VA)

The U.S. Geological Survey is applying Neutron Activation Analysis to the determination of trace concentrations of elements in geological materials. The improved sensitivity of Activation Analysis, for some elements, supplements other analytical techniques in the analysis of rocks, minerals and waters for geochemical studies related to ore formation, magmatic differentiation, alternation, hydrothermal transport, energy reserves (coal, petroleum, geothermal and nuclear) and environmental problems.

The Radioactivation and Radiochemical Analysis project is developing a comprehensive instrument method, using sample changers and computer data reduction to provide data on trace concentrations of Ba, Ce, Co, Cr, Eu, Fe, Gd, Hf, Nd, Rb, Sb, Se, Ta, Th, Yb, Zn and Zr in igneous and metamorphic rocks. Sulfide minerals have been analyzed for Mn, As, Sb, Se, Ag, Hg and Au using instrumental and radiochemical methods. Lunar samples have been analyzed for Al, V, Mn, Hf, and Ta. Thermal waters have been analyzed for gold for the Heavy Metals Program and a comprehensive analytical program is planned for the study of Geothermal Energy. A group separation procedure coupled with high resolution Ge(Li) detectors is being developed to extend the method to the determination of very low concentrations of Cs, Rb, As, Sb, Se, Hg, Ta and the rare earths. Radiochemical separations are being developed and used to satisfy specific analytical problems. The fire assay radiochemical method for the determination of gold has been extended to silver. Sensitivity of gold and silver are 0.1 ppb and 40 ppb respectively.

THE USE OF NEUTRON ACTIVATION ANALYSIS IN SCIENTIFIC CRIME DETECTION

C. H. Hoffman
(U.S. Treasury Department, Washington, DC)

The Treasury Department's ATF Forensic Laboratory has routinely used NAA for examining a wide variety of trace physical evidence such as paint, soil and glass. While other methods have supplanted NAA in the crime laboratory to some extent, it is felt that no other method offers the sensitivity required for examining those tiny traces of materials so vital as evidence in criminal cases.

During FY74, the ATF Forensic Laboratory made 172 irradiations, using 136 hours of reactor time to analyze 4369 samples. The materials examined are summarized below:

Sample Type	Number of Samples
Gunshot Residue	4200
Bullet Lead	72
Human Hair	40
Paint	30
Soil	11
Glass	8
Ink	8

A large scale study of paints and human hair will be started in August, 1974. The trace elemental profiles of these materials will be studied with a view toward establishing the frequency distribution, and the statistical worth of the various elements measured.

LUNAR SAMPLE ANALYSIS FOR 17 TRACE ELEMENTS

E. Anders
(University of Chicago, Chicago, IL)

During the last year we have analyzed 60 samples for 17 trace elements (Ag, Au, Bi, Br, Cd, Ge, Ir, Ni, Rb, Re, Sb, Se, Te, Tl, U, and Zn) by radiochemical neutron activation using the NBS Reactor.

Variations in the abundance of siderophile elements (Au, Ge, Ir, Ni, Re, Sb) in lunar breccias, impact melts and soil separates has enabled the identification of at least 5 types of meteoritic material thought to be derived from major basin-forming events (Ganapathy et al., 1974; Morgan et al., 1974). Measurement of the abundance of volatile trace elements in lunar igneous rocks has made it possible to construct a detailed chemical model for the Earth and Moon based on the seven distinct components seen in meteorites (Ganapathy and Anders, 1974). The model is consistent with petrological and geophysical constraints.

In addition, a suite of 11 anorthosites from W. Greenland were analyzed for the same elements. These rocks are of interest since they appear to be the closest terrestrial analogues to lunar anorthosites, and again provide evidence of the fundamental composition differences between Earth and Moon (Morgan et al., in preparation).

R. Ganapathy and E. Anders (1974), Bulk compositions of the Moon and Earth, estimated from meteorites, *Proc. Fifth Lunar Sci. Conf., Geochim. Cosmochim. Acta,* Suppl. 5, in press.

R. Ganapathy, J. W. Morgan, H. Higuchi, and E. Anders (1974), Meteoritic and volatile elements in Apollo 16 rocks and in separated phases from 14306, *Proc. Fifth Lunar Sci. Conf., Geochim. Cosmochim. Acta,* Suppl. 5 in press

J. W. Morgan, R. Ganapathy, H. Higuchi, and E. Anders (1974), Lunar basins: Tentative characterization of projectiles, from meteoritic elements in Apollo 17 boulders, *Proc. Fifth Lunar Sci. Conf., Geochim. Cosmochim. Acta,* Suppl. 5, in press.

J. W. Morgan, R. Ganapathy, and H. Higuchi (1975), Volatile and siderophile trace elements in anorthositic rocks from Fiskenaesset, W. Greenland: Comparison with lunar and meteoritic analogues. Manuscript in preparation.

TRACE ELEMENTS IN THE ENVIRONMENT AND RADIOACTIVE DECAY STUDIES

W. H. Zoller, G. E. Gordon and W. B. Walters
(University of Maryland, College Park, MD)

Our group has made extensive use of the NBSR for the irradiation of numerous samples for trace element analysis using instrumental neutron activation analysis (INAA). Routinely the samples are analyzed using a two-irradiation sequence. The first irradiation is for the short-lived isotopes, with the samples being counted on our Northern Scientific computer-based, Ge(Li) γ-ray counting system. This system consists of 2-4096 channel analyzers controlled by a mini computer and is portable so that it can be moved to a location near the pneumatic tubes of the NBSR. After the second irradiation for the intermediate (several days) and long-lived isotopes, the samples are returned to the University for γ-ray counting. All data is put onto computer compatible magnetic tape for analysis on the Univac 1108 computer on campus.

During the past year samples from each of the following sources have been analyzed during an extensive air pollution episode: coal- and oil-fired power plants, municipal and sewage sludge incinerators and motor vehicles. Additional related samples of fuels (oil and coal), dust and rock of the surrounding areas have been analyzed by INAA.

Work has continued on samples from the South Pole as part of a study of global atmospheric aerosols. New samples were collected during the last year and will be completed during the next few months from a new sampling facility at Pole Station. Samples were also collected at the Icelandic volcano Heimaey and analyzed. These samples showed fairly high enrichments of the more volatile trace metals in the fumerol deposits and aerosols near the vents.

As part of our program studying the radioactive decay of neutron-rich isotopes, we conducted a set of fission experiments in conjunction with personnel from Lawrence Livermore Laboratory. Dr. Richard A. Meyer and Mr. Jerry Landrum of the LLL radiochemistry group came to do experiments on ^{133m}Te, ^{133g}Te and ^{134}Te separated from the fission of ^{235}U. The decay was studied using our two-parameter Ge(Li)-Ge(Li) coincidence system. Work has proceeded on other studies of the decay of ^{131m}Te, ^{161}Gd, ^{105}Ru, ^{117}Cd.

TRACE ELEMENTS IN OCEANIC FLOOR ROCKS

F. A. Frey
(Massachusetts Institute of Technology, Cambridge, MA)

The NBS Reactor pneumatic facilities are used to do neutron activation analysis of oceanic floor rocks. The primary objective is to determine by gamma ray spectroscopy the abundance in these rocks of elements present in the parts per million range, i.e. trace elements. Such elements are Sc, Cr, Co, Ba, rare-earth elements, Th and U. Neutron activation analysis is the most sensitive analytical technique available for many of these elements.

The following problems are being studied.

1. Basaltic rocks from the ocean floor are believed to have been erupted as magmas from areas of diverging plates such as oceanic ridges, and thus they are an important aspect of sea-floor spreading. A knowledge of trace element abundances in these rocks is useful in understanding melting processes within the earths upper mantle and in determining the chemical composition of the oceanic upper mantle.

2. After eruption as magmas, oceanic basalts are subjected to a variety of chemical alteration processes involving interaction with seawater. Some of these reactions may be important in controlling the composition of seawater; others may be important in concentrating metals which later evolve into continental ore deposits. In some manner oceanic floor rocks must be involved with the formation of volcanoes in island

arcs (e.g. Japan) and continental margins (e.g. Western U.S). A knowledge of trace element behavior during alteration of basalt with seawater is an important aspect of understanding these major geological problems.

SEA AND ATMOSPHERE POLLUTION STUDIES

P. E. Wilkniss
(Naval Research Laboratory, Washington, DC)

During the year, laboratory experiments and chemical analyses were continued in connection with studies on sea water and atmospheric aerosol chemistry, transport and fractionation of chemicals from the sea surface to the atmosphere, and the transport and distribution of pollutants in the ocean and the atmosphere. These studies require the analysis of Hg, Pb, Ag, Fe, Mn, Sc, Na, K, S, Ca, Sr, Br, Cl and I.

The NBS reactor has been used to analyze samples of sea water, rain, fog condensate, atmospheric aerosols and atmospheric dust for microgram amounts of the above named elements. Radioactive tracers for some elements were made at the NBS facility and used in laboratory experiments at NRL. These experiments are to determine transport mechanisms, distribution and partitioning of man-made pollutants and naturally occurring elements in the natural systems under study.

PHOSPHORUS CONTENT OF A VERTEBRATE VISUAL PIGMENT DETERMINED BY NEUTRON ACTIVATION ANALYSIS

W. Robinson, R. Frank and W. Hagins
(National Institutes of Health, Bethesda, MD)

Isolated vertebrate retinal rod outer segments incorporate phosphorous from ATP covalently into rhopodsin when bleached by light.
As much as four moles of phosphorous per mole of rhodopsin can be incorporated. It has recently been reported that there is a light-stimulated incorporation of phosphorous into rhodopsin in the living retina but

no stoichiometry can be determined with the tracer method used.

We are attempting to determine the stoichiometry of this phosphorytation reaction *in vivo* to shed some light on its possible role in photoreception. Retinal rod outer segments from retinas of dark-adapted or light-adapted frogs are solubilized in detergent and fractionated by polyacrylamide gel electrophoresis. The rhodopsin containing band is excised, dried and subjected to slow neutron bombardment (RT4) for 12 hours in the NBS reactor. The irradiated gel slices are then depolymerized with hot H_2O_2, evaporated to dryness and dissolved in a small volume of water. After addition of scintillation fluid, P^{32} can be counted utilizing a narrow window of the scintillation counter.

Trial experiments with casein, a well-characterized phosphoprotein, have demonstrated a linear relationship between the amount of protein applied to the gel and the P^{32} counted. Only very preliminary results have yet been obtained with rhodopsin.

G. STAFF ROSTER

ORGANIZATION CHART

REACTOR RADIATION DIVISION
314.00

Division Office

R. S. Carter, Chief
T. M. Raby, Deputy Chief

E. Maxwell, Admin. Officer*
E. Simms, Receptionist

Technical Support

H. Berger
R. Casella
M. Ganoczy
V. Myers
F. Shorten

314.01
Reactor Operations
T. M. Raby, Chief
J. F. Torrence, Deputy

D. Ahalt, Sec'y

R. Beasley
M. Bell
N. Bickford
H. Brake
D. Cea
A. Chapman
H. Dilks
D. Nelson
J. Ring
R. Scheide
R. Stiber
D. Wilkinson
B. Young

314.02
Engineering Services
J. H. Nicklas, Chief

D. Davitt, Sec'y*

P. Beachley
R. Conway
J. Darr
O. Frizzell
E. Guglielmo
R. Hayes
H. Jackson
J. Sturrock

314.03
Neutron S-S Physics
J. J. Rush, Chief

B. Crowther, Sec'y

A. Cinquepalma
D. Fravel
E. Prince
J. Rowe
W. Rymes
A. Santoro
A. Tudgay
N. Vagelatos*

*Temporary or part-time

STAFF ROSTER

NON-RRD NBS STAFF LOCATED AT REACTOR

Division 240.01

P. R. Cassidy
H. E. DeSpain
E. J. Embree
J. J. Shubiak
F. Moore

Division 241.05

R. A. Dallatore
D. Gilliam
H. T. Heaton
J. A. Grundl
I. G. Schröder
R. Schwartz
V. Spiegel

Division 313.00

B. Mozer

Division 310.08

D. A. Becker
B. S. Carpenter
T. E. Gills
S. H. Harrison
S. R. Lantz
R. M. Lindstrom
G. J. Lutz
E. J. Maienthal
L. T. McClendon
D. Peattie
G. M. Reimer
K. L. Roberts
H. L. Rook
J. Stemple
J. E. Suddueth

GUEST WORKERS AND COLLABORATORS

Division 213.04

D. G. Eitzen

Division 221.03

R. J. Soulen, Jr.
D. B. Utton

Division 232.06

R. D. Deslattes
W. C. Sauder
E. G. Kessler

Division 242.02

L. D. Miller
F. J. Schima

Division 311.03

J. D. Barnes

Division 311.05

B. Dickens
L. W. Schroeder
R. M. Waterstrat

Division 313.01

C. W. Reimann

Division 313.03

R. S. Roth

Division 313.04

G. J. Rosasco

Division 313.05

A. G. Evans

Division 313.06

A. B. Mighell
C. S. Brickencamp

STAFF ROSTER

Aberdeen Proving Grounds

C. M. Cialella

Air Force Materials Laboratory

J. Holloway
R. Rowand

Argonne National Laboratory

H. Flotow
D. L. Price
K. Reimann
K. Sköld

Federal Bureau of Investigation

D. B. Davies
J. W. Kilty
J. M. Little
G. P. Mahoney
J. P. Riley

Food and Drug Administration

M. Friedman*
R. E. Simpson
J. T. Tanner*

General Dynamics - Ft. Worth

W. Dungan

Harry Diamond Laboratory

C. Heimbach
D. McGarry
M. Rosenhaft
C. Soares
T. Wright

National Institutes of Health

G. Flinn, Jr.
R. Frank
W. Hagins
W. Robinson

National Park Service

J. B. Smith

Naval Air Development Center

J. Erthal
F. Williams

Naval Air Systems Command

S. Goldberg

Naval Ordnance Laboratory

H. Alperin*
D. I. Gordon
P. Hesse
D. A. Kubose
S. J. Pickart*
D. Polansky
J. J. Rhyne*
R. S. Sery
R. H. Williams

Naval Ordnance Systems Command

L. Leonard

Naval Research Laboratory

D. J. Bresson
A. C. Ehrlich
G. A. Furgeson
J. Karle
J. H. Konnert
P. E. Wilkniss

Oak Ridge National Laboratory

M. Mostoller
H. G. Smith

Picatinny Arsenal

C. S. Choi*
H. J. Prask*
M. K. Farr*

U.S. Geological Survey

F. W. Brown
R. Finkelman
L. P. Greenland
J. J. Rowe
G. Sellers
F. O. Simon

STAFF ROSTER

U.S. Postal Service

M. Beckman
G. R. Stangohr
J. Upton

U.S. Treasury Department

R. L. Brunelle
P. C. Buscemi
C. M. Hoffman
F. A. Lundgren

V.A. Hospital

J. Smith

American University

R. G. Arnold
B. T. Chertok
R. A. Segnan
R. Simon
D. M. Sweger

Carnegie Institute of Washington

L. W. Finger

University of Maryland

J. Barker
P. Buhl
R. A. Cahill
T. J. Conry
E. Gladney
C. Glinka
G. E. Gordon
J. Graber
S. Harrison
A. Jones
R. Khanna
V. J. Minkiewicz
F. J. Munno
J. Ondov
L. Raber
J. Reednick
W. B. Walters
W. H. Zoller

U.S. Naval Academy

C. S. Schneider

Massachusetts Institute of Technology

F. A. Frey

McGill University

G. Donnay
J. D. H. Donnay
R. F. Martin

Politeenico di Milan

M. Zocchi

Temple University

V. Warkulwiz

University of Chicago

E. Anders
R. Ganapathy

The Ford Motor Company

W. G. Rothschild

Gamma Industries

D. Garrett

Intelcom Rad Tech

D. Rundquist

Old Delft Corp.

D. Bracher

Xonics Corp

P. Scott

*Located full time at Reactor.

H. PUBLICATIONS

COLLABORATIVE PROGRAMS

ALPERIN, H. A., RHYNE, J. J., PICKART, S. J., "Neutron Scattering from an Amorphous Ferrimagnet," *Proceedings*, International Conference on Magnetism, (Nauka, Moscow, USSR, 1974) Vol. IV, p 358.

ALPERIN, H. A., "The Rotation of Polarized Neutrons Scattered From Cr_2O_3," *Proceedings*, International Conference on Magnetism, (Nauka, Moscow, USSR, 1974) Vol. III, p. 12.

CHOI, C. S., PRASK, H. J. and PRINCE, E., "Crystal Structure of NH_4ClO_4 at 298, 78 and 10K by Neutron Diffraction," *J. Chem. Phys.*, in press.

CHOI, C. S., and BULUSU, S., "Crystal Structure of Dinitropentamethylene Nitramine," *Acta Cryst.*, in press.

COPLEY, J. R. D., ROWE, J. M., "Density Fluctuations in Liquid Rubidium. I. Neutron-Scattering Measurements," *Phys. Rev.* A9, 1656 (1973).

COPLEY, J. R. D., ROWE, J. M., "Short-Wavelength Collective Excitations in Liquid Rubidium Observed by Neutron Scattering," *Phys. Rev. Lett.*, 32, 49 (1974).

DICKENS, B., PRINCE, E., SCHROEDER, L. W., and BROWN, W. E., "$Ca(H_2PO_4)_2$, A Crystal Structure Containing Unusual Hydrogen Bonding," *Acta Cryst.* B29, 2057 (1973).

GRUNDL, J. A., DUNDAY, N. D., POPEK, R. J., "Measurement of Absolute Fission Rates," *ANS Transactions* 17, 516 (1973).

LIVINGSTON, R. C., ROTHSCHILD, W. G., RUSH, J. J., "Molecular Reorientation in Plastic Crystals: Infrared and Raman Band Shape Analysis of Noepentane," *J. Chem. Phys.*, 59, 2498-2508 (1973).

LIVINGSTON, R. C., ROWE, J. M., and RUSH, J. J., "Neutron Quasielastic Scattering Study of the Ammonium Ion Reorientations in a Single Crystal of NH_4Br at 373°K," *J. Chem. Phys.* 60, 4541 (1974).

MAREZIO, M., DERNIER, P. D., and SANTORO, A., "Twinning in Cr-Doped VO_2," *Acta Cryst.* A29, 618 (1973).

PICKART, S. J., RHYNE, J. J., and ALPERIN, H. A., "Anomalous Small Angle Scattering from Amorphous $TbFe_2$ and YFe_2," *Phys. Rev. Lett.*, to be published

PICKART, S. J., RHYNE, J. J., ALPERIN, H. A. and SAVAGE, H. T., "Neutron Diffraction of Sputtered and Annealed Tb-Fe Alloys," *Phys. Rev. Lett.* A 47A, 73-74 (1974).

PUBLICATIONS

PRASK, H., TREVINO, S., KEMMEY, P., TSAI, D., McDONALD, R. and YIP, S., "Computer Simulation Studies of the Microscopic Behavior of Shocked Solids," *Proceedings*, Conf. Mechanisms of Explosives and Blast Waves, Yorktown, VA, 1973, in press.

PRASK, H., CHOI, C., IQBAL, Z. and TREVINO, S., "Correlation of the Vibration of Molecular and Stability in Energetic Materials," *Proceedings*, 1974 Army Science Conf., West Point, NY, in press.

PRINCE, E., DICKENS, B. and RUSH, J. J., "A Study of One-Dimensional Hindred Rotation in NH_3OHClO_4," *Acta Cryst.* B30, 1167 (1973).

RHYNE, J. J., PICKART, S. J. and ALPERIN, H. A., "Magnetism in Amorphous Terbium Iorn," AIP Conf. Proc. Series 18, 563 (1974).

RHYNE, J. J., SCHELLING, J. H. AND KOON, N. C., "Anomalous Magnetization of Amorphous $GdFe_2$, $TbFe_2$, and YFe_2," *Phys. Rev.*,to be published.

RHYNE, J. J., "Local Anisotropy and Exchange Effects in Amorphous $TbFe_2$," *Proceedings*, International Conference on Crystalline Electric Fields, (Montreal, Quebec, 1974) to be published.

ROWE, J. M., NICKLOW, R. M., PRICE, D. L. and ZANIO, K., "Lattice Dynamics of Cadmium Telluride," *Phys. Rev.*, to be published.

ROWE, J. M., RUSH, J. J., FLOTOW, H. E., "Neutron-Quasielastic-Scattering Study of Hydrogen Diffusion in a Single Crystal of Tantalum," *Phys. Rev.*, B9, 5039 (1974).

ROWE, J. M., RUSH, J. J., and SMITH, H. G., ""In-Band" Modes of Vibration of $PdH_{0.03}$," *Phys. Rev.* B8, 6013 (1973).

ROWE, J. M., LIVINGSTON, R. C., and RUSH, J. J., "Neutron Quasielastic Scattering Study of SH^- Reorientation in Rubidium Hydrosulfide in the Intermediate Temperature Trigonal Phase," *J. Chem. Phys.* 59, 6652 (1973).

ROWE, J. M., PRICE, D. L., and OSTROWSKI, G. E., "Inelastic Neutron Scattering From a Liquid ^{3}He-^{4}He Mixture," *Phys. Rev. Lett.*, 31 510 (1973).

RUSH, J. J., LIVINGSTON, R. C., deGRAAF, L. A., FLOTOW, H. E. and ROWE, J. M., "Study of Hydrogen Diffusion in Tantalum Hydrides by Inelastic Neutron Scattering," *J. Chem. Phys.* 59, 657 (1973).

RUSH, J. J., "Study of Large-Amplitude Vibrations in Molecules by Inelastic Neutron Scattering," in *Critical Evaluation of Chemical and Physical Structural Information*, edited by David R. Linde, Jr., and Martin A. Paul (National Acad. of Sci., Washington, D.C. 1974).

SAVAGE, H. T., CLARK, A. E., PICKART, S. J., ALPERIN, H. A., RHYNE, J. J., "Effects of Annealing on the Coercivity of Amorphous $TbFe_2$," *Proceedings*, INTERMAG Conf., (Toronto, Canada, May 14-17, 1974) to be published.

SANTORO, A., "Characterization of Twinning," *Acta Cryst.*, A30, 224-241 (1974).

SCHROEDER, L. W., PRINCE, W., and DICKENS, B., "Hydrogen Bonding in $Ca(H_2PO_4)_2 \cdot H_2O$ As Determined by Neutron Diffraction," *Acta Cryst.*, in press.

TREVINO, S. F., PRASK, H. J. and CASELLA, R., "Group Theoretical Selection Rules and Experimental Determination of Lattice Modes in $NaNO_3$ via Inelastic Neutron Scattering," *Phys. Rev.* 10B, 739 (1974).

TREVINO, S. F., PRASK, H. J., SHEN, T. Y., and MITRA, S. S., "Order-Disorder Phenomenon in Sodium Nitrate Studied by Low Frequency Raman Scattering," *Sol. St. Comm.*, in press.

SCHNEIDER, C. S., "A Precise Refractometer for Thermal Neutrons," *Rev. Sci. Instr.* 44, 11, 1594 (1973).

WARKULWIZ, V. P., MOZER, B. and GREEN, M. S., "Observation of the Deviation From Ornstein-Zernike Theory on Critical Scattering of Neutrons From Neon," *Phys. Rev. Lett.*, 32, 1410 (1974).

WATERSTRAT, R. M., and DICKENS, B., "Atomic Ordering in A15-Type Phases in the Vanadium-Nickel and Vanadium-Cobalt Systems," *J. Appl. Phys.*, to be published.

INDEPENDENT PROGRAMS

BECKER, D. A., LAFLEUR, P. D., "Characterization of a Nuclear Reactor for Neutron Activation Analysis," *J. Radioanal. Chem.* 19, 149 (1974).

CARPENTER, B. S., SAMUEL, D., and WASSERMAN, I., "Quantitative Applications of ^{17}O Tracer," *Rad. Effects* 19, 59 (1973).

CARPENTER, B. S., "Lithium Determination by Nuclear Track Technique," *J. Radioanal. Chem.* 19, 233 (1974).

CARPENTER, B. S., and LAFLEUR, P. D., "Nitrogen Determination in Biological Materials by the Nuclear Track Technique," *Anal. Chem.* 46, 8 (1974).

CARPENTER, B. S., GILLIAM, D. M. and REIMER, G. M., "Induced Tracks in Glass From Monoenergetic and Thermal Neutrons," *ANS Transactions* 18, 90 (1974).

PUBLICATIONS

CURRIE, L. A., "On the use of Small Calculators Having Stacked Registers," *Anal. Lett.*, 6, 9, 847 (1973).

FRIEDMAN, M. H., and TANNER, J. T., "An Automated Activation Analysis Data Acquisition System," *Wheat Journal*, to be published.

FRIEDMAN, M. H., FORBES, T. M. and TANNER, J. T., "Instrumental Neutron Activation Analysis for Bromine in Pig Tissue," *Anal. Chim. Acta* 67, 277 (1973).

FRIEDMAN, M. H., MILLER, E., and TANNER, J. T., "Instrumental Neutron Activation Analysis for Mercury in Dogs Administered Methylmercury Chloride: Use of a Low Energy Photon Detector," *Anal. Chem.* 67, 236 (1974).

LUTZ, G. J., "Determination of Lead in Paint With Fast Neutrons From a ^{252}Cf Source," *Anal. Chem.* 46, 4, 618 (1974).

LUTZ, G. J., "The Analysis of Biological and Environmental Samples For Lead by Photon Activation," *J. Radioanal. Chem.* 19, 239 (1974).

McCLENDON, L. T. and LaFLEUR, P. D., "Determination of Rare Earths in Standard Reference Material Glass Using Neutron Activation Analysis and Reversed-Phase Chromatography," *J. Radioanal. Chem.* 16, 123 (1973).

REIMER, G. M. and CARPENTER, B. A., "Thorium Determination in Glass Using the Fission Track Technique," *Nature* 247, 101 (1974).

ROOK, H. L., LUTZ, G. J., and LaFLEUR, P. D., "The Use of a High Efficiency Mass Separator in Activation Analysis," *J. Radioanal. Chem.* 15, 557 (1973).

ROOK, H. L., LaFLEUR, P. D. and SUDDUETH, J. E., "Trace Element Determination Using a High Yield Electromagnetic Isotope Separator and Neutron Activation--The Determination of Cadmium," *Nucl. Instr. and Methods,* 116, 579 (1974).

TANNER, J. T., FRIEDMAN, M. H. and HOLLOWAY, G. E., "Arsenic and Antimony in Laundry Aids by Instrumental Neutron Activation Analysis," *Anal. Chim. Acta,* in press.

TANNER, J. T. and FORBES, W. S., "Determination of Mercury in Total Diet Samples by Neutron Activation," *Anal. Chim. Acta,* in press.

YATES, J T., MADEY, T. E. and ROOK, H. L., "Wear of English Monumental Brasses Caused by Brass Rubbing," *Nature* 243, 422 (1973).

NBS-114A (REV. 7-73)

U.S. DEPT. OF COMM.
BIBLIOGRAPHIC DATA SHEET

1. PUBLICATION OR REPORT NO. NBS Tech. Note 860

2. Gov't Accession No.

3. Recipient's Accession No.

4. TITLE AND SUBTITLE

NBS Reactor: Summary of Activities July 1973 to June 1974

5. Publication Date April 1975

6. Performing Organization Code

7. AUTHOR(S) Robert S. Carter

8. Performing Organ. Report No.

9. PERFORMING ORGANIZATION NAME AND ADDRESS

NATIONAL BUREAU OF STANDARDS
DEPARTMENT OF COMMERCE
WASHINGTON, D.C. 20234

10. Project/Task/Work Unit No.

11. Contract/Grant No.

12. Sponsoring Organization Name and Complete Address *(Street, City, State, ZIP)*

13. Type of Report & Period Covered 7-1-73 to 6-30-74

14. Sponsoring Agency Code

15. SUPPLEMENTARY NOTES

16. ABSTRACT *(A 200-word or less factual summary of most significant information. If document includes a significant bibliography or literature survey, mention it here.)*

This report summarizes all those programs which depend on the NBS reactor. It covers the period from July 1973 through June 1974. The programs range from the use of neutron beams to study the structure and dynamics of materials through nuclear physics, and neutron standards and neutron radiography to sample irradiations for activation analysis, isotope production and radiation effects studies.

17. KEY WORDS *(six to twelve entries; alphabetical order; capitalize only the first letter of the first key word unless a proper name; separated by semicolons)*

Activation analysis; crystal structure; diffraction; isotopes; molecular dynamics; neutron; nuclear reactor; radiation; radiography.

18. AVAILABILITY ☒ Unlimited

☐ For Official Distribution. Do Not Release to NTIS

☒ Order From Sup. of Doc., U.S. Government Printing Office
Washington, D.C. 20402, SD Cat. No. C13 46:860

☐ Order From National Technical Information Service (NTIS)
Springfield, Virginia 22151

19. SECURITY CLASS (THIS REPORT) UNCLASSIFIED

20. SECURITY CLASS (THIS PAGE) UNCLASSIFIED

21. NO. OF PAGES 143

22. Price $2.05

USCOMM-DC 29042-P74

☆ U.S.GOVERNMENT PRINTING OFFICE:1975- 583-018/45

NBS TECHNICAL PUBLICATIONS

PERIODICALS

JOURNAL OF RESEARCH reports National Bureau of Standards research and development in physics, mathematics, and chemistry. It is published in two sections, available separately:

- **Physics and Chemistry (Section A)**

Papers of interest primarily to scientists working in these fields. This section covers a broad range of physical and chemical research, with major emphasis on standards of physical measurement, fundamental constants, and properties of matter. Issued six times a year. Annual subscription: Domestic, $17.00; Foreign, $21.25.

- **Mathematical Sciences (Section B)**

Studies and compilations designed mainly for the mathematician and theoretical physicist. Topics in mathematical statistics, theory of experiment design, numerical analysis, theoretical physics and chemistry, logical design and programming of computers and computer systems. Short numerical tables. Issued quarterly. Annual subscription: Domestic, $9.00; Foreign, $11.25.

DIMENSIONS/NBS (formerly Technical News Bulletin)—This monthly magazine is published to inform scientists, engineers, businessmen, industry, teachers, students, and consumers of the latest advances in science and technology, with primary emphasis on the work at NBS. The magazine highlights and reviews such issues as energy research, fire protection, building technology, metric conversion, pollution abatement, health and safety, and consumer product performance. In addition, it reports the results of Bureau programs in measurement standards and techniques, properties of matter and materials, engineering standards and services, instrumentation, and automatic data processing.

Annual subscription: Domestic, $9.45; Foreign, $11.85.

NONPERIODICALS

Monographs—Major contributions to the technical literature on various subjects related to the Bureau's scientific and technical activities.

Handbooks—Recommended codes of engineering and industrial practice (including safety codes) developed in cooperation with interested industries, professional organizations, and regulatory bodies.

Special Publications—Include proceedings of conferences sponsored by NBS, NBS annual reports, and other special publications appropriate to this grouping such as wall charts, pocket cards, and bibliographies.

Applied Mathematics Series—Mathematical tables, manuals, and studies of special interest to physicists, engineers, chemists, biologists, mathematicians, computer programmers, and others engaged in scientific and technical work.

National Standard Reference Data Series—Provides quantitative data on the physical and chemical properties of materials, compiled from the world's literature and critically evaluated. Developed under a world-wide program coordinated by NBS. Program under authority of National Standard Data Act (Public Law 90-396).

NOTE: At present the principal publication outlet for these data is the Journal of Physical and Chemical Reference Data (JPCRD) published quarterly for NBS by the American Chemical Society (ACS) and the American Institute of Physics (AIP). Subscriptions, reprints, and supplements available from ACS, 1155 Sixteenth St. N. W., Wash. D. C. 20056.

Building Science Series—Disseminates technical information developed at the Bureau on building materials, components, systems, and whole structures. The series presents research results, test methods, and performance criteria related to the structural and environmental functions and the durability and safety characteristics of building elements and systems.

Technical Notes—Studies or reports which are complete in themselves but restrictive in their treatment of a subject. Analogous to monographs but not so comprehensive in scope or definitive in treatment of the subject area. Often serve as a vehicle for final reports of work performed at NBS under the sponsorship of other government agencies.

Voluntary Product Standards—Developed under procedures published by the Department of Commerce in Part 10, Title 15, of the Code of Federal Regulations. The purpose of the standards is to establish nationally recognized requirements for products, and to provide all concerned interests with a basis for common understanding of the characteristics of the products. NBS administers this program as a supplement to the activities of the private sector standardizing organizations.

Federal Information Processing Standards Publications (FIPS PUBS)—Publications in this series collectively constitute the Federal Information Processing Standards Register. Register serves as the official source of information in the Federal Government regarding standards issued by NBS pursuant to the Federal Property and Administrative Services Act of 1949 as amended, Public Law 89-306 (79 Stat. 1127), and as implemented by Executive Order 11717 (38 FR 12315, dated May 11, 1973) and Part 6 of Title 15 CFR (Code of Federal Regulations).

Consumer Information Series—Practical information, based on NBS research and experience, covering areas of interest to the consumer. Easily understandable language and illustrations provide useful background knowledge for shopping in today's technological marketplace.

NBS Interagency Reports (NBSIR)—A special series of interim or final reports on work performed by NBS for outside sponsors (both government and non-government). In general, initial distribution is handled by the sponsor; public distribution is by the National Technical Information Service (Springfield, Va. 22161) in paper copy or microfiche form.

Order NBS publications (except NBSIR's and Bibliographic Subscription Services) from: Superintendent of Documents, Government Printing Office, Washington, D.C. 20402.

BIBLIOGRAPHIC SUBSCRIPTION SERVICES

The following current-awareness and literature-survey bibliographies are issued periodically by the Bureau:

Cryogenic Data Center Current Awareness Service

A literature survey issued biweekly. Annual subscription: Domestic, $20.00; foreign, $25.00.

Liquefied Natural Gas. A literature survey issued quarterly. Annual subscription: $20.00.

Superconducting Devices and Materials. A literature survey issued quarterly. Annual subscription: $20.00. Send subscription orders and remittances for the preceding bibliographic services to National Technical Information Service, Springfield, Va. 22161.

Electromagnetic Metrology Current Awareness Service

Issued monthly. Annual subscription: $100.00 (Special rates for multi-subscriptions). Send subscription order and remittance to Electromagnetics Division, National Bureau of Standards, Boulder, Colo. 80302.

U.S. DEPARTMENT OF COMMERCE
National Bureau of Standards
Washington, D.C. 20234

OFFICIAL BUSINESS

Penalty for Private Use, $300

POSTAGE AND FEES PAID
U.S. DEPARTMENT OF COMMERCE
COM-215

FOURTH CLASS MAIL

U.S.MAIL

AMERICAN REVOLUTION BICENTENNIAL
1776-1976